Exploring Drivers of Gene Flow in Jaguars and Pumas in Southern Mexico via Molecular Scatology and Eco-Evo Simulations

Jennifer Mae-White Day

A dissertation

Submitted in partial fulfillment of the

Requirements for the degree of

Doctor of Philosophy

University of Washington

2017

Reading Committee:

Samuel K. Wasser, Chair

Joshua J. Lawler

Kerry-Ann Naish

Program Authorized to Offer Degree:

Biology

University of Washington

Abstract

Exploring Drivers of Gene Flow in Jaguars and Pumas in Southern Mexico via Molecular Scatology and Eco-Evo Simulations

Jennifer Mae-White Day

Chair of the Supervisory Committee:
Samuel K. Wasser
Biology

The profound fragmentation and degradation of Neotropical forests over the past 50-100 years poses a significant threat to the wildlife populations in Mesoamerica. Neotropical large carnivores, jaguars (*Panthera onca*) and pumas (*Puma concolor*), are at particular risk from forest conversion due to their large spatial requirements and high vagility, and are key contributors to ecosystem function in their roles as top predators. Diminishing structural connectivity of the landscape is likely to impede gene flow for both species, with potential impacts on population or species persistence. However, the mechanistic drivers behind gene flow are poorly understood. In this dissertation, I explore how landscape patterns and habitat selection interact to influence gene flow of jaguars and pumas in southern Mexico.

The first half of this dissertation is dedicated to the quantification of jaguar and puma landscape use, gene flow, and genetic diversity in southern Mexico, where we know little about the remaining populations (Chapters 1 & 2). This work was based on noninvasive genetic samples, collected with the aid of wildlife detector dogs, in the Uxpanapa valley of Veracruz, and northern Quintana Roo. Resource selection analysis suggests less ubiquitous use of the landscape by jaguars due to greater habitat specificity for natural vegetation, rugged terrain, and avoidance of human activity, as compared to use of a broader array of habitats by pumas. However, I did not find evidence of gene flow restriction within Uxpanapa despite low predicted connectivity between forest patches. At the regional scale between

study locations, pumas exhibited greater genetic discontinuity than sympatric jaguars. These findings are also echoed in the literature and highlight an apparent disconnect between predicted structural connectivity at fine-scales and gene flow at broader scales, suggesting that behavioral components of movement ecology may differ between resource use within home ranges and juvenile dispersal.

In the second half of this dissertation, I turned to computer simulations to explore the possible drivers of gene flow by scaling-up fine-scale processes, such as resource selection, to broader-scale patterns, such as gene flow (Chapters 3 & 4). I explored the utility of an individual-based modeling (IBM) platform, HexSim, for integrating population dynamics, movement ecology and behavior, and evolutionary processes on spatially explicit landscapes. I then employed this modeling platform to build a biologically and spatially realistic eco-evo IBM of large felid gene flow. I used this model to conduct a pilot test of hypothesized drivers of gene flow through Mexico, Guatemala, and Belize. Results suggest that gene flow was decreased by territorial habitat specialization and increased by sensitivity to landscape features during dispersal. My results showcase the model's ability to investigate how specific components of complex movement behavior drive of gene flow.

The large-felid eco-evo IBM offers a powerful tool for future investigations of mechanistic connections between fine-scale resource selection and gene flow at broader scales, as well as for forecasting the effects of habitat preservation versus connectivity conservation. Jaguars appear to have greater forest selectivity and sensitivity to human activity as compared to pumas, highlighting the need to bolster the existing national incentives for forest preservation in order to protect this declining species. Finally, my results stress the need for state or federal protection of the Uxpanapa valley, Veracruz, as a biological hotspot that provides a stepping stone for movement between Central and North American wildlife populations.

CONTENTS:

CHAPTER 1: Resource Selection and Habitat Connectivity of Jaguar (*Panthera onca*), Puma (*Puma concolor*), and Baird's Tapir (*Tapirus bairdii*) in the Isthmus of Tehuantepec, Mexico.

Jennifer M.W. Day[1], Brenda Solorzano[2], Samuel K. Wasser[1]

[1] Center for Conservation Biology, Department of Biology, University of Washington, Seattle, USA

[2] Universidad Nacional Autonoma de Mexico, Mexico City, Mexico

ABSTRACT:

The Isthmus of Tehuantepec of southern Mexico is a vital biogeographic bridge through central Mesoamerica. The three native large mammals within this region are puma (*Puma concolor*), jaguar (*Panthera onca*), and the endangered Baird's tapir (*Tapirus bairdii*). All three are species of conservation concern, threatened with deforestation, urbanization, and road development through Tehuantepec. Determining how these species interact with the landscape can help inform conservation actions such as corridor design or species-specific habitat protection plans. Landscape use information is especially needed within human-dominated landscapes, outside of protected parks, where regional connectivity and species resilience is likely to be decided. Our study quantifies landscape use for these three species in the Uxpanapa valley, Veracruz, a human-dominated unprotected area in the center of Tehuantepec.

The Uxpanapa valley study site (~ 5,000 km^2) contains remnant forest fragments embedded in a matrix of pasture and agriculture. Prior to this study, it was unknown if jaguar or Baird's tapir were extant within the valley or if they had been extirpated by poaching and habitat loss. We employed wildlife detector dogs to collect noninvasive scat samples, which we identified to species using mitochondrial DNA sequencing. We used the confirmed species locations (scat and tracks) to conduct multiple-scale resource selection analyses, which were in turn, used as the basis for modeling connectivity through the valley using a circuit-theory approach.

We collected 126 putative felid samples and 26 tapir dung samples over survey transects totaling approximately 550 km. Of the putative felid samples, we confirmed 44 jaguar, 18 puma, and 20 unknown felid, via genetic analysis or identification of the felid hair within the scat. An additional 10 scats were identified as unknown felid, based on large-bodied prey content. We also recorded 9 large-felid track locations and 20 tapir track locations. Resource selection models for jaguars indicate a selection for rugged terrain and tall forest, and avoidance of pasture and villages. Puma models indicate

a selection for moderate terrain and avoidance of areas with high stream density. Tapir models indicate a selection for higher elevation (correlated with interior of forest fragments) and avoidance of human-dominated land cover and roads. Selection for land cover by the large felids appears to occur at a relatively fine spatial scale (625 m radius) rather than at the scale of a home-range. Conversely, selection by tapirs appears to occur at broader spatial scales (2.5-5 km radius). Structural connectivity modeling highlighted movement corridor locations that differed between jaguar and puma, and suggest a lower overall connectivity throughout the valley for jaguar than for puma. The level of forest patch connectivity appears positively correlated with the density of individuals.

Baird's tapir appear to be obligate forest specialists in this region, making conservation of forest habitat of paramount importance for this endangered species. Our results support the relative forest specialization and sensitivity to human activity of jaguars as compared to puma. While we are pleased to confirm the existence of all three species within the Uxpanapa valley, our study highlights an immediate need for controlling the rate of deforestation to ensure the continued presence of these species in Uxpanapa.

Keywords: deforestation, conservation, large carnivores, resource selection, habitat connectivity, noninvasive genetics, wildlife detector dogs

INTRODUCTION:

The profound fragmentation and degradation of neo-tropical forests over the past 50 years has led to ambitious large-scale wildlife conservation initiatives. The delineation and monitoring of a network of Jaguar Conservation Units (JCUs) from Argentina through northern Mexico is one such international initiative (Sanderson et al. 2002; Rabinowitz and Zeller 2010; Olsoy et al. 2016). Approximately 50% of the historical jaguar (*Panthera onca*) species range remains today (Sanderson et al. 2002; Zeller 2007). Jaguars in the Isthmus of Tehuantepec JCU in southern Mexico connect the populations in northern Mexico and the Yucatan Peninsula / Central America (Rabinowitz and Zeller 2010). The Tehuantepec JCU area has experienced approximately 25-50% woody deforestation between 2001-2010 alone (Clark, Aide, and Riner 2012). The two other megafauna species within the Tehuantepec JCU, are puma (*Puma concolor*), and Baird's tapir (*Tapirus bairdii*) (an herbivorous odd-toed ungulate). Jaguars are considered near-threatened and Baird's tapir are considered endangered by the International Union for Conservation of Nature (IUCN) and both are listed as Appendix I species under the Convention on International Trade in Endangered Species (CITES).

Large carnivores and tapirs contribute to Neotropical ecosystem function in their roles as top predators (Terborgh et al. 2001; Terborgh 1992) and large-seed dispersers (Fragoso 1997), respectively. These large mammals are at particular risk from forest conversion. The large spatial extent of their home-ranges require large contiguous tracts of habitat. Additionally, their high vagility increases the chance of human conflicts. Protected forested reserves, while important, will likely be insufficient to sustain megafauna species through the Anthropocene (Woodroffe and Ginsberg 1998). For example, the proposed JCUs, while an ambitious conservation goal, cover just 14% of the estimated jaguar habitat within Mexico (Rodríguez-Soto et al. 2011). Their resilience will depend, in part, on the degree of connectivity provided by the non-forest matrix between forest patches, in human-dominated landscapes (Chazdon et al. 2009; Franklin and Lindenmayer 2009). Connectivity is driven by a

combination of landscape pattern (e.g. quality of the non-forest matrix), biology (e.g. movement ability, dietary requirements, or sensory ability), and behavioral traits (e.g. tolerance of roads or preference for concealment). The goal of our study is to quantify landscape use for these species in a human-dominated unprotected area in the center of Tehuantepec for the purpose of predicting connectivity patterns relevant to conservation strategies, including corridor identification and species-specific management recommendations. Our methodological approach couples noninvasive molecular scatology with resource selection analyses to predict connectivity for the three species in the Uxpanapa valley, on the northern border of the Tehuantepec JCU in Veracruz, Mexico.

All three species are classified as under threat of extinction in Uxpanapa (Sandoval-Mendoza et al. 2007). We lack confirmed georeferenced reports for any of the wild felids in the Uxpanapa valley (Figure 1), and it is unknown if jaguars or Baird's tapir persist in the valley (Sandoval-Mendoza et al. 2007). The landscape use by pumas is unknown within the region. Pumas are generally considered capable of using many different land-cover types, are less constrained by the matrix surrounding habitat patches, and more adaptable to changes in the landscape (De Angelo, Paviolo, and Di Bitetti 2011; Elbroch and Wittmer 2012; Goulart et al. 2009). Conversely, jaguar are reported to be more sensitive to human activity, and more constrained to undisturbed vegetation (Monroy-Vilchis et al. 2009; Petracca et al. 2014; Carly Vynne, Keim, et al. 2011; Zeller 2007). However, in other regions, patterns of habitat preference and human-avoidance behavior appear reversed (Foster, Harmsen, and Doncaster 2010). What little is known about Baird's tapir in Mexico indicates that the estimated 2,600 individuals are located in isolated populations scattered across southern Mexico (Naranjo 2009). Baird's tapir are reported to use a variety of lands cover types, with habitat use being influenced by hunting pressure (Naranjo 2009). We predict that selection for forest cover and avoidance of human-dominated landscapes will be stronger for jaguar and tapir than for puma, resulting in lower predicted connectivity through the valley for these "specialists" versus the more "generalist" puma.

Our study includes three objectives building to our goal of understanding landscape use by these species. First and foremost, we determine if all three species are extant in the valley, or whether jaguar or tapir have been extirpated. Secondly, we quantify patterns of resource use, including the identification of selected or avoided landscape features, and the spatial scale of these behaviors. The third objective is to use the results of our resource selection analyses to predict connectivity through the valley, including the identifying movement corridor locations and determining if connectivity influences species density within habitat patches. Addressing these objectives will help determine whether conservation priorities can benefit multiple species at once, or if species-specific plans are needed.

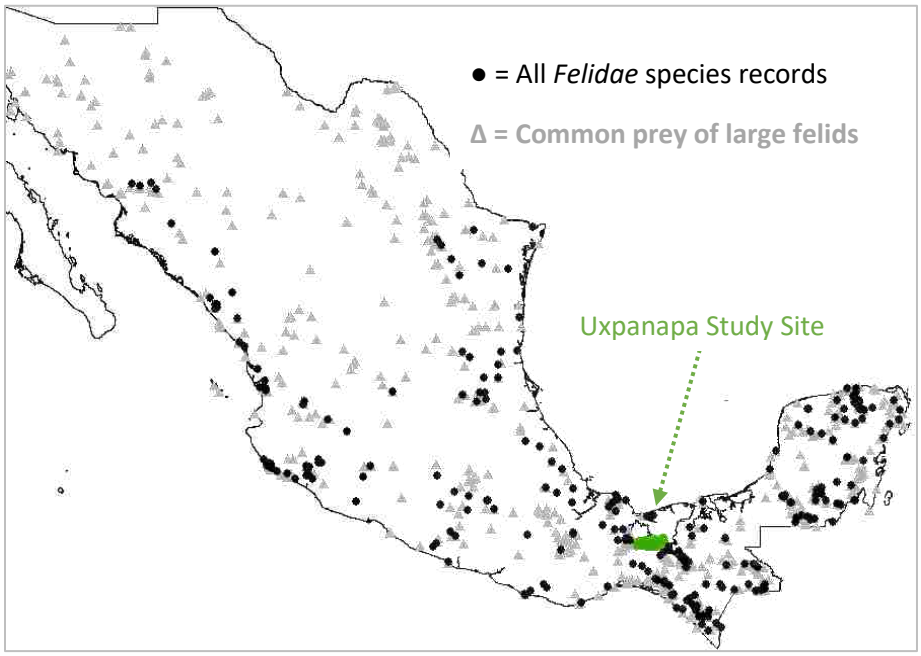

Figure 1. Global Biodiversity Information Facility (GBIF) species records for jaguars, pumas, and smaller cats, as well as their common prey species in Mexico. There are no GBIF records within the Uxpanapa valley study site.

METHODS:

Study Site and Noninvasive Sample Collection: The Uxpanapa valley study area is approximately 4,775km^2, and is a mosaic dominated by pasture (26%) and secondary forest (38%), with smaller portions consisting of small corn plantations and rubber tree cultivations (15%), remnant mature tall canopy forest (16%), and village settlements (5%) (Figure 2). Vegetation data were collected by a single field team member throughout the survey for continuity in classification of vegetation types. These data were used to inform a supervised classification of five SPOT 5 satellite images captured in the dry season of March and April 2011 (88.25% classification accuracy, Kappa coefficient = 0.8482). Of the 2,535km^2 forest remaining in 2011, approximately 1,266km^2 were mid-successional secondary forest, 491km^2 were late-successional secondary forest, and 778km^2 were mature tall-canopy forest.

Land ownership in the valley is primarily in the form of small communities (ejidos), but also includes areas of national land. There are two areas within Veracruz's Uxpanapa valley that are contiguous with Selva Zoque to the south of the study site in Oaxaca and Chiapas states (Figure 2). Selva Zoque is a large area of steep cliffs and dense jungle, that makes up the majority of the Tehuantepec JCU (Rabinowitz and Zeller 2010).

We divided the study area into 275 grid cells of 5 km x 5 km. We targeted cells that contained over 36% forest cover, assuming wildlife are more likely to inhabit areas that contain some natural vegetation. Surveys of each targeted cell consisted of one to two transects approximately 10 km long. A typical survey began at an access point closest to a forest fragment, continued through ranchland for 1-10 km, followed by a quasi-circular path through a forest fragment, returning through pasture to the access point. Surveys often followed human or game trails, but also included off-trail and roads. The extent to which we were able to survey each targeted cell was determined by our guides' knowledge of the local forest. The western portion of the valley was surveyed from March-May 2010, and the eastern portion (including some revisits to the western side) from March-May 2011.

Scat samples were found with the aid of wildlife scat detection dogs from the University of Washington Conservation Canines program. We chose to use noninvasive sample collection with wildlife detector dogs for the following reasons. Trapping and collaring approaches to large mammal research are often cost prohibitive over large tracts of land where terrain limits access. Noninvasive methods requiring repeated checks of static sample locations, such as camera-traps or hair-snags, become untenable when the target species exist in low densities across large spatial extents. Additionally, these methods often rely on luring wildlife to a station location, potentially disrupting movement behavior. Therefore, we employed detection dogs to locate puma, jaguar, and tapir scats, allowing us to cover a large area effectively without requiring the target species to alter their movement behavior. Wildlife detector dogs are less biased and more systematic compared to opportunistic scat collection by humans because the olfactory search of the dogs does not rely on visually-conspicuous scat deposition on trails or roads, a behavior that may be sex-biased (Vynne et al. 2011).

The survey team included a dog and dog-handler, orienteer, and one to two guides hired from the ejido. The detection dog was trained to find scat from jaguars, pumas, and Baird's tapirs. Smaller carnivore samples that were investigated but passed-up by the detector dog were also collected, as they were suspected to be from the smaller wild felids (ocelots, margays, or jaguarondis). Survey tracks were recorded continuously via a GPS unit worn by the detector dog. We collected vegetation and microhabitat data at each scat location along with a description of the scat's visible condition and content. A portion of the scat was collected in sterile urine cups with silica desiccation beads (3:1 ratio of silica beads to scat volume) separated from the sample by filter paper. Given sufficient size of the sample, a portion was left in the field to minimize disruption of any territorial marking behavior. Immediately upon returning to the field station each day, scat samples were swabbed for epithelial cells using sterile cotton swabs soaked in PBS buffer. During the first field survey, swabs were stored in 1.5mL tubes with either silica beads, ethanol, or lysis buffer, and kept refrigerated. Based on a limited

analysis of these storage methods, lysis buffer was chosen as the optimal storage technique for the second season (data not shown). The remaining fecal material was frozen in a -20°C freezer in the field station, and later freeze-dried for long-term preservation.

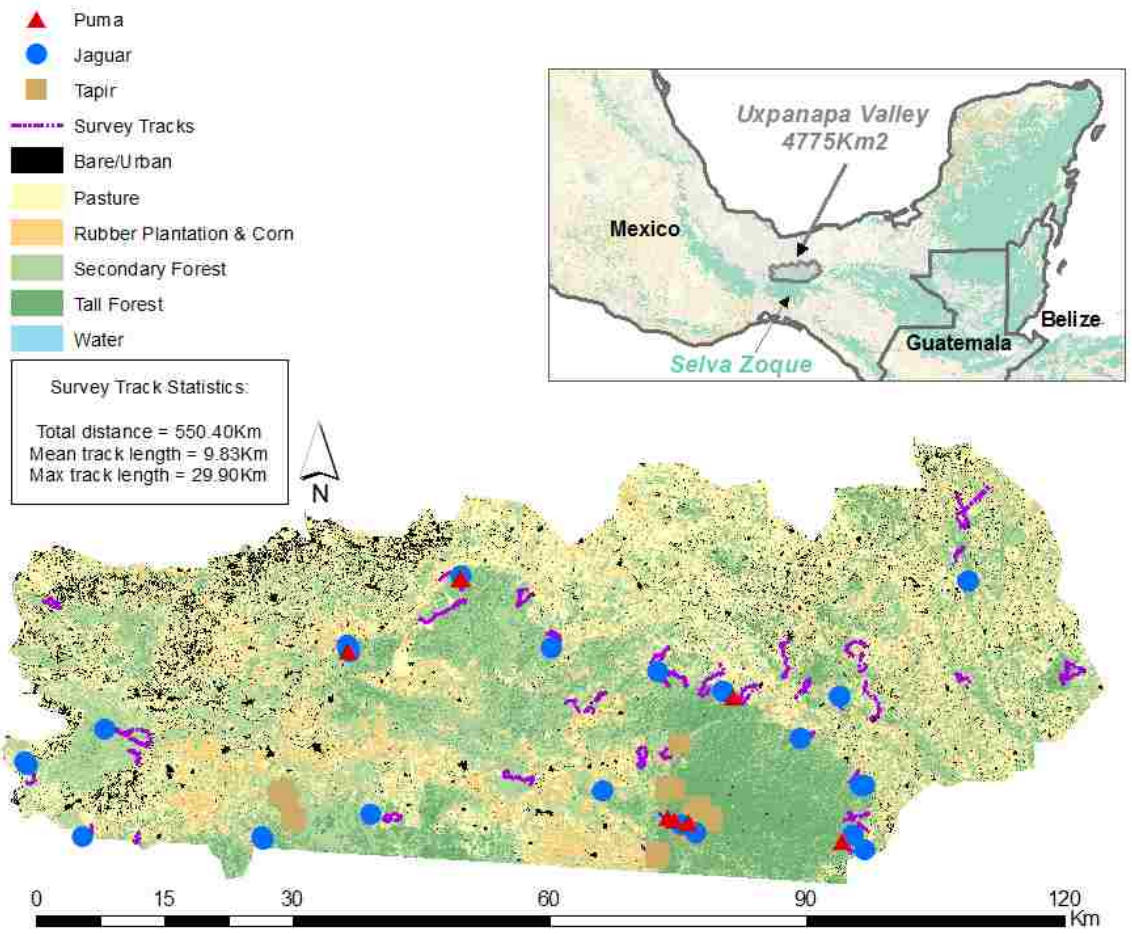

Figure 2. Uxpanapa valley study site in Veracruz, Mexico. Confirmed locations of puma, jaguar, and Baird's tapir.

Species Identification of Scat Samples: We extracted DNA from the sample swabs using the Qiagen Tissue kit (Qiagen, Inc., Valencia, CA). Because jaguar and puma scats are visually indistinguishable from each other, we identified the species using forward and reverse sequencing of the ATP6 ribosomal region (~175bp) of mitochondrial DNA (mtDNA) (primers: F 5'- AAC GAA AAT CTA TTC GCC TCT -3', R 5'- CCA GTA TTT GTT TTG ATG TTA GTT G -3')(Chaves et al. 2012), and fragment length polymorphism within the mtDNA control region (D-loop) using primers HSF21 (GTA CAT GCT TAT ATG CAT GGG) and LTPROB13 (CCA CTA TTA ACA CCC AAA GC) (S. K. Wasser et al. 1997; C. Vynne et al. 2012). Each 10uL PCR amplification reaction consisted of 1uL 10X PCR buffer, 0.6uL 50mM mgCl2, 0.3uL 10mM dNTPs, 1uL Bovine Serum Albumin (BSA), 0.6 5uM Forward Primer, 0.6uM Reverse Primer, 0.15 5U/uL Taq Polymerase, 3.75uL water, and 2uL DNA extract. PCR thermocycling program began with a 5 minute 95°C denaturation, followed by 40 amplification cycles (30 s 95 °C denaturation, 30 s 62 °C annealing, 30 s 72 °C elongation), followed by a final 8 minute 72°C elongation.

ATP6 sequences were aligned using SEQUENCHER, and assigned to species by alignment to reference sequences obtained from all sympatric carnivore species from either the University of Washington Burke Museum (UWBM) Genetic Resources Collection, or from fecal samples from captive animals at Zoologico Miguel Alvarez del Toro (ZOOMAT), Chiapas, Mexico (*Panthera onca*: UWBM # 76494 Tissue # JR 1521; *Puma concolor*: UWBM # 81677 Tissue # JEB 1488, UWBM # 81679 Tissue # JEB 1490, UWBM # 81680 Tissue # JEB 1491, UWBM # 81682 Tissue # JEB 1493). Sequence identification was also confirmed via National Center for Biotechnology Information (NCBI) Basic Locus Alignment Search Tool (BLAST). Baird's tapir scat was visually identified by its unique, cuboid, morphology (the majority of locations lacked sympatric animals with comparable scat content, such as horse or donkey). Tapir scats were also frequently accompanied by their distinctive three-toed tracks. Analysis of the hair contained within the carnivore scat (both predator and prey) was conducted by a student trained by B.

Sorlozano in morphological identification hair scale pattern and cuticle morphology and based on published reference guides (Baca-Ibarra and Sánchez-Cordero 2004; Juarez et al. 2010).

Preparation of Geographic Information: We considered four categories of landscape variables: Human Activity, Water, Vegetation, and Terrain. For puma, we also considered the presence of jaguars as a potential determinant of landscape use due to competitive exclusion. Geographic analysis was done within ArcGIS10.2-3 and the Geospatial Modeling Environment 0.7.3-4 (GME) (Beyer, n.d.). Geographic data layers included roads (manually classified into three use levels), villages, large rivers, detailed streams, classified vegetation, and digital elevation model (DEM) (appendix Table S1). The field team observed that there were different qualities to the "rugged" terrain within the study area. There were steep slopes in the southwestern part of the study area that were difficult to navigate, but other areas of jagged karstic limestone substrate that were impossible to traverse. This observed heterogeneity was not captured by any of the numerous metrics commonly used to quantify ruggedness. Therefore, we created a novel ruggedness metric, termed "Insuperable Terrain Index" (*ITI*), designed to distinguish these two types of terrain. We calculated ITI based on DEM within an eight-cell neighborhood as follows:

$$[(\text{Mean}-\text{Min})/(\text{Max}-\text{Min})] \mid \text{slope}>30$$

ITI was classified into three levels (rough, moderate, and flat) based on ground-truthed locations of jagged karstic rock slopes, non-jagged slopes, and valley floor, respectively (appendix Text S1).

For each geographic layer, we extracted geographic data relative to each sample. For each location, we quantified distance to nearest feature (e.g. distance to road), value at the location (e.g. land-cover class), or amount of feature within circular zones around each sample (e.g. amount of pasture within 2.5 km). For the latter, we chose four radii around each sample (625m, 1.25km, 2.5km,

and 5km) to assess the scale of landscape use behavior (appendix Text S2). The larger two radii approximate female and male jaguar home range sizes. We had two linear features of interest, roads and large rivers, for which we wanted to account for both proximity and density simultaneously. To do so, we created buffers surrounding the features (Road Buffers: 100 m and 1 km, River Buffers: 1 km, 5 km, and 10 km) and then measured the amount of those buffers within the circular zones (e.g. % of a 2.5 km zone covered by 100 m Road Buffer). We used ArcGIS for distance to nearest feature or sampling the value at a given location. We used the GME *isectpolyrst* function to calculate the % of feature within each circular radius, as the *Tabulate Intersection* tool within ArcGIS does not calculate these values correctly. In total, we calculated 77 geographic metrics for downstream analysis (Table 1)

Table 1. Geographic metrics calculated for used (scat) and available locations for use in resource selection analysis. .

Human Activity	Distance to Nearest	Within 625m Radius	Within 1.25km Radius	Within 2.5km Radius	Within 5km Radius
(17 metrics)	Village	Number of Villages	Number of Villages	Number of Villages	Number of Villages
	Road	% 100m Road Buffer	% 100m Road Buffer	% 100m Road Buffer	% 100m Road Buffer
	Primary Road	% 1km Road Buffer	% 1km Road Buffer	% 1km Road Buffer	% 1km Road Buffer
	Secondary Road				
	Tertiary Road				
Water	Distance to Nearest	Within 625m Radius	Within 1.25km Radius	Within 2.5km Radius	Within 5km Radius
(15 metrics)	River	Total meters of Streams	Total meters of Streams	Total meters of Streams	Total meters of Streams
	Stream	% 1km River Buffer	% 1km River Buffer	% 1km River Buffer	% 1km River Buffer
		% 5km River Buffer	% 5km River Buffer	% 5km River Buffer	% 5km River Buffer
					% 10km River Buffer
Vegetation	Value at Location	Within 625m Radius	Within 1.25km Radius	Within 2.5km Radius	Within 5km Radius
(31 metrics)	VegClass (HC,P,CR,SF,TF)	% HC	% HC	% HC	% HC
	VegForestClass (SF, TF, or AH)	% P	% P	% P	% P
	VegSimple (Forest/Human)	% CR	% CR	% CR	% CR
		% All Human (HC+P+CR)	% All Human (HC+P+CR)	% All Human (HC+P+CR)	% All Human (HC+P+CR)
		% SF	% SF	% SF	% SF
		% TF	% TF	% TF	% TF
		% All Forest (SF+TF)	% All Forest (SF+TF)	% All Forest (SF+TF)	% All Forest (SF+TF)
Terrain	Value at Location	Within 625m Radius	Within 1.25km Radius	Within 2.5km Radius	Within 5km Radius
(14 metrics)	ITI Class (Flat, Mod., Rough)	% Flat ITI	% Flat ITI	% Flat ITI	% Flat ITI
	Elevation (DEM)	% Moderate ITI	% Moderate ITI	% Moderate ITI	% Moderate ITI
		% Rough ITI	% Rough ITI	% Rough ITI	% Rough ITI

* Human Settlement or Clear (HC), Pasture (P), Citrus or Rubber (CR), Secondary Forest (SF), Tall forest (TF)

Resource Selection Analysis: Resource selection models examine use of landscape features relative to what is available. Landscape characteristics were measured at "used" (scat) locations and at

1,000 randomly generated "available" locations. To limit bias in our assessment of what is considered "available", generated locations were restricted to within a 50 m buffer around each survey track. Although local vegetation and wind will obviously influence the odor distribution from any given sample, this approach provides a conservative estimate of the effective olfactory search area of the detector dog (Wasser et al. 2012). We have chosen a used-versus-available resource selection approach for analysis of habitat associations, as opposed to a use-only approach or species distribution modeling, for the following two reasons. First, resource selection is arguably more pertinent for conservation applications than a resource use-only approach, which has the potential to undervalue landscape resources that are relatively rare in the landscape. Secondly, resource-selection is constrained by eco-physiological limits (such as thermal tolerances) at coarse spatial scales and realized by more plastic behavioral dynamics occurring at finer spatial scales (such as food-seeking movement behavior). We argue that it is at this intermediate spatial scale, of home range or smaller (second/third-order spatial scale; Johnson 1980), that our results will be most applicable for connectivity conservation within Tehuantepec.

The majority of the geographic covariates that were quantified as percentages (e.g. *% 1Km Road Buffer within 625m Radius*) required logit transformation to improve normality in the data distribution. Others required $\log_{10}$ or square-root transformation prior to analysis, or were unusable due to skewness (appendix Table S2). Resource Selection (RSF) and Resource Selection Probability Functions (RSPF) use a logistic-regression framework (binomial response variable of 0 = *available* and 1 = *used*) to model the effect of geographic variables on the probability that a location is used or unused if encountered (Lele et al. 2013; Lele and Keim 2006; Keim, DeWitt, and Lele 2011). In brief, RSF is a relative metric (e.g. a forest site has a 4.6x higher probability of being used than a pasture site) and models are fit with an exponential function. RSPF is an absolute metric (e.g. a forest site has a 0.8 probability of being used if encountered) and models are fit with a logistic function. It is recommend to use both model forms for analysis, as either may fit a given dataset best (Lele et al. 2013; Keim, DeWitt, and Lele 2011). RSF and

RSPF analyses were implemented with the R *Resource Selection* package (settings: *m* = 0, *B* = 99)(Lele, Keim, and Solymos 2014). Model selection was based on information criteria of Log-likelihood scores.

Analysis was done in two phases: 1. Determination of optimal spatial scale for those geographic variables measured at multiple scales and, 2. Model building across categories. In the first phase, for each covariate (e.g. *% Secondary Forest* [*SF*]), RSF and RSPF models were fit for each scale of measurement (e.g. *%SF within 625 m Radius*, *%SF within 1.25 Radius*, etc.). The top RSF/RSPF models were chosen via BIC for consideration in phase two of analysis (*see* Text S2 *for an example of the impact of scale selection*). The second phase of analysis combined the top variables from the first phase across all categories of geographic metrics. To examine the potential of species-specificity in resource selection, we conduced both phases of analysis on each species separately, as well as for all felids together. The later included scat locations that were confirmed as jaguar or puma, as well as samples that were from unknown felids. Unknown felid samples were either scat samples for which genetic species identification was inconclusive, scat samples that contained large-bodied prey (peccary or deer), and large-felid track locations.

Predicted values from the top resource selection models (<2 delta BIC) were mapped across the study area and averaged to create a composite resource selection map for each species. Resource selection functions are not constrained to range between 0-1 as are RSPF. Therefore, we re-scaled those top models that were fit with the RSF exponential function to range between 0-1, prior to building the composite map.

Connectivity Analysis: We modeled connectivity using a resistance framework within the program CIRCUITSCAPE (B. McRae, Shah, and Mohapatra 2013; B. H. McRae 2006). In brief, CIRCUITSCAPE models movement as electrical current through a network of nodes and resistors. In our case, the electrical network is in the form of a raster grid, where each cell contains an electrical

conductance value. The higher the conductance, the greater the amount of movement (current) through that cell. We used our composite species-specific resource selection maps as conductance grids.

In addition to the conductance grid, CIRCUITSCAPE requires an electrical source and ground(s) to model current through the landscape. We modeled two different scenarios of source-ground input, to address two different biological questions of connectivity within the Uxpanapa valley. First, we modeled connectivity between putative population source and sink locations within the valley to identify movement corridors and pinch points relevant to maintaining populations of our target species. For this scenario, we considered the majority of the remnant forest fragments of Uxpanapa to be potential population sinks due to their small area in relation to average home-range sizes (Stoner et al. 2013). These forest patches were modeled as electrical grounds. The probable source population is within the Selva Zoque, the large forest at the southern edge of Uxpanapa. There are two areas within Uxpanapa that are contiguous with Selva Zoque, and it is these two areas that are modeled as electrical sources within this first scenario. With our second scenario, we wanted to quantify the amount of modeled connectivity between the various forest fragments in the study area, and compare across species. To do so, we modeled connectivity in a pairwise manner between all forest fragment centroids, each one acting as an electrical source and ground. We compared species-specific connectivity estimates via a paired-t-test.

To test for the effect of forest patch connectivity on species density, we calculated the average density of individuals per km^2 surveyed by our field team for each forest patch. To limit bias due to recaptures of the same individual, we considered all scats within 1.5 km of each other as one observation, as they have a higher probability of being from the same individual (Haag et al. 2009; Day et al. *this dissertation Chapter 2*). We plotted density against connectivity results from both scenarios above: the amount of current reaching each fragment from Selva Zoque (first scenario), or the average

movement resistance to other patches (second scenario). For the purposes of visualization, we assigned high current values to the patches contiguous with the Selva Zoque source, as they are receiving infinite current under the first scenario.

RESULTS:

Species Identification and Vegetation at Sample Locations: The survey path lengths totaled approximately 550 km, ~68% within forest (recovering, secondary, or tall forest) and 32% within human dominated land cover (pasture, agriculture, or urban areas) (Figure 2). Our field team collected 29 putative Baird's tapir samples and 126 putative felid samples (123 scat and 3 wads of regurgitated grass) from the study area in approximately 100 active survey days over approximately five months. Of the 126 putative felid scat samples, we identified 82 as felid (jaguar = 44, puma = 18, unknown felid = 20) via genetic analysis or identification of the felid hair within the scat (Figure 3). The genetic markers used are designed to amplify all carnivores, yet none of the amplified samples were identified as non-felid, attesting to the specificity of the detector dog method. The remaining 27% of unidentified samples were too degraded for DNA analysis. At times, single sequence reads (either forward or reverse) of single replicates were identified as domestic dog, while the other sequences from that sample were identified as wild felid, possibly due to contamination from CK9 DNA at the field station. There were several samples suspected to be linked to jaguar predation, included a gnawed cattle horn, remains of a goat, pierced pieces of armadillo shell, and a tube-like bundle of porcupine quills. These samples were swabbed for genetic analysis, but unfortunately did not yield DNA for predator species identification. Many of the samples located by the team were degraded to the point where only prey hair remained (a tube of peccary hair was not uncommon), and yet some of these samples yielded DNA. Additionally,

one of the three regurgitated grass samples yielded jaguar DNA sequences. These results suggest caution when culling samples prior to analysis based on visual inspection.

An additional 10 scat samples were identified as unknown felid based on the identification of hair from large-bodied prey (deer or peccary) and scat morphology. An additional jaguar location was based on a CK9 alert at an obvious urine deposit with strong felid musk odor at a frequented location for jaguar urine marking, and the genetic identification of a jaguar scat further along the same trail. Despite the short length of the ATP6 mtDNA sequence, we were able to reconstruct the basic phylogenetic relationships between the wild felids (appendix Figure S1). A portion of our unidentified felid samples phylogenetically clustered to reference samples of each of the other small sympatric felids, including jaguarondi, ocelot, and margay (Figure S1). We collected 29 putative tapir dung samples. However, three were removed from further analysis due to questionable morphology and the presence of horses within the vicinity. We also recorded 9 unique track locations of felids and 20 of tapir. Species locations are shown in Figure 2.

The local perception is that these species are only present in the valley during the wet season, and migrate to higher elevations within Selva Zoque during the dry season. During the wet season, local residents report seeing tracks of all three species, but as the soil turns rigid in the dry season, the tracks are eroded away and no new tracks are created, giving the perception that the animals “leave”. The large quantity of scat and dung samples located during our dry-season survey and the presence of freshly deposited samples are inconsistent with that assumption. Furthermore, fecal material is rapidly recycled by insects and bacteria (Peck and Forsyth 1982; Sanchez et al. 2004), making it unlikely that the samples we located during the dry season were deposited months prior during the wet season. Therefore, we conclude that there is a resident population of all three species in the Uxpanapa valley.

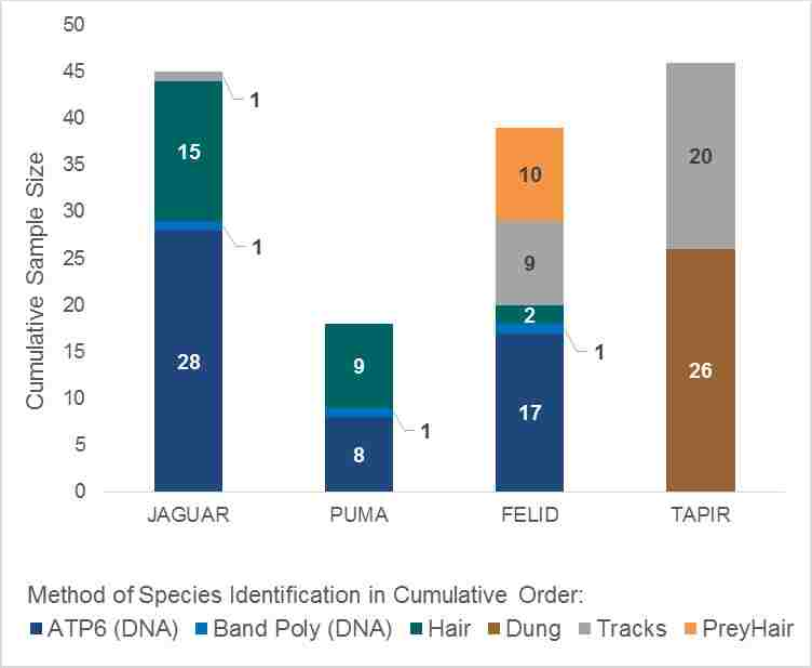

Figure 3. Method of species location ID. Samples were often identified using multiple methods. Numbers here indicate unique locations added by each method, beginning with scat samples identified by ATP6 mtDNA sequencing.

Elevation of scat locations reflected the relatively small range in elevation in the study area, with felid samples generally located below 500m. However, tapir locations had a higher average elevation than did the felid locations (appendix Figure S2). Most samples were found in natural vegetation including various successional stages of secondary forest (appendix Figure S3). Felid scat samples were found in a wider range of vegetation types than tapir dung (Figure 4). Jaguar scat samples were predominantly found in forested vegetation, but forest quality varied from low canopy recovering secondary forest to high-canopy mature forest. One jaguar scat sample was found on an unpaved road, and several were found within corn fields and pasture. Baird's tapir samples were only found in forest, with the majority in mature tall-canopy forest.

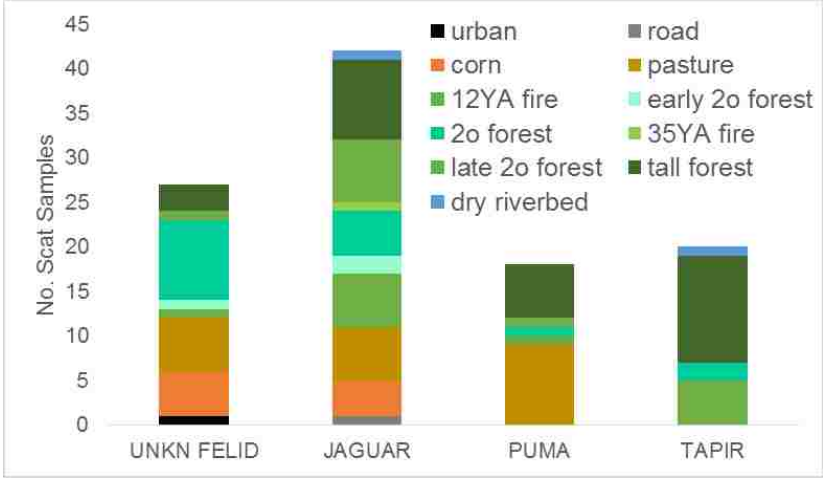

Figure 4. Vegetation identified in the field by confirmed Scat Samples

Resource Selection Results: The optimal scale for the zonal measurement of geographic features varied between metrics and between species. Tapir resource selection was best predicted by zonal covariates measured at the larger geographic scales, either 2.5 km or 5.0 km radius. Within the felid selection models, several scales did equally well for terrain, water, and human impact metrics. However, the top performing vegetation metrics were almost uniformly measured at the smallest scale of a 625 m radius.

Both exponential RSF and logistic RSPF models were included in the final suite of top models ($\Delta BIC < 2$). The top models for all felid locations together (including unknown felid samples) revealed a pattern of selection for rough terrain and tall forest vegetation, with avoidance of roads (Table 2; Figure 5) (appendix Table S3-4). The top jaguar-specific resource selection models share a collection of four variables: positive selection for tall forest and rough terrain (similar to the combined cat models), and avoidance of human-dominated land cover (including pasture, agriculture, or rubber plantations) and villages. The top puma-specific models demonstrate a selection for moderate rather than rough terrain,

and an avoidance of areas with high stream density. The top tapir resource selection models demonstrate a selection for higher elevation and avoidance of roads and human land cover.

Table 2. Top resource selection models (Δ BIC <2). CATS models includes sample locations of unknown felid as well as both jaguar and puma locations. Arrows indicate either positive or negative beta-parameter estimates, suggesting selection or avoidance, respectively. Values in parentheses indicate the spatial scale of the metric (radius around each location).

		MODEL COVARIATES, SYNTAX, AND BETA PARAMETER DIRECITONALITY							
		Terrain		Vegetation		Human Activity		Water	
CATS:	Exponential RSF	↑ITIRough(2.5km)	*	↑TallForest(625m)	+	↓100m RoadBuffer(1.25km)			
	Exponential RSF	↑ITIRough(2.5km)	*	↑TallForest(625m)	+	↓1km RoadBuffer(625m)			
JAGUAR:	Logistic RSPF	↑ITIRough(2.5km)	+	↑TallForest(625m)					
	Logistic RSPF	↑ITIRough(2.5km)	+	↑TallForest(625m) + ↓Human Landcover					
	Exponential RSF	↑ITIRough(2.5km)	*	↓Pasture(625m)	+	↓Villages(5km)			
	Exponential RSF	↑ITIRough(2.5km)	*	↑TallForest(625m)	+	↓Villages(5km)			
	Exponential RSF	↑ITIRough(2.5km)	*	↓Pasture(625m)					
PUMA:	Logistic RSPF	↑ITIModerate(625m)					*	↓StreamDensity(5km)	
	Logistic RSPF	↑ITIModerate(1.25km)					*	↓StreamDensity(2.5km)	
TAPIR:	Logistic RSPF	↑Elevation			+	↓1km RoadBuffer (2.5km)			
	Logistic RSPF	↑Elevation	+	↓Human Landcover	+	↓1km RoadBuffer (2.5km)			

*Human Landcover: 0 = Forest, 1 = Pasture, Human Settlement, or Corn/Rubber Plantations

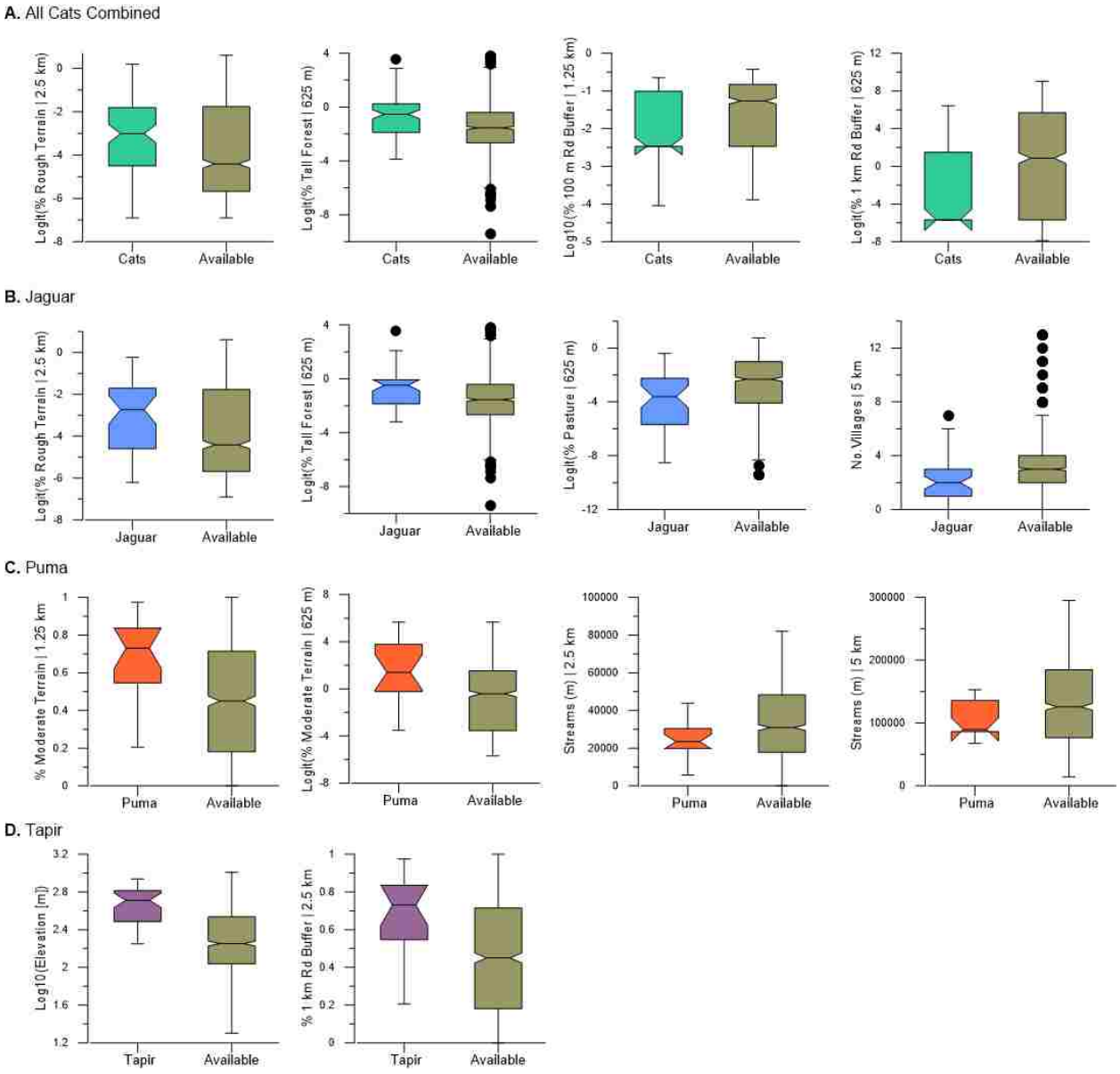

Figure 5. Used and Available notched median-quartile plots for top covariates from resource-selection analyses. Non-overlapping notches between used (species) and Available indicate significant difference between medians. The spatial scale of measurement is indicated after the "|" (e.g. "Streams (m) | 5 km" is the total amount of stream lengths within a 5 km radius around each location).

Connectivity Modeling Results: For jaguar, the small scale of the top covariates and large beta-parameter coefficients in the top resource selection models resulted in a patchy predicted distribution of selected habitat (Figure 6). The areas of high predicted resource selection are composed of rough

terrain and tall forest, with a penalty if there are numerous villages in the vicinity or human land cover. For puma, the larger spatial scale of the top performing covariates and smaller beta-parameter coefficient resulted in a more diffuse predicted habitat. In stark contrast, the magnitude the of the beta-parameter coefficients in the top tapir selection models resulted in a binary landscape of suitable habitat and completely avoided matrix. The lack of a resource selection gradient in the predicted tapir maps precluded further connectivity modeling.

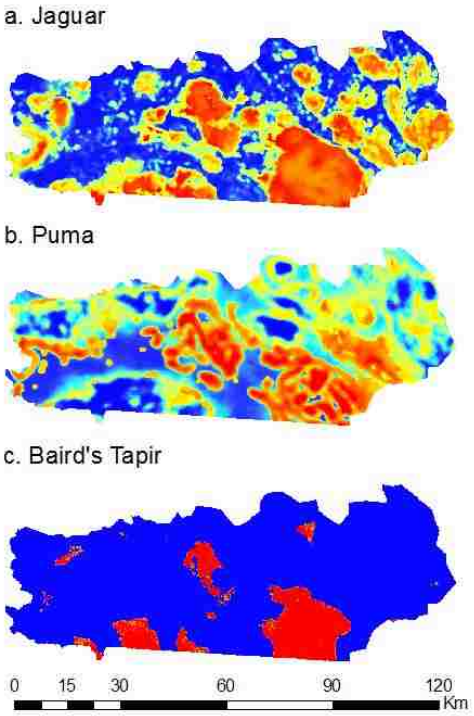

Figure 6. Predicted resource selection, averaged over top resource selection models for each species. Hot colors are higher predicted resource selection, cool colors are lower (colors are stretched equalized over the data histogram).

The predicted resource selection maps were used as conductance grids to model structural connectivity under two scenarios (Figure 7). Under our first scenario, connectivity was modeled as a source-sink dynamic generated by the Selva Zoque (green shaded areas; Figure 7 *left*) with forest fragments (black bolts) as grounds. The location of predicted movement corridors are different between species. For example, both species have corridors in the south-west of the valley span the

single paved, highest trafficked road in the study area. However, the strongest jaguar corridor is further east than for puma. Similarly, the narrow corridors connecting the fragment furthest west (named "Media Luna") differ in location by species. For both species, we identified wide corridors connecting the central forest patches to the eastern Selva Zoque area, and little to no predicted connectivity extending to the forest fragments in the degraded landscape of Chimalapas in the northeast.

Under our second scenario, connectivity was modeled between each forest fragment (outlined in green; Figure 7 *right*). These models reveal an overall difference in the level of connectivity across the study site, reflecting the patchiness of habitat selection. Jaguar resource selection models predicted low selection between forest fragments which resulted in higher resistance to movement between forest fragments in the connectivity model (Figure 8). Conversely, the more diffuse puma resource selection predictions result in a lower movement resistance between forest fragments.

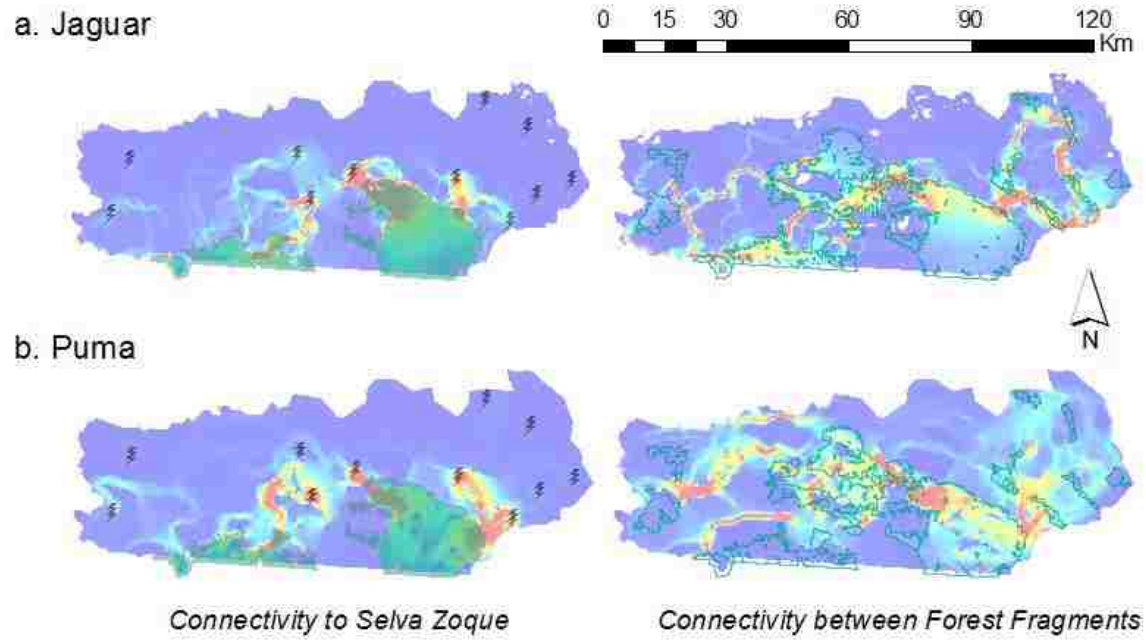

Figure 7. LEFT: Connectivity (current) from southerly Selva Zoque source population (shaded green) to remaining forest fragments sinks (bolts). RIGHT: connectivity between Uxpanapa forest fragments (outlined in green lines). Warm colors = high, cool colors = low (colors are stretched over data standard deviations). .

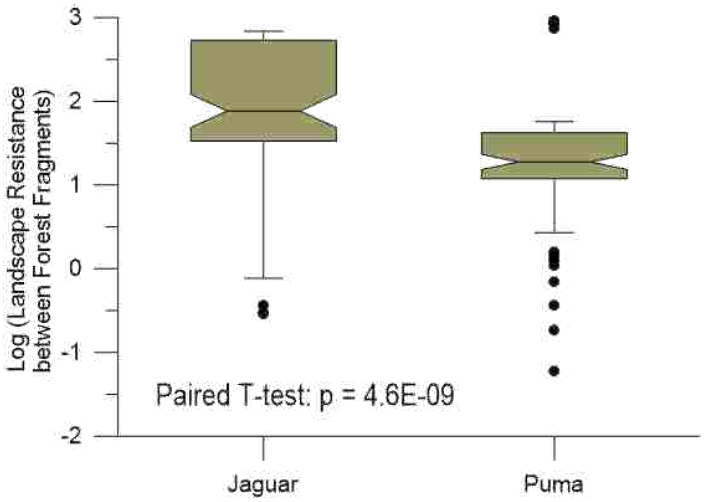

Figure 8. Landscape resistance between forest fragments in Uxpanapa study site.

Connectivity, as modeled by either scenario, appears to be positively correlated with the sample density. Sample density increased with current received from Selva Zoque under the first, source-sink scenario (Figure 9 left). Sample density decreases with resistance between forest fragments under the second scenario (Figure 9 right).

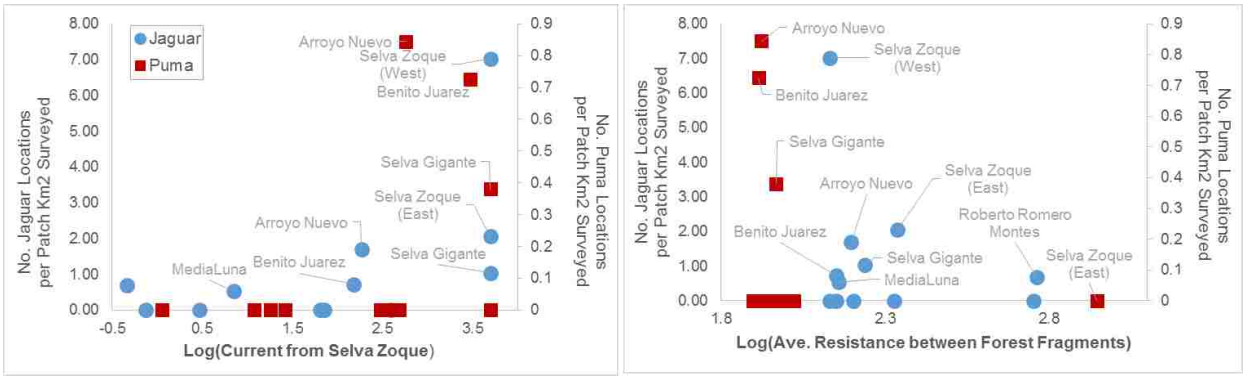

Figure 9. Modeled connectivity influences sample density within survey tracks. Left – Connectivity modeled as current received from Selva Zoque under a source-sink scenario. Right – Connectivity modeled as resistance to patch from other patches.

DISCUSSION:

Our study identifies key differences in landscape use and habitat connectivity between the three large mammal species of Tehuantepec, Mexico. The presence of jaguar samples in both pasture and corn fields suggests that their movements may not be exclusively restricted to forests (Foster, Harmsen, and Doncaster 2010). However, when we compare used locations to availability, we see a clear pattern of selection for rugged terrain covered by tall forest, with some evidence for avoidance of villages. These results confirm the relative forest specialization of this species and sensitivity to human presence. The insuperability of the rugged terrain likely creates a natural fortification preventing expansion of cattle ranchland or human settlement. We were limited in our ability to survey this rough terrain, and it is unknown how or if wildlife populations can be sustained within such areas. Therefore, all areas of tall forest should remain a top conservation priority for jaguar habitat in Uxpanapa.

The endangered Baird's tapir appears to be an extreme forest specialist in this region, avoiding of human activity at large spatial scales. While we are pleased to confirm the presence of Baird's tapir in Uxpanapa, the rate of deforestation in the valley represents a direct threat to their continued presence. This is an especially urgent concern given the predicted lack of structural connectivity to other populations.

The moderately rugged terrain selected for by puma, primarily lays between the flat valley floor, where human activity is highest, and the rugged terrain selected by jaguar. Therefore, selection of moderate terrain may be evidence of simultaneous avoidance of high human activity and of competitive exclusion by jaguars. However, areas of high predicted jaguar resource use were not uniformly avoided by pumas, and close proximity of scat samples from both species reduces the support for spatial avoidance, but does not preclude temporal avoidance. The apparent avoidance of areas of high stream density was an unexpected result, potentially resulting from water avoidance behavior, spatial

avoidance of jaguars in areas with high stream density, undocumented prey distribution, or an artifact of our small number of puma locations.

Jaguar selection for tall forest appears to occur at a spatial scale that is much smaller than a home range, suggesting fine-grain movement behavior. Selection for other features occurred at the scale approximating a female home range. Including multiple scales in resource selection analyses can thus provide insight into movement behavior of a species (Lyra-Jorge et al. 2009; Cudworth and Koprowski 2011). Other movement patterns relevant to conservation include the possible use of linear features by jaguars, as one sample was found on a disused road and another in a dry riverbed. However, results from our combined felid models suggest avoidance of actively-used roads.

Our connectivity models identified that, while both jaguar and puma selection is highest in forest patches, movement corridors in the matrix between patches are in different locations depending on species. For both species, connectivity to the western "Media Luna" forest patch is threatened by the one primary road, and connectivity to the remnant patches in the northeastern portion are threatened by matrix degradation and isolation. Overall, structural connectivity between the remaining forest patches is lower for jaguars than for pumas. For both felid species, the level of connectivity to a forest patch appears to affect the density of species locations within a given patch. Therefore, while habitat protection of forest patches remains important, connectivity through the matrix may also play a significant role in maintaining the populations of jaguars and puma within Uxpanapa.

Our study has highlighted Uxpanapa as a biodiversity hotspot, providing habitat for three species of conservation concern as well as other smaller wild felids. These results speak to the prioritization of Uxpanapa for state and/or federal protection. Road development and deforestation of Uxpanapa are a threat to the species within this critical stepping-stone through Mesoamerica, as well as to the ecosystem services provided to the local communities. We hope our study has provided the information and impetus to invest in the future of the Uxpanapa valley.

ACKNOWLEDGEMENTS:

Centro de Investigaciones Tropicales (CITRO), U.Veracruzana for logistical support and vehicles. Carlos Muñoz-Robles, CITRO, performed the supervised classification of satellite imagery. Primary funding from Fundo-Mixto CONACYT/Gobierno Del Estado de Veracruz de Ignacio De la Llave. Additional funding from the Wingfield-Ramenofski UW Biology Graduate Award and the Katherine Hahn UW-Biology Writing Fellowship. U.Veracruzana students conducted prey hair analysis. We thank the director and staff at Zoologico Miguel Alvarez del Toro, for providing fecal material from captive animals, and the UW Burke Museum of Natural History and Culture, Genetic Resources Collection for tissue samples.

PERMIT INFORMATION:

Wildlife detector dogs were cared for under the *Scat Detection Dog Program* IACUC approved protocol #2850-08. All samples collected from the wild were naturally deposited fecal samples. Sample collection was conducted under the license SGPA/DGVS/07120/09 (22-Oct-09), provided by M.V.Z. Martin Vargas Prieto of the Dirección General de Vida Silvestre (Semarnat). Faecal samples were exported from Mexico to USA under the export licenses MX #49045 (14-Oct-10) and MX #54703 (01-Dic-11) of the Secertaria de Medio Ambiente/CITES.

LITERATURE CITED:

Baca-Ibarra, Itzel I., and Victor Sánchez-Cordero. 2004. “Catálogo de Pelos de Guardia Dorsal En Mamíferos Del Estado de Oaxaca, México.” *Anales Del Instituto de Biologia, Universidad Nacional Autonoma de Mexico*, Serie Zoologia, 75 (2): 383–437.

Beyer, Hawthorne L. n.d. *Geospatial Modeling Environment* (version 0.7.2 RC2). www.spatialecology.com/gme.

Chaves, Paulo B., Vanessa G. Graeff, Marília B. Lion, Larissa R. Oliveira, and Eduardo Eizirik. 2012. “DNA Barcoding Meets Molecular Scatology: Short mtDNA Sequences for Standardized Species Assignment of Carnivore Noninvasive Samples.” *Molecular Ecology Resources* 12 (1): 18–35.

Chazdon, Robin L., Celia A. Harvey, Oliver Komar, Daniel M. Griffith, Bruce G. Ferguson, Miguel Martínez-Ramos, Helda Morales, et al. 2009. “Beyond Reserves: A Research Agenda for Conserving Biodiversity in Human-Modified Tropical Landscapes.” *Biotropica* 41 (2): 142–53.

Clark, Matthew L., T. Mitchell Aide, and George Riner. 2012. “Land Change for All Municipalities in Latin America and the Caribbean Assessed from 250-M MODIS Imagery (2001–2010).” *Remote Sensing of Environment* 126 (November): 84–103.

Cudworth, Nichole L., and John L. Koprowski. 2011. “Importance of Scale in Nest-Site Selection by Arizona Gray Squirrels.” *Journal of Wildlife Management* 75 (7): 1668–74.

De Angelo, Carlos, Agustín Paviolo, and Mario Di Bitetti. 2011. “Differential Impact of Landscape Transformation on Pumas (Puma Concolor) and Jaguars (Panthera Onca) in the Upper Paraná Atlantic Forest.” *Diversity and Distributions* 17 (3): 422–36.

Elbroch, L. Mark, and Heiko U. Wittmer. 2012. “Puma Spatial Ecology in Open Habitats with Aggregate Prey.” *Mammalian Biology* 77 (5): 377–84.

Foster, Rebecca J., Bart J. Harmsen, and C. Patrick Doncaster. 2010. “Habitat Use by Sympatric Jaguars and Pumas Across a Gradient of Human Disturbance in Belize.” *Biotropica* 42 (6): 724–31.

Fragoso, José M. V. 1997. “Tapir-Generated Seed Shadows: Scale-Dependent Patchiness in the Amazon Rain Forest.” *Journal of Ecology* 85 (4): 519–29.

Franklin, Jerry F., and David B. Lindenmayer. 2009. “Importance of Matrix Habitats in Maintaining Biological Diversity.” *Proceedings of the National Academy of Sciences* 106 (2): 349–50.

Goulart, Fernando Vilas Boas, Nilton Carlos Cáceres, Maurício Eduardo Graipel, Marcos Adriano Tortato, Ivo Rohling Ghizoni Jr, and Luiz Gustavo Rodrigues Oliveira-Santos. 2009. “Habitat Selection by Large Mammals in a Southern Brazilian Atlantic Forest.” *Mammalian Biology* 74 (3): 182–90.

Haag, Taiana, Anelisie S. Santos, Carlos De Angelo, Ana Carolina Srbek-Araujo, Dênis A. Sana, Ronaldo G. Morato, Francisco M. Salzano, and Eduardo Eizirik. 2009. “Development and Testing of an Optimized Method for DNA-Based Identification of Jaguar (Panthera Onca) and Puma (Puma Concolor) Faecal Samples for Use in Ecological and Genetic Studies.” *Genetica* 136 (3): 505–12.

Johnson, Douglas H. 1980. “The Comparison of Usage and Availability Measurements for Evaluating Resource Preference.” *Ecology* 61 (1): 65–71.

Juarez, D., C. Estrada, M. Bustamante, Y. Quintana, J. Moreira, and J.E. Lopez. 2010. “Guía Ilustrada de Pelos Para La Identificación de Mamíferos Medianos Y Mayores de Guatemala.” Direccion General de Investigacion (DIGI), Universidad de San Carlos de Guatemala.

Keim, Jonah L., Philip D. DeWitt, and Subhash R. Lele. 2011. “Predators Choose Prey over Prey Habitats: Evidence from a Lynx–hare System.” *Ecological Applications* 21 (4): 1011–16.

Lele, Subhash R., and Jonah L. Keim. 2006. “Weighted Distributions and Estimation of Resource Selection Probability Functions.” *Ecology* 87 (12): 3021–28

Lele, Subhash R., Jonah L. Keim, and Peter Solymos. 2014. *ResourceSelection: Resource Selection (Probability) Functions for Use-Availability Data*.

Lele, Subhash R., Evelyn H. Merrill, Jonah Keim, and Mark S. Boyce. 2013. "Selection, Use, Choice and Occupancy: Clarifying Concepts in Resource Selection Studies." *Journal of Animal Ecology* 82 (6): 1183–91.

Lyra-Jorge, Maria Carolina, Milton Cezar Ribeiro, Giordano Ciocheti, Leandro Reverberi Tambosi, and Vânia Regina Pivello. 2009. "Influence of Multi-Scale Landscape Structure on the Occurrence of Carnivorous Mammals in a Human-Modified Savanna, Brazil." *European Journal of Wildlife Research* 56 (3): 359–68.

McRae, Brad H. 2006. "Isolation by Resistance." *Evolution* 60 (8): 1551–61.

McRae, Brad, Viral Shah, and Tanmay Mohapatra. 2013. *Circuitscape 4 Users Guide* (version 4.0). The Nature Conservancy. http://www.circuitscape.org.

Monroy-Vilchis, Octavio, Clarita Rodríguez-Soto, Martha Zarco-González, and Vicente Urios. 2009. "Cougar and Jaguar Habitat Use and Activity Patterns in Central Mexico." *Animal Biology* 59 (2): 145–57.

Naranjo, Eduardo J. 2009. "Ecology and Conservation of Baird's Tapir in Mexico." *Tropical Conservation Science* 2 (2): 140–58.

Olsoy, Peter J., Kathy A. Zeller, Jeffrey A. Hicke, Howard B. Quigley, Alan R. Rabinowitz, and Daniel H. Thornton. 2016. "Quantifying the Effects of Deforestation and Fragmentation on a Range-Wide Conservation Plan for Jaguars." *Biological Conservation* 203 (November): 8–16.

Owen, Myrfyn. 1972. "Some Factors Affecting Food Intake and Selection in White-Fronted Geese." *Journal of Animal Ecology* 41 (1): 79–92.

Peck, Stewart B., and Adrian Forsyth. 1982. “Composition, Structure, and Competitive Behaviour in a Guild of Ecuadorian Rain Forest Dung Beetles (Coleoptera; Scarabaeidae).” *Canadian Journal of Zoology* 60 (7): 1624–34.

Petracca, Lisanne S., Sandra Hernández-Potosme, Lenin Obando-Sampson, Roberto Salom-Pérez, Howard Quigley, and Hugh S. Robinson. 2014. “Agricultural Encroachment and Lack of Enforcement Threaten Connectivity of Range-Wide Jaguar (Panthera Onca) Corridor.” *Journal for Nature Conservation* 22 (5): 436–44.

Rabinowitz, Alan, and Kathy A. Zeller. 2010. “A Range-Wide Model of Landscape Connectivity and Conservation for the Jaguar, Panthera Onca.” *Biological Conservation* 143 (4): 939–45.

Riley, Shawn J., Stephen D. DeGloria, and Robert Elliot. 1999. “A Terrain Ruggedness Index That Quantifies Topographic Heterogeneity.” *Intermountain Journal of Sciences* 5 (1–4): 23–27.

Rodríguez-Soto, Clarita, Octavio Monroy-Vilchis, Luigi Maiorano, Luigi Boitani, Juan Carlos Faller, Miguel Á. Briones, Rodrigo Núñez, Octavio Rosas-Rosas, Gerardo Ceballos, and Alessandra Falcucci. 2011. “Predicting Potential Distribution of the Jaguar (Panthera Onca) in Mexico: Identification of Priority Areas for Conservation.” *Diversity and Distributions* 17 (2): 350–61.

Sanchez, Dana M., Paul R. Krausman, Troy R. Livingston, and Philip S. Gipson. 2004. “Persistence of Carnivore Scat in the Sonoran Desert.” *Wildlife Society Bulletin* 32 (2): 366–72.

Sanderson, Eric W., Kent H. Redford, Cheryl-Lesley B. Chetkiewicz, Rodrigo A. Medellin, Alan R. Rabinowitz, John G. Robinson, and Andrew B. Taber. 2002. “Planning to Save a Species: The Jaguar as a Model.” *Conservation Biology* 16 (1): 58–72.

Sandoval-Mendoza, Juana B., Anibal F. Ramirez-Soto, Ixchel M. Shesena-Hernandez, Carlo Sormani, Fortunato Ruiz-DeLaMerced, Daniel Jarvio-Arellano, and Eder Farid-Mora. 2007. “Evaluacion Del

Estado de Conservacion de Los Ecosistemas Forestales de La Region Denominada Uxpanapa 2006-2007." SEDARPA & ProNatura asociacion civil.

Stoner, David C., Michael L. Wolfe, Clint Mecham, McLain B. Mecham, Susan L. Durham, and David M. Choate. 2013. "Dispersal Behaviour of a Polygynous Carnivore: Do Cougars Puma Concolor Follow Source-Sink Predictions?" *Wildlife Biology* 19 (3): 289–301.

Terborgh, John. 1992. "Maintenance of Diversity in Tropical Forests." *Biotropica* 24 (2): 283–92.

Terborgh, John, Lawrence Lopez, Percy Nuñez, Madhu Rao, Ghazala Shahabuddin, Gabriela Orihuela, Mailen Riveros, et al. 2001. "Ecological Meltdown in Predator-Free Forest Fragments." *Science* 294 (5548): 1923–26.

Vynne, C., M. R. Baker, Z. K. Breuer, and S. K. Wasser. 2012. "Factors Influencing Degradation of DNA and Hormones in Maned Wolf Scat." *Animal Conservation* 15 (2): 184–94.

Vynne, Carly, Jonah L. Keim, Ricardo B. Machado, Jader Marinho-Filho, Leandro Silveira, Martha J. Groom, and Samuel K. Wasser. 2011. "Resource Selection and Its Implications for Wide-Ranging Mammals of the Brazilian Cerrado." *PLoS ONE* 6 (12): 1–12.

Vynne, Carly, John R. Skalski, Ricardo B. Machado, Martha J. Groom, Anah T. A. Jácomo, Jader Marinho-Filho, Mario B. Ramos Neto, et al. 2011. "Effectiveness of Scat-Detection Dogs in Determining Species Presence in a Tropical Savanna Landscape." *Conservation Biology* 25 (1): 154–62.

Wasser, S. K., C. S. Houston, G. M. Koehler, G. G. Cadd, and S. R. Fain. 1997. "Techniques for Application of Faecal DNA Methods to Field Studies of Ursids." *Molecular Ecology* 6 (11): 1091–97.

Wasser, Samuel K., Lisa S. Hayward, Jennifer Hartman, Rebecca K. Booth, Kristin Broms, Jodi Berg, Elizabeth Seely, Lyle Lewis, and Heath Smith. 2012. "Using Detection Dogs to Conduct

Simultaneous Surveys of Northern Spotted (Strix Occidentalis Caurina) and Barred Owls (Strix Varia).” *PLoS ONE* 7 (8): e42892.

Woodroffe, Rosie, and Joshua R. Ginsberg. 1998. “Edge Effects and the Extinction of Populations Inside Protected Areas.” *Science* 280 (5372): 2126–28.

Zeller, Kathy. 2007. “Jaguars in the New Millennium. Data Set Update: The State of the Jaguar in 2006. WCS Report.” *Wildlife Conservation Society, New York*, 1–82.

SUPPLEMENTARY TABLES AND FIGURES:

Table S1. Sources of Geographic Information

Geographic Data Layer	Source	Provider
Digital Elevation Model:	Shuttle Radar Topography Mission (STRM) 3 Arc Second (~90 m)	NASA & NGA (National Geospatial-Intelligence Agency)
Roads:	Capa de Datos - Vias de comunicacion	INEGI (Instituto Nacional de Estadistica y Geografia
Villages:	Capa de Datos - Toponimos (INTR_VILL)	INEGI (Instituto Nacional de Estadistica y Geografia
Streams:	Capa de Datos - Hidrografico	INEGI (Instituto Nacional de Estadistica y Geografia
Rivers:	Digital Chart of the World	DIVA-GIS

Table S2. Type of Data Transformation for each geographic covariate. No transformation necessary (black), Logit transformation (orange), Log10 transformation (green), SQRT transformation (blue), unusable metric due to skewness (grey)

Human Activity	Distance to Nearest	Within 625m Radius	Within 1.25km Radius	Within 2.5km Radius	Within 5km Radius
(17 metrics)	Village	Number of Villages	Number of Villages	Number of Villages	Number of Villages
	Road	% 100m Road Buffer	% 100m Road Buffer	% 100m Road Buffer	% 100m Road Buffer
	Primary Road	% 1km Road Buffer	% 1km Road Buffer	% 1km Road Buffer	% 1km Road Buffer
	Secondary Road				
	Tertiary Road				
Water	Distance to Nearest	Within 625m Radius	Within 1.25km Radius	Within 2.5km Radius	Within 5km Radius
(15 metrics)	River	Total meters of Streams	Total meters of Streams	Total meters of Streams	Total meters of Streams
	Stream	% 1km River Buffer	% 1km River Buffer	% 1km River Buffer	% 1km River Buffer
		% 5km River Buffer	% 5km River Buffer	% 5km River Buffer	% 5km River Buffer
					% 10km River Buffer
Vegetation	Value at Location	Within 625m Radius	Within 1.25km Radius	Within 2.5km Radius	Within 5km Radius
(31 metrics)	VegClass (HC,P,CR,SF,TF)	% Human Settlement (HC)	% Human Settlement (HC)	% Human Settlement (HC)	% Human Settlement (HC)
	VegForestClass (SF, TF, or AH)	% Pasture (P)	% Pasture (P)	% Pasture (P)	% Pasture (P)
	VegSimple (Forest/Human)	% Citrus or Rubber (CR)	% Citrus or Rubber (CR)	% Citrus or Rubber (CR)	% Citrus or Rubber (CR)
		% All Human (HC+P+CR)	% All Human (HC+P+CR)	% All Human (HC+P+CR)	% All Human (HC+P+CR)
		% Secondary Forest (SF)	% Secondary Forest (SF)	% Secondary Forest (SF)	% Secondary Forest (SF)
		% Tall Forest (TF)	% Tall Forest (TF)	% Tall Forest (TF)	% Tall Forest (TF)
		% All Forest (SF+TF)	% All Forest (SF+TF)	% All Forest (SF+TF)	% All Forest (SF+TF)
Terrain	Value at Location	Within 625m Radius	Within 1.25km Radius	Within 2.5km Radius	Within 5km Radius
(14 metrics)	ITI Class (Flat, Moderate, Rough)	% Flat ITI	% Flat ITI	% Flat ITI	% Flat ITI
	Elevation (DEM)	% Moderate ITI	% Moderate ITI	% Moderate ITI	% Moderate ITI
		% Rough ITI	% Rough ITI	% Rough ITI	% Rough ITI

Table S3. Model Selection using Information Criteria (BIC). Top models for each species, using logistic Resource Selection Probability Function (RSPF) and exponential Resource Selection Function (RSF). Delta BIC was calculated across both RSPF and RSF models.

	Resource Selection Probability Function					Resource Selection Function				
	ID		df	BIC	delta	ID		df	BIC	deltaBIC
CATS	m228e	ITIBigRough*VegSmallTF+RdMedium100	5	1364.294	4.625	m228e	ITIBigRough*VegSmallTF+RdMedium100	4	1359.669	0.000
	m228f	ITIBigRough*VegSmallTF+RdSmallOne	5	1364.479	4.810	m228f	ITIBigRough*VegSmallTF+RdSmallOne	4	1359.854	0.185
	m228	ITIBigRough*VegSmallTF	4	1367.971	8.302	m228	ITIBigRough*VegSmallTF	3	1363.346	3.677
	m227	ITIBigRough*VegMediumAH	4	1370.691	11.022	m228c	ITIBigRough*VegSmallTF+VegSimple	4	1366.520	6.851
	m028	ITIBigRough+VegSmallTF	3	1371.096	11.427	m228g	ITIBigRough*VegSmallTF*RdMedium100	7	1368.700	9.031
JAGUAR	m011	ITIBigRough+VegSmallTF	3	604.238	0.287	m210b	ITIBigRough*VegSmallP+VillageGiant	4	603.951	0.000
	m011c	ITIBigRough+VegSmallTF+VegSimple	4	604.575	0.625	m211b	ITIBigRough*VegSmallTF+VillageGiant	4	605.743	1.792
	m071	VegMediumW + VegSmallTF	3	606.261	2.311	m210	ITIBigRough*VegSmallP	3	605.811	1.860
	m268	VegGiantW*VegSmallTF	4	606.480	2.529	m211	ITIBigRough*VegSmallTF	3	606.842	2.891
	m211b	ITIBigRough*VegSmallTF+VillageGiant	5	607.013	3.062	m211e	ITIBigRough*VegSmallTF+VegForestClass	5	607.984	4.033
PUMA	m233	ITISmallMod*RiosGiant	4	227.254	0.000	m112	ITIMediumMod+RiosBig+RdSmallOne	3	231.195	3.941
	m221	ITIMediumMod*RiosBig	4	229.118	1.864	m110	ITIMediumMod+RiosGiant+RdSmallOne	3	231.734	4.480
	m311	ITIMediumMod*RiosBig+RdMedium100	5	231.057	3.802	m111	ITIMediumMod+RiosBig+RdMedium100	3	231.943	4.688
	m235	ITISmallMod*VegGiantP	4	231.494	4.240	m109	ITIMediumMod+RiosGiant+RdMedium100	3	232.372	5.117
	m224	ITIMediumMod*VegGiantP	4	231.892	4.638	m307	ITIMediumMod*RiosBig+RdSmallOne	4	232.393	5.139
TAPIR	m002	DEM+RdBigOne	3	430.424	0.000	m102	RdSecondaryDist*VegGiantHC	4	439.592	9.168
	m002c	DEM+RdBigOne+VegSimple	4	431.147	0.723	m103	RdGiantOne*VegGiantHC	3	440.341	9.917
	m104	RdMediumOne*VegGiantHC	4	433.453	3.029	m109	RdMediumOne*VegGiantP	3	441.014	10.590

Table S4. Top resource selection models (ΔBIC<2)

	Model Form	Model Equation with Beta-Parameter Estimates
CATS	Exponential RSF	Exp((-0.19232 ITIBigRough)+(-0.35293 VegSmallTF)+(-0.41881 RdMedium100)+(-0.20467 ITIBigRough* VegSmallTF))
	Exponential RSF	Exp((-0.18444 ITIBigRough)+(-0.35543 VegSmallTF)+(-0.7001 RdSmallOne)+(-0.20137 ITIBigRough*VegSmallTF))
JAGUAR	Logistic RSPF	Exp(11.031+(1.336 ITIBigRough)+(2.409* VegSmallTF)) / (1+(Exp(11.031+(1.336 ITIBigRough)+(2.409 VegSmallTF)))
	Logistic RSPF	Exp(11.488+(1.432 ITIBigRough)+(2.066 VegSmallTF)+(-2.408 VegSimple)) / (1+(Exp(11.488+(1.432 ITIBigRough)+(2.066 VegSmallTF)+(-2.408 VegSimple)))
	Exponential RSF	Exp((0.50944 ITIBigRough)+(0.21254 VegSmallP)+(-0.22685 VillageGiant)+(0.14317 ITIBigRough*VegSmallP)))
	Exponential RSF	Exp((-0.21708 ITIBigRough)+(-0.31007* VegSmallTF)+(-0.21110 VillageGiant)+(-0.20721 ITIBigRough* VegSmallTF))
	Exponential RSF	Exp((0.57952 ITIBigRough)+(0.19129 VegSmallP)+(0.13849 ITIBigRough* VegSmallP))
PUMA	Logistic RSPF	Exp(0.0002143+(0.004017 ITISmallMod)+(-0.1450 RiosGiant)+(-0.02129 RiosGiant*ITISmallMod)) / (1+(Exp(0.0002143+(0.004017 ITISmallMod)+(-0.1450 RiosGiant)+(-0.02129 RiosGiant* ITISmallMod)))
	Logistic RSPF	Exp(-6.924+(20.72 ITIMediumMod)+(-0.00009328 RiosBig)+(0.0004505 ITIMediumMod*RiosBig)) / (1+(Exp(-6.924+(20.72 ITIMediumMod)+(-0.00009328 RiosBig)+(0.0004505 ITIMediumMod* RiosBig)))
TAPIR	Logistic RSPF	Exp(-18819.2+(8818.2 DEM)+(-245.9 RdBigOne)) / (1+(Exp(-18819.2+(8818.2 DEM)+(-245.9 RdBigOne)))
	Logistic RSPF	Exp(-7175.14+(3341.54 DEM)+(-80.22 RdBigOne)) +(-3473.08 Human Landcover)) / (1+Exp(-7175.14+(3341.54 DEM)+(-80.22 RdBigOne)) +(-3473.08 Human Landcover)))

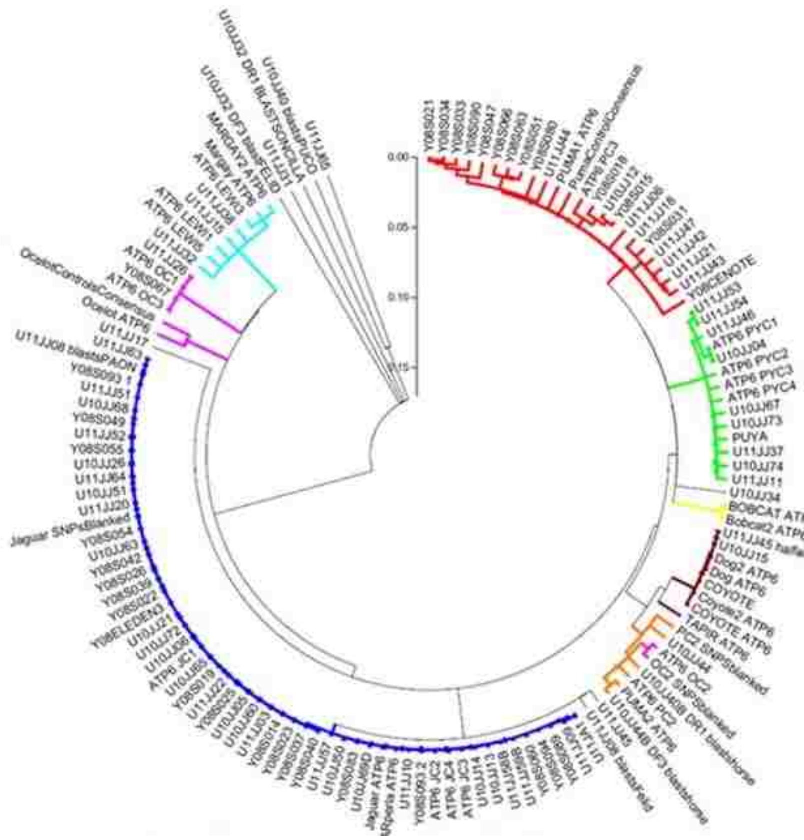

Figure S1. Neighbor-joining phylogenetic relationship of samples and control sequences, based on ATP6 mtDNA (~176bp). Samples from field begin with either "U" (Uxpanapa) or "Y" (Quintana Roo), while reference samples begin with either "ATP6" or common name. Dark blue = jaguar, red = puma, green = jaguarondi, teal = margay, pink = ocelot, yellow = bobcat controls, brown = canids, orange = unknown.

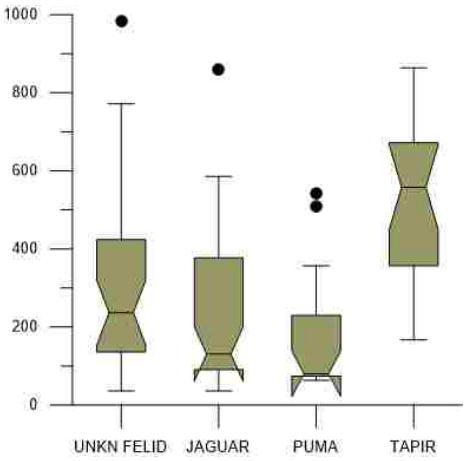

Figure S2. Elevation of confirmed scat samples as measured by field GPS

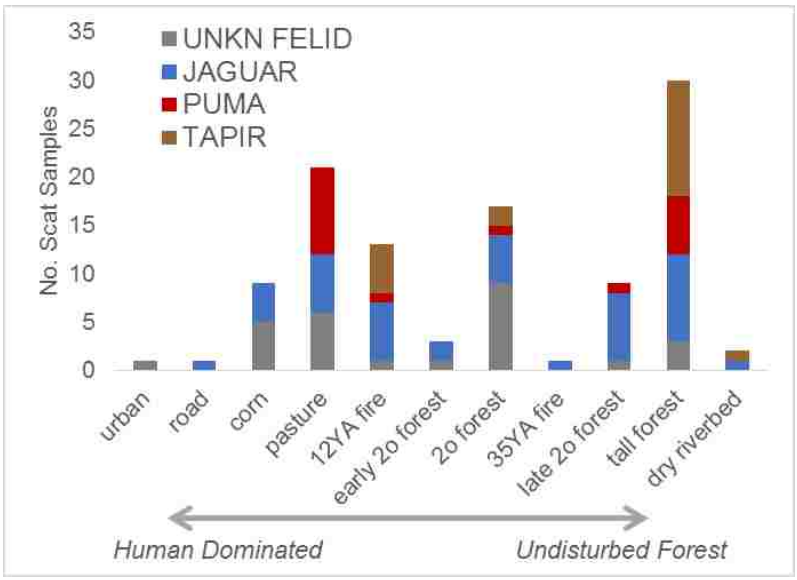

Figure S3. Confirmed Scat Samples ID in each Vegetation Class identified in the Field

SUPPLEMENTARY TEXT:

Text S1. Navigating "roughness" metrics: The path to analyzing terrain roughness (unevenness, texture, rugosity, surface relief, ruggedness, etc.) can be, well, rocky. The "roughness" ArcGIS tool calculates the neighborhood elevation variance. If elevational variance does not capture the pattern of roughness of interest, there are many other options for evaluating terrain unevenness, nicely summarized in "Terrain Roughness – 13 ways" at S. Cooley's blog, *GIS 4 Geomorphology*. Different metrics will perform better for different goals, levels of elevational relief, and spatial extents.

Of the numerous available metrics, Riley's Terrain Ruggedness Index (TRI) is widely used in the literature (Riley, DeGloria, and Elliot 1999). The appeal of Riley's TRI is its calculation simplicity and a perception that it creates a standardized classification system. However, the goal of standardization is undermined by ambiguity in the original paper. Many people are misled to average the squared differences before taking the square root [equation here] rather than taking the sum [equation here]. This will give you very different values. Moreover, neither of these formulas produce the values of worked example within the manuscript, adding to the confusion because users cannot check their understanding of the equation. Elsewhere you can find "Riley's TRI" cited as a neighborhood min and max [SquareRoot(Abs((Square("3x3max") – Square("3x3min"))))], other equations, or without specific equations listed. Therefore, it is hard to consider TRI as a standardized "index" across studies, especially when specific equations used are not supplied.

For the purposes of evaluating resource selection of jaguars and pumas within the Uxpanapa valley, Veracruz, we needed to capture the ruggedness difference observed in two areas. One is exposed karstic limestone and extremely jagged and pitted, and the other has steep ridges, but the slopes are relatively smooth. Using a 3 arc second DEM (~90m2 pixels), neither Riley's TRI nor any of the other metrics available successfully captured the terrain difference between these locations. Surface

Relief Ratio (SRR) did capture the heterogeneity within the study area. However, upon scaling up to southern Mexico, there were areas that were flat, but with high SRR. Therefore, I produced a new metric, Insuperable Terrain Index (ITI) as SRR|slope>30 to capture areas that are impassable due to combined steepness and jaggedness.

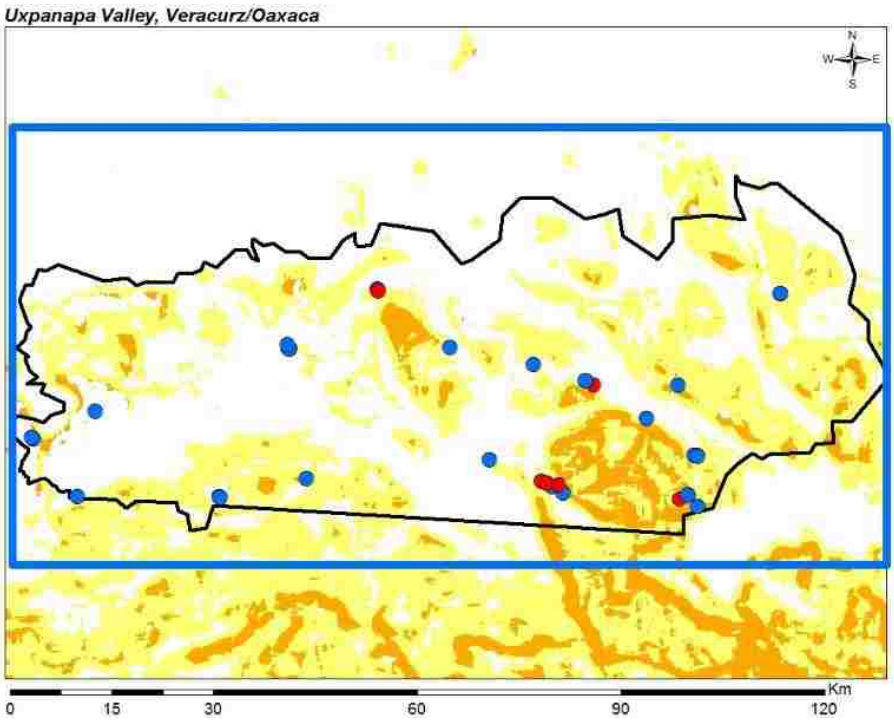

Text S1 Figure 1. Novel ruggedness metric: Insuperable Terrain Index (ITI). Rough (orange) areas were very steep and jagged, primarily composed of exposed karstic limestone. Moderate terrain (yellow) included rolling to steep hills, but lacked the impassable limestone. Flat terrain (white) dominated the valley floor. Locations of confirmed jaguar (blue dots) and puma (red dots).

Text S2. Considerations of Scale in Resource Selection:

Selection of landscape features by wildlife can be exercised at different spatial scales (Owen 1972). In 1980, Johnson formalized this idea into the following hierarchy: First Order = species range, Second-order = individual home-range, Third order = Usage of habitat (e.g. feeding site), Fourth order = Where actions contribute to reproduction (e.g. procurement of food).

Evaluating geographic features at point locations, or distance to nearest feature, may fail to capture the nature of the geographic feature. For example, sampling the nearest road does not necessarily capture information regarding the density of roads. Similarly, taking a land cover value at a point fails to capture the amount of that land cover in the vicinity. Therefore, given the distribution of a given geographic feature, it may be best quantified within zones around identified locations. But, how big should these zones be? A common approach is to use the average home range size of the study species, as it is a biologically justifiable and often reported in the literature. This second-order scale seems appropriate for assessing habitat capacity or delineating population boundaries. However, the resource-selection analysis explicitly assess third-order scale behavior, the probability of use of a location with given characteristics if that location is encountered. This third-order spatial scale is suitable for addressing questions such as wildlife interaction with human-dominated land cover or movement connectivity. Using larger scale sizes may fail to capture the importance of a given landscape variable at smaller scales.

In our study of resource selection, we examined a geometric progression of zonal scales around our sample locations. The larger two zone sizes approximate male and female jaguar home range size, and the smaller two were decreased by a factor of 0.5 from there. We found evidence of the importance of scale in several of our geographic metrics. Below, we show an example of where, at the largest scale, there is no discernable difference in the density of observations (in this case, the % forest

within the zone) between the used (scat sample) versus available locations. However, at smaller zone sizes, a pattern of selection for higher % forest cover becomes evident. The importance forest would have been missed if we had only evaluated this metric at a home-range scale.

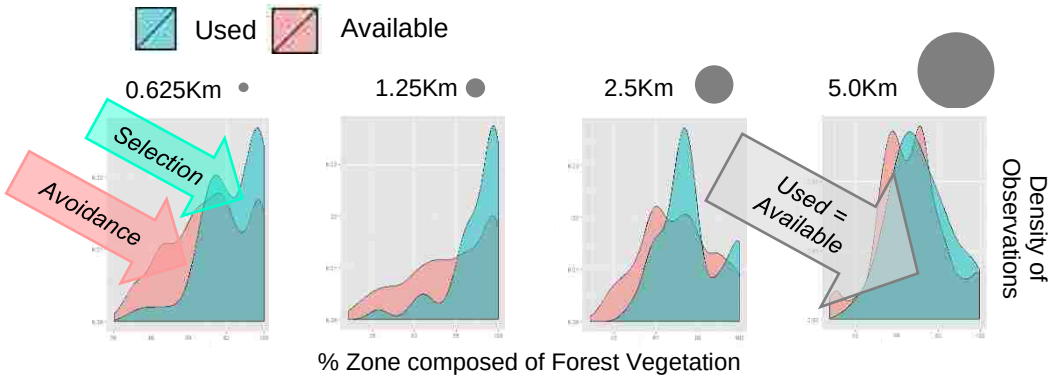

Text S2 - Figure 1. Resource selection of a single geographic variable at four spatial scales ranging from 0.625 m to 5 km radius around each used (scat samples) or available (randomly generated locations within surveyed area) location. The pattern of selection for high forest cover (left) is lost at larger spatial scales (right).

CHAPTER 2: Effects of Deforestation on Gene flow in Jaguars (*Panthera onca*) and Pumas (*Puma concolor*) in the Isthmus of Tehuantepec, Filling in Gaps of the Mesoamerican Puzzle.

Jennifer M.W. Day[1]*, Brenda Solorzano[2], Samuel K. Wasser[1]

[1] Center for Conservation Biology, Department of Biology, University of Washington, Seattle, USA

[2] Universidad Autonoma, Mexico City, Mexico

ABSTRACT:

The Isthmus of Tehuantepec in southern Mexico is a biogeographic link between North and Central American populations of both jaguars and pumas. Little is known about the demographic status or the genetic diversity of the putative populations within the isthmus. Our study fills this gap in our knowledge regarding the genetic diversity of jaguar and puma in central Tehuantepec, while examining whether gene flow has been restricted by deforestation within the Uxpanapa valley, Veracruz. Additionally, we compare regional gene flow for jaguar to regional gene flow for puma by examining the level of genetic differentiation between Uxpanapa and northern Quintana Roo, Mexico.

We collected noninvasive genetic samples with the aid of wildlife detection dogs, in Uxpanapa (UX) (4,775 km^2) and northern Quintana Roo (QR) (4,202 km^2). We identified 7 individual jaguars and 5 pumas in Uxpanapa, and 9 jaguars and 6 pumas in Quintana Roo, using 10 nuclear microsatellite markers. These results refute the notion that jaguars have been extirpated from Uxpanapa. Individual-based analysis of gene flow within Uxpanapa did not find significant relationships between landscape resistance and relatedness between individuals for either species, suggesting that deforestation has not limited gene flow between forest patches at this small scale. Genetic diversity estimates for jaguars (Ar = 3.81 UX, 3.21 QR, He = 0.63 UX, 0.58 QR, Ho = 0.72 UX, 0.62 QR) fall within published ranges from the surrounding areas, suggesting that the deforestation over the past 50-100 years has not resulted in a reduction of genetic diversity to date. At the regional scale, we found less genetic differentiation between the jaguars of Uxpanapa and northern Quintana Roo (Fst = 0.0719) as compared to the sympatric pumas (Fst = 0.1770). Our data support an emerging pattern at the species-range scale, of lower genetic diversity in Mexican populations of jaguars than in Central or South America.

Our study suggests that gene flow of both species persists through the non-forest matrix at the local level (within Uxpanapa), but is greater for jaguars than for puma at the regional level (between

locations). The drivers producing greater gene flow in jaguars as compared to sympatric puma populations, remain unclear. Our results highlight the importance of the Uxpanapa valley as a stepping-stone for gene flow through the Isthmus of Tehuantepec for both species. Preserving large-scale gene flow of these highly vagile large carnivores is a key component of their species conservation.

INTRODUCTION:

The Isthmus of Tehuantepec is a critical movement corridor between Central and North American wildlife populations. Tehuantepec is at the center of the Mesoamerican global biodiversity hotspot (Myers et al. 2000) and is at the northern most extent of the Mesoamerican Biological Corridor (MBC). Wildlife populations within this region have the potential to serve as connectivity stepping stones between the MBC and populations in central-northern Mexico. There is a paucity of demographic or genetic data for the two top carnivores in this region, jaguar (*Panthera onca*) and puma (*Puma concolor*) (Zeller 2007; Zanin et al. 2016; Wultsch et al. 2016). The two most comprehensive studies of Mesoamerican jaguar genetic population structure and diversity to date, both published this year, highlight the need for data from Tehuantepec. Wultsch et al. (2016b) report seven jaguars genotyped in Mexico, and only a portion of those were from a site within the isthmus (Sierra Mixe, Oaxaca). Zanin et al. (2016) successfully genotyped 22 puma in Tehuantepec, but only one jaguar.

The overarching goal of this project is to investigate potential impacts of deforestation on gene flow at multiple spatial scales, while filling in our knowledge gap for jaguars and pumas in Tehuantepec. We used wildlife detection dogs to aid in the collection of noninvasive genetic samples at two study sites, and we genotyped samples using 10 microsatellite loci.

Our two study sites are the Uxpanapa valley, Veracruz, in central Tehuantepec, and northern Quintana Roo in the Yucatan Peninsula (Figure 1). Uxpanapa is one of Veracruz's last remaining biological hotspots, laying across the northern edge of the Selva Zoque, a large swath of dense jungle and steep cliffs that makes up the bulk of the *Isthmus of Tehuantepec Jaguar Conservation Unit* (JCU) (Sanderson et al. 2002). Until now, it was unknown if these large Neotropical felids have been extirpated from Uxpanapa (Sandoval-Mendoza et al. 2007) despite potential sightings and tracks reported by local residents. Our first study objective is to ascertain if jaguars and puma have been extirpated from the valley, by determining the number of unique individuals represented in our

noninvasive scat samples, and identification of any genetic recaptures (matching genotypes) using nuclear microsatellite genotyping. We also measure the geographic distance between recaptures of the same individuals, providing a limited estimate of movement distances.

Uxpanapa has undergone intensive land conversion from forest to agriculture and pasture within the past 100-50 years (Gomez-Irving, Edward A., and Gomez-Cesar A. 2011; Sandoval-Mendoza et al. 2007) and deforestation continues today. It is unknown if jaguars and pumas are able to disperse between the remnant forest patches which are separated by 7-20 km of intervening non-habitat matrix (Day et al. *this dissertation Chapter 1*), or if this isolation has been in place for a long enough period of time to impact gene flow between forest patches, despite the generational lag-time (Epps and Keyghobadi 2015). Our second study objective addresses this question by using an individual-based analysis to determine if genetic relatedness is associated with landscape resistance within the Uxpanapa valley.

Deforestation within and surrounding Uxpanapa/Selva Zoque may also have resulted in reduced population genetic diversity (allelic richness and heterozygosity) as compared to other sites in Mesoamerica. To address this third objective, we collected and genotyped noninvasive samples in northern Quintana Roo for comparison to Uxpanapa. The Quintana Roo study site is approximately 1,000 km to the northeast of Uxpanapa, and has greater purported habitat connectivity to the rest of the species' ranges (Rabinowitz and Zeller 2010).

In additional to investigating fine-scale gene flow within Uxpanapa, we were interested in how movement ecology at fine scales, such as resource use, scale-up to broader-scale processes, such as gene flow. If we make the assumption that intrinsic dispersal ability is comparable between species (there is a void of information regarding dispersal capacity of jaguar), then realized dispersal distance will depend on the interaction of movement behavior and landscape pattern. Jaguars are considered to be more selective of forest habitat and less tolerant of human activity as compared to puma (Day et al.

this dissertation Chapter 1; Sunquist and Sunquist 2002). If we scale up local resource selection to the regional level, there are two alternate predictions: P1) habitat selectivity of jaguars influences the search for suitable territory, leading to greater gene flow between populations due to prolonged searches, as compared to sympatric puma populations, or P2) habitat selectivity of jaguars impacts dispersal behavior, leading to less gene flow between populations due to dispersal restriction, as compared to sympatric puma populations.

Previous studies provide conflicting evidence regarding the relative amount of gene flow between sympatric jaguar and puma populations. In support of P1 (jaguar gene flow > puma gene flow), previous range-wide analysis of jaguar population structure found little evidence of genetic structuring (Eizirik et al. 2001). In contrast, within the same spatial extent, there are eight genetically distinct puma sub-species (Culver et al. 2000). Additionally, within Belize, puma populations are more genetically distinct from each other than sympatric jaguar populations (Wultsch, Waits, and Kelly 2016) and within the Yucatan Peninsula, there is evidence for more sub-populations of puma than jaguar (Zanin et al. 2016). In support of P2 (jaguar gene flow < puma gene flow) recent studies have refuted genetic panmixia of Mesoamerican jaguars (Wultsch et al. 2016), and found greater genetic isolation of jaguars in western Mexico than sympatric pumas (Zanin et al. 2016). Our fourth objective was to investigate whether gene flow at the regional level (Mesoamerica) is more restricted for jaguars versus puma by comparing indirect metrics of gene flow (e.g. genetic distance between sampling localities, and partitioning of genetic variance within and among sampling localities) between Uxpanapa and Quintana Roo, adding a valuable data point to the existing literature on species differences in gene flow.

In summary, this study uses noninvasive genetic sample collection and microsatellite genotyping for four specific objectives: (1) Assess the potential for a resident population of each species in Uxpanapa, by determining the number of unique individuals represented in our noninvasive sample collection and presence of recaptures. (2) Evaluate genetic connectivity between the forest fragments

within Uxpanapa using individual-based analysis of gene flow. (3) Determine if isolation of the Uxpanapa valley has impacted jaguar and puma population genetic diversity relative to northern Quintana Roo. (4) Compare the level of gene flow between Uxpanapa and Quintana Roo locations, for jaguar versus puma.

METHODS

Field Collection of Noninvasive Samples: The Uxpanapa valley study area (UX) is approximately 4,775km^2 (Figure 1). Uxpanapa consists of a mosaic of land cover, dominated by pasture (26%) and secondary forest (38%), with smaller portions consisting of small corn plantations and rubber tree cultivations (15%), remnant mature tall canopy forest (16%), and village settlements (5%). The 4,202km^2 study site in northern Quintana Roo study site (QR) is dominated by low-canopy secondary forest, interspersed with ranchland and urban developments. Sample collection surveys were conducted in the spring 2008 (QR), 2010 (UX- western half), and 2011 (UX – eastern half and revisits to the western half). Scat samples were found with the aid of wildlife scat detection dogs from the University of Washington Conservation Canines (CK9) program. A portion of each scat sample was collected in sterile plastic cups containing silica desiccation beads separated from the sample by filter paper (3:1 ratio of silica beads to scat volume). Previous molecular scatology studies caution against culling samples based on visual appearance, because visual appearance does not always indicate DNA quality (White 2010). Therefore, all samples were collected, regardless of the degradation appearance. Whenever possible, a portion of the sample was left in the field to minimize disruption of territorial marking behavior. In Uxpanapa, each scat sample was swabbed for epithelial cells using sterile cotton swabs soaked in PBS buffer, immediately upon returning to the field station each day. Swabs were stored in 1.5mL tubes with Qiagen ATL lysis buffer, and kept frozen for further DNA extraction and amplification via polymerase chain reaction (PCR). The remaining fecal material was kept refrigerated (4°C), and later freeze-dried for

long-term preservation. In Quintana Roo, fecal samples were immediately frozen (-20°C) in 2008, and were swabbed for epithelial cells two years later (2010) following unsuccessful DNA amplification by a laboratory in Mexico.

Laboratory Analysis: Scat samples were identified as either jaguar or puma by sequencing the ATP6 region of mitochondrial DNA (mtDNA) (Day et al. *this dissertation Chapter 1*). Only samples that were confirmed to species were further processed for nuclear markers, as it is unlikely that nuclear DNA will amplify if the significantly more abundant mtDNA fails to amplify. All DNA extracts were done in duplicate, with epithelial samples taken from different areas along the scat surface, to account for uneven distribution of DNA in feces. DNA extraction was done using the Qiagen Tissue kit (Qiagen, Inc., Valencia, CA). Jaguar and puma samples were genotyped at 10 unlinked microsatellite loci originally developed for domestic cat (Menotti-Raymond et al. 1999) and widely applied to wild felids, including jaguar and puma (see appendix Table S1 for primer sequences). Due to the cost associated with the repeated PCRs required when analyzing noninvasive samples, we minimized the number of PCR reactions by multiplexing loci as follows: Multiplex#1 (FCA026, FCA090, FCA132), Multiplex#2 (FCA008, FCA043, FCA096), Multiplex#4 (FCA082, FCA275), with FCA126 and FCA057 run in independent PCR reactions. Each 10uL PCR amplification reaction consisted of 0.05uL Bovine Serum Albumin (BSA), 5uL 1X Qiagen Master Mix (Quiagen, Inc., Valencia, CA), 1uL (0.2uM of each primer), 0.5uL water, and 3uL DNA extract. PCR thermocycling program began with a 15 minutes 95°C denaturation, followed by 45 amplification cycles (30 s 94 °C denaturation, 90 s 55 °C annealing, 60 s 75 °C elongation), followed by a final 30 minute 60 °C elongation. PCR amplification of each extract was replicated (multiple-tubes approach) and genotyping followed standard allele confirmation protocols for noninvasive samples: a minimum of two amplifications to identify alleles of a heterozygous genotype, and a minimum of three amplifications to identify a homozygous genotype. Due to the small amount of target DNA per sample,

we included a PCR negative (reagents only) in all PCR plates to control for possible contamination from other samples caused by pipetting errors. PCR positives (one jaguar and one puma sample of known genotype with relatively high quality DNA) were included in each plate to monitor for possible PCR failure related to laboratory protocols as opposed to lack of genetic material in samples. DNA extraction and PCR preparation were conducted in a separate laboratory space and using designated equipment kept free from post-PCR product.

Sample PCR amplification and genotyping proceeded through an initial triage phase using a subset of seven loci (Multiplex #2, #4, FCA125, and FCA 057) and four replicates (two extracts, each with 2 PCR replicates). If these four replicates confirmed fewer than two of the 14 alleles, no further genotyping was attempted for that sample. This conservative approach was performed to focus resources on samples that might yield multi-locus genotypes with further PCR replicates. Genotyping was considered "successful", and those individuals included in downstream statistical analysis, if a minimum of 9 of 20 alleles and genotypes at 3 of 10 loci were confirmed. Out of the successfully genotyped individuals, the average number of confirmed alleles was 17.89 (median = 20) and the average number of confirmed genotypes was 8.44 (median=10). Genotypes were considered to be from the same individual if they matched at 16 of 20 alleles and if remaining differences were due to a lack of a unique allele in one individual, either due to a homozygous genotype or missing data. In other words, samples would be considered a match if 8 loci matched perfectly, but one locus had only one matching allele due a homozygote (e.g. 1/1 versus 1/2) and another due to missing data (e.g. 1/2 versus 1/NA). Probability that these matching genotypes were from different individuals ranged from 2.91E-06 – 1.21E-04 (P_{ID}) or, if they were siblings, 0.005 – 0.021 (P_{SIB}), calculated using CERVUS (Kalinowski, Taper, and Marshall 2007)

Data Analyses: We measured the geographic distance between samples from the same individual (matching genotypes) to estimate minimum distance moved within the time period of scat

degradation (which is unknown, yet assumed to be especially rapid in tropical environments). We checked for the possible presence of null alleles with MICROCHECKER (Van Oosterhout et al. 2004). There was no evidence for null alleles within the jaguar genotypes. The small sample size of puma genotypes prevented an analysis for null alleles. All downstream statistical analyses of multi-locus genotypes were conducted in R statistical computing platform version 3.3.1, unless otherwise noted (R Core Team 2016).

Genetic Diversity by Study Site: Allelic richness and inbreeding coefficient (F_{IS}) at study site were calculated using the R *diveRsity* package *divBasic* function (Keenan et al. 2013). Number of alleles and observed and expected heterozygosity at each location was calculated using the *adegenet* package using *summary(genind)* (Jombart 2008). Tests for departures from Hardy-Weinberg equilibrium were calculated for each sampling location using *diveRsity*, and overall using the R package *pegas/adegenet*, with significance tests based on 1000 Monte-Carlo permutations of alleles (Paradis 2010).

Relatedness between Individuals: The reliability and precision of genetic relatedness estimators depend on the characteristics of the microsatellite markers (e.g. polymorphism) and the dataset (e.g. amount of missing data, which is common in data from scat samples) and it is difficult to predict which estimator will be the most reliable for a given data set and suite of loci (Van De Casteele, Galbusera, and Matthysen 2001). Therefore, we calculated six estimators via the R *related* package (Pew et al. 2016) and performed an ad hoc evaluation of their reliability for our dataset. Initial inspection revealed that the two samples with the most missing data had significantly increased the average relatedness values using the relationship coefficient of Wang (2002) and the similarity index of Li et al. (1993)(Appendix Figure S1). Accordingly, we dropped the two samples from relatedness analysis and rejected those estimators. From the remaining four estimators, we chose one marker-based estimator and one likelihood-based estimator: the relationship coefficient of Queller and Goodnight (1989) and the dyadic likelihood estimator of relatedness (Milligan 2003).

Individual-based Analysis of Gene flow within Uxpanapa: To test whether geographic variables impact pairwise relatedness between individuals, we calculated the amount of connectivity (measured as "current") between each pair of samples through movement resistance surfaces using CIRCUITSCAPE in pair-wise mode with each individual as a focal node (B. H. McRae 2006; B. McRae, Shah, and Mohapatra 2013). We chose 10 geographic features for the generation of resistance surfaces based on their significance in our previous resource selection analysis (Day et al. *this dissertation Chapter 1*). They included three terrain ruggedness metrics (Insuperable Terrain Index [ITI]), three vegetation metrics, two stream density metrics, and three human activity metrics (Table 1). The values within each geographic layer were considered as either conductivity or resistance to movement, depending on whether that feature was selected or avoided, respectively (Table 1). We used a Multiple Regression on Distance Model (MRDM) approach to quantify the effect of landscape connectivity on pairwise relatedness (Balkenhol, Waits, and Dezzani 2009). The MRDM regression treats each pair-wise matrix of landscape connectivity between individuals as an independent variable, with the genetic relatedness matrix as the dependent variable. In addition to the 10 connectivity matrices generated from single geographic variables, we also calculated pairwise connectivity based on the top multivariate resource selection functions (RSF) from our previous study, one for each species. These RSF surfaces take multiple geographic variables into account at once, with beta-parameters weighting each variable in the function. We also calculated the pair-wise Euclidean distance between each pair of samples. We tested 32 MRDM models for jaguar, and 30 for puma (See Appendix Table S2). Each candidate model contained either one or two independent variables, with either the Queller-Goodnight or dyadic-likelihood relatedness values as the dependent variables. MRDM analysis was conducted with the R *ecodist* package *MRM* function, with 100 permutations to estimate statistical significance of regression coefficients and R^2 (Goslee and Urban 2007).

Table 3. Geographic features used in analysis of landscape effects on genetic relatedness between individuals. Geographic features were chosen based on previous study of resource selection and fall into four general categories of Human Activity, Water, Vegetation, and Terrain ruggedness (See Chapter 1 for further detail regarding geographic features). Connectivity Influence indicates whether the values of each geographic feature were considered as resistance or conductance to movement when calculating connectivity between individuals.

	Geographic feature	Connectivity Influence
Human Activity	% 1km Road Buffer within 626m Radius	Resistance
	% 100m Road Buffer within 1.25km Radius	Resistance
	Number of Villages within 5km Radius	Resistance (Jaguar only)
Water	Total meters of Streams within 2.5km Radius	Resistance (Puma only)
	Total meters of Streams within 5km Radius	Resistance (Puma only)
Vegetation	% Pasture within 625m Radius	Resistance (Jaguar only)
	% Tall forest within 625 Radius	Conductance
	Forest (0) Human(1) Landcover	Resistance (Jaguar only)
Terrain	% Moderate ITI within 625m Radius	Conductance (Puma only)
	% Moderate ITI within 1.25km Radius	Conductance (Puma only)
	% Rough ITI within 2.5km Radius	Conductance

** ITI = Insuperable Terrain Index of ruggedness*

Genetic Differentiation between Locations, Comparison of Jaguar versus Puma: The relative genetic differentiation between the two locations for jaguars versus pumas was assessed using five approaches. Our goal was to use a comparative approach to determine whether there was a consensus pattern describing differences in population structure between the two sympatric species. First, we use the Bayesian clustering program, STRUCTURE, to determine the number of clusters of related individuals for each species (Pritchard, Stephens, and Donnelly 2000). Second, we compared the relatedness between individuals within-versus-among locations (*see* Iacchei et al. 2013 *for an example of this approach*). Our third approach was to calculate the summary statistics of genetic distance between locations for each species, including Gst, G'st, Djost, and Weir and Cockerham's Fst (Weir and Cockerham 1984; Jost 2008; Hedrick 2005; Nei and Chesser 1983). The fourth was to partition molecular variance into hierarchical components, including within versus among locations (Analysis of Molecular Variance [AMOVA]) (Excoffier, Smouse, and Quattro 1992). Our final approach was to

determine the level of differentiation based on Discriminant Analysis of Principle Components (DAPC) for each species (Jombart, Devillard, and Balloux 2010).

If jaguar gene flow is more restricted between Uxpanapa and Quintana Roo, than puma gene flow, then one would predict the following for each approach. 1) Analysis of population genetic structure will have highest support for two genetic clusters of jaguar and one for puma. 2) Individual jaguars within a location will be more related to each other than they are to individuals in the other location, but pumas will be (on average) as related to individuals in their own location as they are to individuals in the other. 3) Genetic distance will be greater between the two locations for jaguar than for puma. 4) When partitioning genetic variance, the hierarchical level with the most genetic variance will be between locations for jaguar, and either within individuals (heterozygosity) or within locations for puma. 5) There will be a greater separation of the locations based on DAPC for jaguar than for puma.

(1) Genetic Structure*:* STRUCTURE analyses were run with a burn-in period of 10,000 iterations, with an additional 10,000 analysis iterations. We performed 20 replicate trials for each possible K value (number of genetic clusters) using the default settings. We limited possible K values to 5, due to the small number of samples. We ran two sets of analyses, one with and one without using the sample location as a prior for cluster identification. The best supported *K* values were identified using two methods: 1) plotting the replicate average *Ln P(D|K)*, and visually determining the minimum *K* of the curve's asymptote (Pritchard, Wen, and Falush 2010), and 2) using Evanno's Δ*K* method (Evanno, Regnaut, and Goudet 2005). Assignment plots for each supported K>1 were organized by sample location.

(2) Individual Relatedness within versus among Locations: Average relatedness between individuals was calculated with the R *related* package, *grouprel* permutation function. This function randomly shuffles individual genotypes among groups (locations in our case) while maintaining group

sizes. We choose to use 500 permutations since the number of permutations should not be much larger than the binomial coefficient $\binom{n}{k}$, where n = number of observations and k = number of groups, which in our case is $\binom{11}{5}$ = 462 for puma, and $\binom{16}{7}$ = 11,440 for jaguar.

(3) Summary statistics of Genetic Distance: F-statistics were calculated using the *diveRsity* including Gst, G'st, and D(Jost) in addition to Weir and Cockerham's Fst.

(4) Analysis of Molecular Variance: AMOVA was conducted via R *poppr* v2.2.1 package *poppr.amova* function with the *quasieuclid* correction, method from the *ade4* package and ignoring missing data (alternate options were not tenable given our data) (Kamvar, Brooks, and Grünwald 2015; Kamvar, Tabima, and Grünwald 2014). Each hierarchical variance component (partition level) was tested for statistical significance using a Monte-Carlo permutation test (Excoffier, Smouse, and Quattro 1992) with 99 permutations (*randtest.amova* function).

(5) Discriminant Analysis of Principle Components: DAPC was conducted using the R *adegenet* package *dapc.genind* function with default settings. DAPC first uses a principle component analysis to reduce the number of genetic variables (alleles) into synthetic variables that maximize between-group variance and minimize within-group variance. The axis that provides the most discriminatory power between groups is the first discriminant function. In our case, we specified individual cluster assignment *a priori*, with 2 clusters (K=2) specifically to test for the relative amount of differentiation between the two study sites. We visualize the differentiation between clusters by plotting density of individuals along the discriminant function axis.

Further Exploration of Gene flow between Jaguar Populations: In order to place our analysis of gene flow into a larger context, we attempted an ad hoc merger of our jaguar microsatellite genotypes to those published from other studies. A suite of three microsatellite loci (FCA043, FCA090, and FCA126) were used by this study and two others, Roques et al. (2015) in the Yucatan Peninsula, and

Wultsch et al. (2016) in Belize (see Figure 7). Assuming a significant amount of gene flow between these sites, differences in the range allele sizes between these studies are most likely due to laboratory conditions causing shifts in the size ranges. For each locus, we adjusted allele sizes hand by adding or subtracting integers until we maximized visual concordance between allele size ranges. The process of visual alignment was relatively straightforward, as the range of allele sizes and the shape of the frequency distributions were similar across the three studies (Appendix Figure S2). In order to examine the relative levels of gene flow between the three study areas, we calculated Fst between the three sites based on these three microsatellite loci. This is a non-traditional approach to pooling microsatellite data across labs, and was done for preliminary investigation only, in the hopes of enticing further collaboration between research labs.

RESULTS

Field Collection and Genotyping of Noninvasive Samples: We obtained 16 unique jaguar genotypes (9UX+ 7QR) and 11 unique puma genotypes (6UX + 5QR). Within Uxpanapa (UX), 29 confirmed jaguar scats yielded 9 unique jaguar genotypes (11 genotypes with 2 sets of matching genotypes from the same individuals) and 9 confirmed puma scats yielded 6 unique puma genotypes (38% and 67% genotyping success for jaguar and puma, respectively) (Figure 1 & 3) (see appendix Table S3 for sample genotypes). One of the jaguar genotypes was from the pelt of a locally poached animal. That individual was not included in the downstream analyses that required a precise geographic location. Within the Quintana Roo study area (QR), 18 confirmed jaguar scat samples yielded 7 unique jaguar genotypes (10 genotypes with a set of 2 and another set of 3 matching genotypes) and 11 confirmed puma scats yielded 5 unique puma genotypes (8 genotypes with 3 matching sets)(56% and

73% genotyping success for jaguar and puma, respectively). Our nuclear marker amplification success of samples confirmed to species via mtDNA markers (44% jaguar, 70% puma) was comparable to those reported for other studies (Michalski et al. 2011)(Allele frequencies: appendix Figure S3-S4)

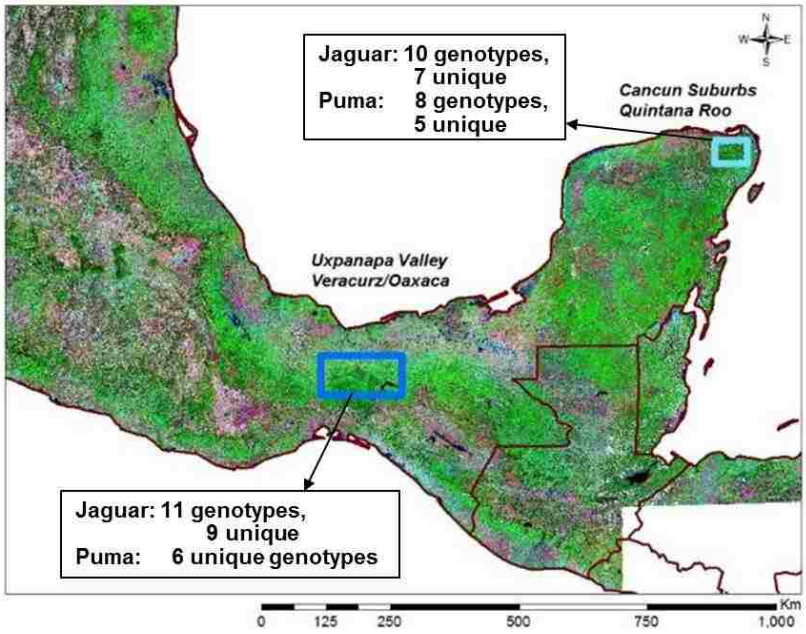

Figure 1. Sampling locations and number of genotypes obtained for each species within Mexico with satellite imagery.

Distance between genetic recaptures of the same individual ranged from <1 – 4,543 m (Figure 2). The longest distances between scat samples with matching genotypes were approximately 2km for jaguar, and 4.5km for puma.

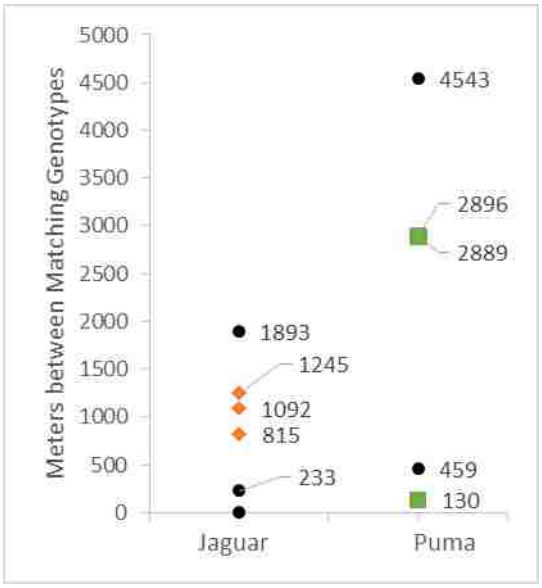

Figure 2. Geographic distance (m) between recaptures of individuals. Each black circle represents the distance between two locations of a unique individual (two locations for a single individual = one distance between those locations = one black circle). Colored symbols are distances between multiple recaptures of one individual. One jaguar (orange) had three locations (three locations = three distances between those locations = three orange diamonds), one puma (green) had three locations.

Individual-based Analysis of Gene flow within Uxpanapa: Multiple Regression on Distance Modeling did not reveal any statistically significant association between the relatedness metrics and geographic metrics for either jaguar or puma within Uxpanapa (appendix Table S2). Genetic relatedness estimates between individuals within Uxpanapa varied from -0.6307-0.1692 for the Queller-Goodnight estimator, and from 0-0.3077 for the dyadic likelihood estimator (*latter visualized in* Figure 3). Euclidean geographic distance alone was also not a significant predictor of genetic distance, suggesting no isolation by distance at this spatial scale (appendix Table S2).

A. Jaguar

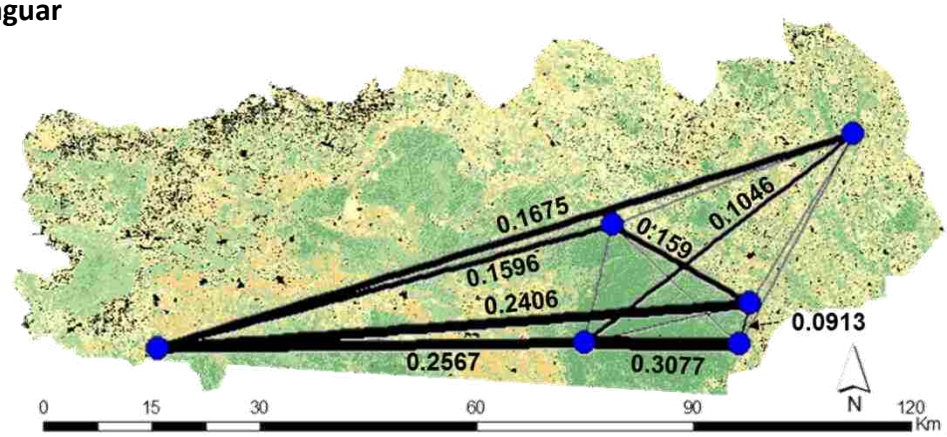

B. Puma

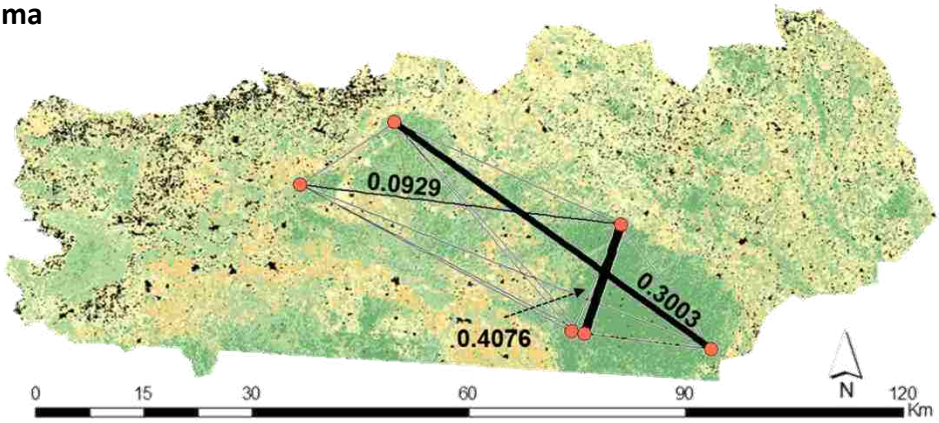

Figure 3. Genetic relatedness between individuals as measured by the dyadic likelihood estimator of genetic relatedness. Line thickness scaled to relatedness, unlabeled lines had an estimated relatedness of zero. Recaptured individuals are represented by a single dot, as all recaptures within Uxpanapa were <1km from each other.

Genetic Diversity by Study Site: Results from tests of departure from Hardy-Weinberg equilibrium (HWE) were inconclusive. One locus (FCA132) was significantly out of HWE for puma samples, both within and across sampling locations (appendix Table S4). It is unclear if this is a biological result or an artifact of the small number of samples. Standard measures of genetic diversity were calculated for Uxpanapa (UX) and Quintana Roo (QR) as well overall, summarized by locus in Table 2.

Table 2. Genetic diversity of jaguar and puma populations in Uxpanapa, Veracruz (UX) and northern Quintana Roo (QR) Mexico. Number of unique alleles observed per locus (No.Alleles/Locus), rarefacted allelic richness, and Observed (Obs) and Expected (Exp) Heterozygosity.

		FCa008	FCa043	FCa096	FCa126	FCa026	FCa090	FCa132	FCa082	FCa275	FCa056
JAGUAR	UX No.Alleles/Locus	5	3	7	3	3	4	3	2	3	6
	QR No.Alleles/Locus	4	2	3	3	3	4	1	2	4	2
	Overall No.Alleles/Locus	6	3	7	4	3	4	3	3	4	6
	UX Allelic Richness	4.05	3.16	6.22	3.51	3.29	4.67	2.78	2.41	2.79	5.26
	QR Allelic Richness	3.98	1.98	3.73	3.85	3.34	4.15	1.91	2.64	3.99	2.55
	UX Obs Heterozygosity	1	0.67	0.89	0.89	0.56	0.89	0.43	0.38	0.78	0.78
	QR Obs Heterozygosity	0.57	0.17	1	0.71	0.71	0.43	0.4	0.83	0.86	0.5
	Overall Obs Heterozygosity	0.8	0.47	0.93	0.81	0.62	0.69	0.42	0.57	0.81	0.67
	UX Exp Heterozygosity	0.7	0.6	0.83	0.65	0.56	0.78	0.58	0.32	0.54	0.78
	QR Exp Heterozygosity	0.67	0.49	0.72	0.7	0.58	0.68	0.32	0.54	0.67	0.4
	Overall Exp Heterozygosity	0.71	0.56	0.82	0.7	0.57	0.76	0.52	0.44	0.61	0.69
PUMA	UX No.Alleles/Locus	3	5	6	3	3	6	5	4	4	3
	QR No.Alleles/Locus	2	4	3	2	4	3	3	5	4	5
	Overall No.Alleles/Locus	4	6	7	4	5	7	5	5	5	5
	UX Allelic Richness	2.59	3.79	4.54	2.59	2.83	4.03	3.77	3.68	3.68	2.96
	QR Allelic Richness	1.69	4.18	2.35	1.68	3.53	3.35	3.25	3.93	3.5	4.26
	UX Obs Heterozygosity	1	1	0.83	0.5	0.83	0.67	0.67	0.83	0.83	0.83
	QR Obs Heterozygosity	0.2	1	0.2	0.2	1	1	0.4	0.8	0.6	1
	Overall Obs Heterozygosity	0.64	1	0.55	0.36	0.91	0.82	0.55	0.82	0.73	0.91
	UX Exp Heterozygosity	0.57	0.69	0.79	0.49	0.57	0.62	0.72	0.61	0.71	0.65
	QR Exp Heterozygosity	0.18	0.74	0.34	0.18	0.66	0.64	0.64	0.74	0.7	0.76
	Overall Exp Heterozygosity	0.48	0.78	0.78	0.38	0.64	0.66	0.75	0.74	0.72	0.76

Overall metrics of genetic diversity for the Uxpanapa and Quintana Roo jaguar and puma populations were similar to published values, with a few exceptions (Table 3). Jaguar allelic richness and expected heterozygosity within the two populations are lower than those published in other areas such as Colombia, Brazil, and Venezuela, but are similar to those reported from Mexico and Belize. The observed heterozygosity in the puma populations are similar to others reported from Mexico, and higher than reported from populations within the USA. Comparisons between studies should be viewed with caution, given that each study used different suites of microsatellite loci (with some loci overlapping between studies).

Table 3. Comparison of genetic diversity metrics of Uxpanapa and Quintana Roo populations from this study (our study, Day 2016, in bold at top) to other published records. The one other entry for Tehuantepec, Mexico is under Puma, by Zanin et al. 2016 in Los Ocotones. Genetic diversity metrics include rarefracted allelic richness, observed (Obs) and expected (Exp) heterozygosity and inbreeding coefficient (Fis).

	First Author & Year	Location	Allelic Richness	Obs Het	Exp Het	F_{IS}
JAGUAR	**Day 2016**	**Uxpanapa, Mexico (*n=9*)**	**3.81 (3.1-4.4 CI)**	**0.72**	**0.63**	**-0.1422 (-0.2989 - -0.0150 BC CI)**
		Quintana Roo, Mexico (*n=7*)	**3.21 (2.7-3.6 CI)**	**0.62**	**0.58**	**-0.0689 (-0.2819 - 0.1008 BC CI)**
	Zanin 2016	ElEden& Zapotal, Mexico	2.79	0.62	0.58	-0.06
		Petcab, Caoba & Calakmul, Mexico	3.24	0.70	0.66	-0.03
		ElCarmen, Mexico	2.57	0.64	0.59	-0.03
	Wultch 2016	Belize	3.36	0.57	0.57	0.04
	Ruiz-Garcia 2001	Columbia			0.76	
	Ruiz-Garcia 2006	Columbia	10.083±2.570		0.835±0.083	
		Guatemala, Paraguay, Peru, Bolivia, Venezuela & Brazil	11.33±2.570		0.846±0.066	
	Haag 2010	Brazil (Atlantic Forest)	7.23	0.682 (0.548-0.782)	0.732 (0.498-0.782)	
	Roques 2016	Mexico	4.45	0.684	0.645	
		Brazil	9.45	0.734-0.848	0.709-0.837	
	Eizirik 2001	range-wide	8.31		0.739	
	Wultch 2016	Mexico	3.14	0.52	0.54	0.13 (0.00-0.29 CI)
		Mesoamerica mean (incl Mex)	3.43	0.59	0.59	0.05
PUMA	**Day 2016**	**Uxpanapa, Mexico (*n=6*)**	**3.45 (2.7-4.0 CI)**	**0.8**	**0.64**	**-0.2441 (-0.4101 - -0.1418 BC CI)**
		Quintana Roo, Mexico (*n=5*)	**3.17 (2.3-3.8 CI)**	**0.64**	**0.56**	**-0.147 (-0.4236 - -0.0159 BC CI)**
	Zanin 2016	**Loc Ocotones, Mexico**	**1.67**	**0.69**	**0.55**	**-0.22**
		ElEden& Zapotal, Mexico	3.22	0.61	0.65	0.12
		Petcab, Caoba & Calakmul, Mexico	3.29	0.65	0.66	0.06
		ElCarmen, Mexico	4.00	0.71	0.76	0.12
	Wultch 2016	Belize	4.20	0.60	0.57	0.06
	Ruiz-Garcia 2001	Columbia			0.75	
	Benson 2016	Southern CA, USA	2.220 (SE 0.123)	0.388 (SE 0.040)	0.352 (SE 0.032)	0.127 (SE 0.022)
	Andreasen 2012	Great Basin, Nevada & Sierra Nevadas, USA	3.8-4.7	0.50-0.57	0.50-0.57	

Genetic Differentiation between Locations, Comparison of Jaguar and Puma:

1) Genetic Structure: We conclude that the jaguar samples collected from the two locations represent one genetic cluster, while puma represent two genetic clusters. Evanno's ΔK method supported either K=2 or K=4 for jaguar and puma (see Appendix Figure S5 & S6). However, visual inspection of the assignment bar plots refuted K=4 for both species, as all individuals had approximately equal assignment probability to alternative clusters (Appendix Figure S7). Likewise, no assignment pattern was seen for K=2 in jaguar, regardless of whether location information was used as a prior. However, the assignment probabilities of pumas for K=2 using location as prior supported two significant clusters.

2) Individual Relatedness within versus among Locations*:* Individual jaguars within each location (group) are no more related (on average) than they are to individuals at the other location (regardless of which relatedness estimator was used). However, pumas within the groups are more related to each other than between groups. Average relatedness between individuals within the same location was calculated for both species (Figure 4, red arrows). Shuffling jaguar individuals between groups did not significantly change the average relatedness between individuals within a group (Figure 4, histogram), from the observed average. However, shuffling individual pumas between groups produced lower within-group average relatedness than observed (Figure 4). To make sure that the significant difference in the puma results was not due to excessive permutations, we reanalyzed with 100 permutations (far below the binomial coefficient) and still obtained statistically significant difference between observed and permuted average within-group relatedness (p <0.01).

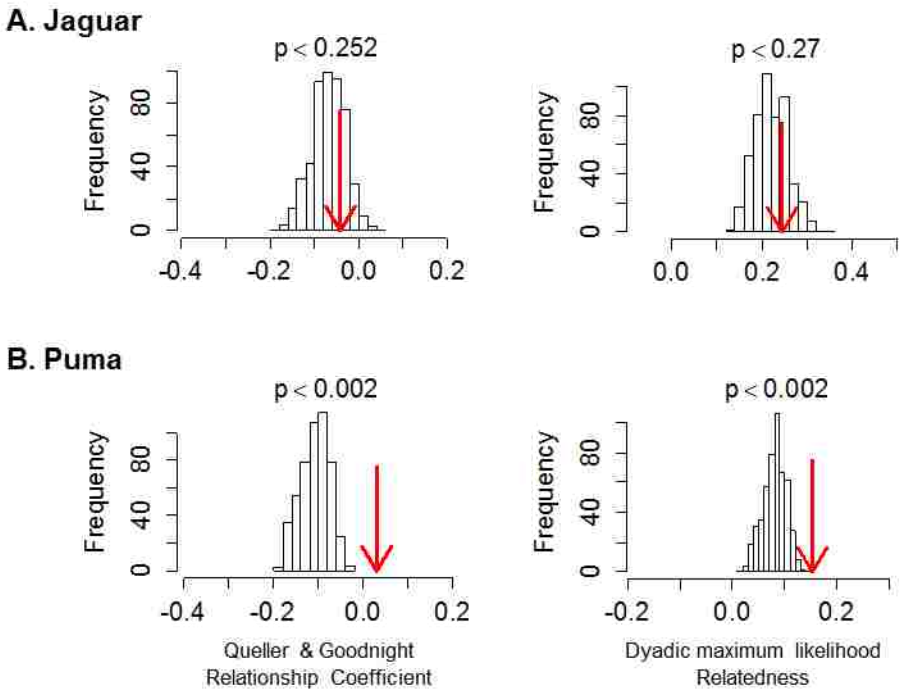

Figure 4. Observed average within-group genetic relatedness between individuals (red arrow). Permuted within-group average relatedness based on shuffling genotypes between groups (Uxpanapa and Quintana Roo) for 500 permutations (histogram). P-values are the % of expected observations that are greater or equal to the observed value.

3) Summary statistics of Genetic Distance: Despite differences in magnitude between metrics, all genetic distance metrics showed the same pattern of greater differentiation between the puma populations than the sympatric jaguar populations (Table 4).

Table 4. Genetic distance between Uxpanapa and Quintana Roo for jaguar and puma. Nei's Gst, Hedrick's G'st, Jost's D (Djost), and Weir and Cockerham's Fst (Fst[WC]).

		Gst	G'st	Djost	Fst (WC)
JAGUAR	Estimate	0.0343	0.1391	0.0386	0.0719
(*n=16*)	95% CI	0.0056-0.0814	0.0241-0.2868	0.0000-0.1215	0.0124-0.1558
	Bias Correcte	0.0023	0.0110	-0.0001	0.0062
	95% CI	-0.0264-0.0494	-0.1041-0.1586	-0.0387-0.0828	-0.0533-0.0901
PUMA	Estimate	0.0887	0.3625	0.1553	0.1770
(*n=11*)	95% CI	0.0432-0.1527	0.1966-0.5364	0.0591-0.3067	0.0964-0.2861
	Bias Correcte	0.0501	0.2455	0.0669	0.1040
	95% CI	0.0046-0.1141	0.0795-0.4193	-0.0293-0.2182	0.0234-0.2131

4) Analysis of Molecular Variance: The amount of genetic variance that was partitioned into the between-locations hierarchical level (as opposed to within-samples or between-samples) was significant for puma (p = 0.02), but not for jaguar (p = 0.46) (Table 5; Figure 5). However, for both species, the amount of variance was small as compared to the amount of genetic variance attributed to within samples (heterozygosity) (Table 5).

Table 5. Hierarchical Analysis of Molecular Variance

	Source	d.f.	Sum of Squares	Variance Component	Variation %	*P* value
JAGUAR	Between Populations	1	2.674	-0.007	-0.242	0.46
	Between Samples within Populations	14	39.047	-0.224	-7.446	0.9
	Within Samples	16	51.786	3.237	107.688	0.89
	Total	31	93.507	3.005	100	
PUMA	Between Populations	1	7.108	0.382	10.399	0.02
	Between Samples within Populations	9	26.483	-0.347	-9.449	0.86
	Within Samples	11	40.000	3.636	99.049	0.73
	Total	21	73.591	3.671	100	

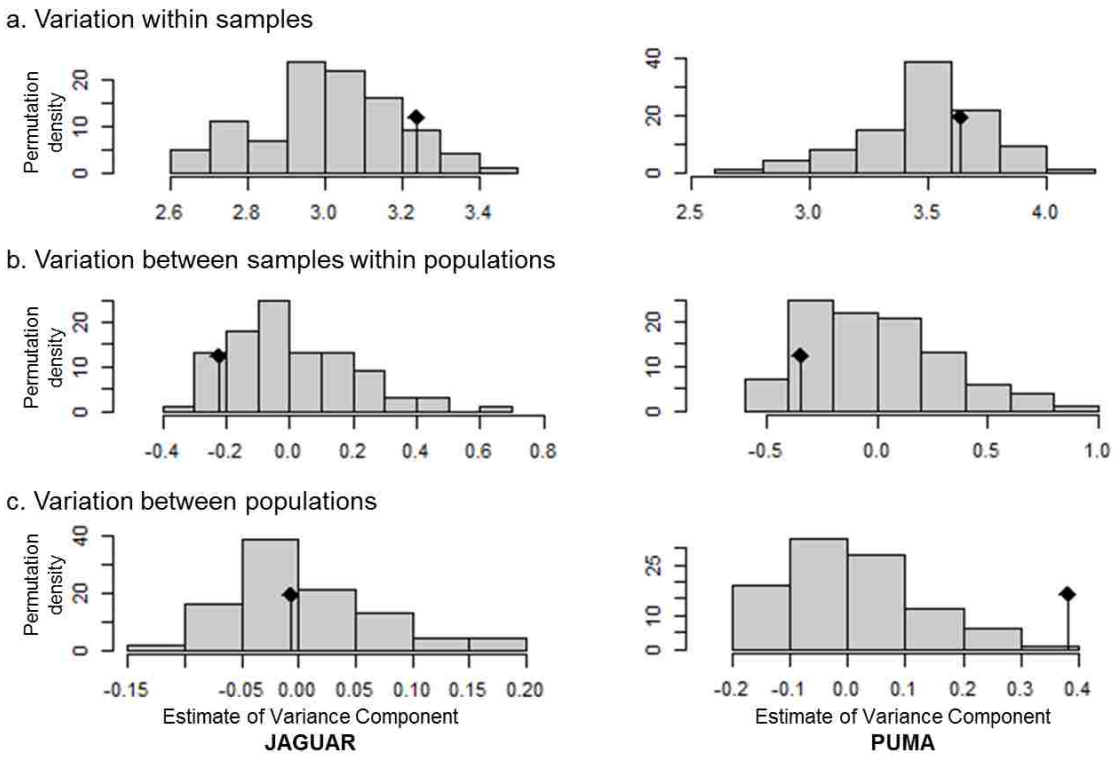

Figure 5. Visualization of significance tests of hierarchical AMOVA for JAGUAR (left) and PUMA (right). Variance component estimates observed from our data (sticks) and expected by Monte-Carlo permutations (histogram). All of the observed values fall within the random distribution, indicating non-significant variance component at that hierarchical level, with one exception; the observed variance component between puma populations (lower right) is significantly outside of the permuted distribution, indicating significant structure between puma populations.

5) Discriminant Analysis of Principle Components: The DAPC clustering approach showed greater differentiation between the two puma populations than the two jaguar populations (Figure 6). The density of individuals along the first discriminant function axis had greater overlap between the two locations for jaguar than for puma.

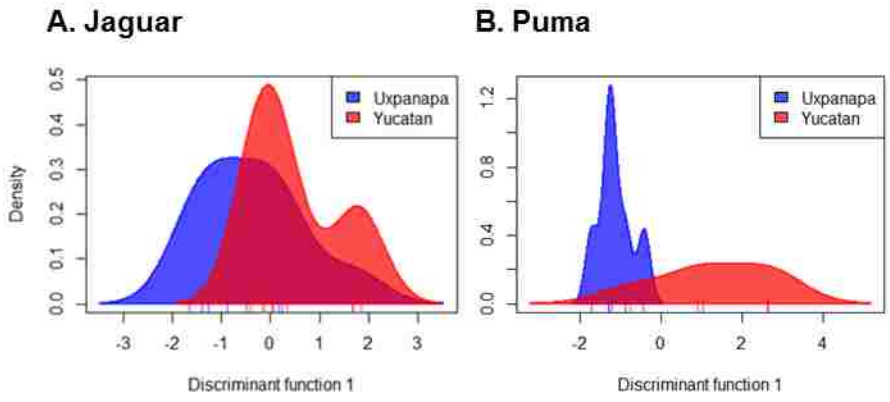

Figure 6. Discriminant Analysis of Principle Components for two locations (K=2). Density of individuals along the first discriminant function axis show greater overlap in between the two locations for jaguar, and less overlap for puma. .

Further Exploration of Gene flow between Jaguar Populations: By adjusting the allele sizes for three microsatellite loci, we pooled jaguar genetic data from three studies to examine genetic distance between our sites and those in Belize. The estimates of Fst between the three jaguar populations studied shows a greater distance between the Uxpanapa valley and Belize populations than between QR and either population (Figure 7). Preliminary results from our ad hoc merger of three shared microsatellite loci suggest less genetic connectivity between the Uxpanapa valley and Belize, than between the Yucatan Peninsula populations and either region, indicating benefits of the network of protected areas throughout the Yucatan Peninsula and/or greater movement barriers between Belize and Uxpanapa. Future collaboration with these other research groups, including genetic sample exchange, will determine the validity of this approach.

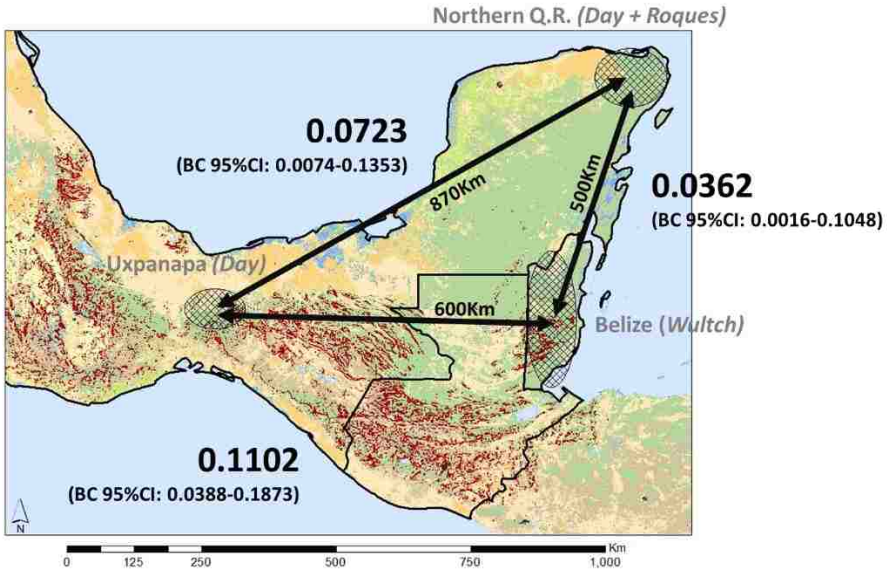

Figure 7. Genetic distance (Fst) between three jaguar populations surveyed by three research groups (First authors Day, Roques, and Wultsch). Fst values are based on three microsatellite loci. Bias-corrected (BC) 95% confidence intervals (CI) are based on 100 bootstrap iterations.

DISCUSSION

Our study suggests that gene flow of these highly vagile species is not restricted between forest fragments within Uxpanapa, nor has the genetic diversity within the valley been reduced by surrounding deforestation. Alternatively, our results could be due to a combination of the following: A) our sample size was too small to detect patterns in genetic relatedness or reduction in genetic diversity, B) the habitat fragmentation that has occurred over the past 50 years (Gomez-Irving, Edward A., and Gomez-Cesar A. 2011) has not yet influenced the pattern of relatedness between individuals due generational lag-time (Epps and Keyghobadi 2015; Landguth et al. 2010), or C. the number and polymorphism of the genetic markers used were insufficient to capture landscape genetic patterns. Therefore, we urge continued monitoring of the large felids in Uxpanapa, especially given the ongoing deforestation and habitat degradation within and surrounding the valley.

At the regional scale, all of our analyses of genetic differentiation between locations concur that pumas at the two locations are more genetically distinct from each other than the sympatric jaguars. Wultsch et al. (2016) identified spatial autocorrelation in the genetic structure of jaguars to the distance of ~340km. However, we found no evidence of genetic structure between jaguars at our two sites separated by approximately 1,000km. We do not think this failure to find genetic structure can be attributed to sample size alone, as other studies have found genetic structure with similar sample sizes, albeit between sites farther apart. Additionally, despite our limited number of samples, our estimate of Fst between the puma populations is remarkably similar to that reported by Zanin et al. 2016 (0.1770 and 0.1700 respectively), lending credence to our conclusions. The greater genetic differentiation between puma populations than jaguar has been generally hypothesized to be due to a shorter dispersal distance of pumas versus jaguars. However, this has not been substantiated by field observation. The behavioral drivers of dispersal distance in large Neotropical felids remains an open question. Future studies of movement ecology may shed light on how local resource selection processes scale-up to regional processes such as gene flow, leading to species differences in gene flow such as we've found in our study.

Our study confirms the persistence of both jaguar and puma within the Uxpanapa valley. Our success in identifying numerous individuals within this challenging region is testimony to the utility of using detection dogs to locate big cat samples; previous attempts have been relatively unsuccessful using either observer located scats (Zanin et al. 2016) or camera trapping (Figel, Duran, and Bray 2011). The geographic distances between genetic recaptures are similar to the 2.4km average daily jaguar movement estimated from radio-telemetry data in the Brazilian Pantanal (Crawshaw and Quigley 1991) and are under the maximum 10km/day or 14km/day estimated for jaguar (Colchero et al. 2011) or puma (Elbroch and Wittmer 2012) respectively. Unfortunately, we did not observe a sufficient number of recaptures to enable a genetics-based mark-recapture or territory delineation. However, these

approaches may be feasible with greater sampling effort, offering a noninvasive alternative to trapping and marking or collaring animals.

At the species-range scale, our study contributes to an emerging pattern of lower genetic diversity in the jaguar populations of Mexico and neighboring Belize as compared to populations in South America. Additionally, puma population expected heterozygosity appears slightly higher in Mexico than the more northerly populations in the USA. This difference in species genetic diversity may be due to niche-centrality (Lira-Noriega and Manthey 2014; Eckert, Samis, and Lougheed 2008), Mexican jaguars being further away from their species range center than puma. An alternate hypotheses, as postulated by Zanin et al. (2016), is that the lower genetic diversity in Mexican jaguars could be due to reduced gene flow through parts of Nicaragua and Honduras (Sanderson et al. 2002).

Our study has provided a glimpse into three spatial scales of gene flow dynamics for jaguars and pumas, and highlights the need for further work elucidating potential behavioral drivers governing movement during juvenile dispersal versus movements within home-ranges (Roffler et al. 2016). Our study fills a gap in genetic data for the Mesoamerican jaguars, which we hope will contribute to international efforts monitoring genetic connectivity throughout their species ranges. We argue that the Uxpanapa valley has the potential to contribute to the long-term preservation of both species by providing a stepping-stone for gene flow through Mesoamerica.

ACKNOWLEDGEMENTS: Centro de Investigaciones Tropicales (CITRO), U.Veracruzana for logistical support and vehicles. Primary funding from Fundo-Mixto CONACYT/Gobierno Del Estado de Veracruz de Ignacio De la Llave. Additional funding from the Wingfield-Ramenofski UW Biology Graduate Award and the Katherine Hahn UW-Biology Writing Fellowship.

PERMIT INFORMATION:

Wildlife detector dogs were cared for under the *Scat Detection Dog Program* IACUC approved protocol #2850-08. All samples collected from the wild were naturally deposited fecal samples. Sample collection was conducted under the license SGPA/DGVS/07120/09 (22-Oct-09), provided by M.V.Z. Martin Vargas Prieto of the Dirección General de Vida Silvestre (Semarnat). Faecal samples were exported from Mexico to USA under the export licenses MX #49045 (14-Oct-10) and MX #54703 (01-Dic-11) of the Secertaria de Medio Ambiente/CITES.

LITTERATURE CITED:

Balkenhol, Niko, Lisette P. Waits, and Raymond J. Dezzani. 2009. “Statistical Approaches in Landscape Genetics: An Evaluation of Methods for Linking Landscape and Genetic Data.” *Ecography* 32 (5): 818–30.

Colchero, F., D. A. Conde, C. Manterola, C. Chávez, A. Rivera, and G. Ceballos. 2011. “Jaguars on the Move: Modeling Movement to Mitigate Fragmentation from Road Expansion in the Mayan Forest.” *Animal Conservation* 14 (2): 158–66.

Crawshaw, P. G., and H. B. Quigley. 1991. “Jaguar Spacing, Activity and Habitat Use in a Seasonally Flooded Environment in Brazil.” *Journal of Zoology* 223 (3): 357–70.

Culver, M., W. E. Johnson, J. Pecon-Slattery, and S. J. O’Brien. 2000. “Genomic Ancestry of the American Puma (Puma Concolor).” *Journal of Heredity* 91 (3): 186–97.

Eckert, C. G., K. E. Samis, and S. C. Lougheed. 2008. “Genetic Variation across Species’ Geographical Ranges: The Central–marginal Hypothesis and beyond.” *Molecular Ecology* 17 (5): 1170–88.

Eizirik, Eduardo, Taiana Haag, Anelisie S. Santos, Francisco M. Salzano, Leandro Silveira, Fernando CC Azevedo, and Mariana M. Furtado. 2008. “Jaguar Conservation Genetics.” *Cat News Special Issue*.

Eizirik, Eduardo, Jae-Heup Kim, Marilyn Menotti-Raymond, Peter G. Crawshaw JR., Stephen J. O’Brien, and Warren E. Johnson. 2001. “Phylogeography, Population History and Conservation Genetics of Jaguars (Panthera Onca, Mammalia, Felidae).” *Molecular Ecology* 10 (1): 65–79.

Elbroch, L. Mark, and Heiko U. Wittmer. 2012. “Puma Spatial Ecology in Open Habitats with Aggregate Prey.” *Mammalian Biology* 77 (5): 377–84.

Epps, Clinton W., and Nusha Keyghobadi. 2015. “Landscape Genetics in a Changing World: Disentangling Historical and Contemporary Influences and Inferring Change.” *Molecular Ecology*, November.

Evanno, G., S. Regnaut, and J. Goudet. 2005. “Detecting the Number of Clusters of Individuals Using the Software Structure: A Simulation Study.” *Molecular Ecology* 14 (8): 2611–20.

Excoffier, Laurent, Peter Smouse, and Joseph Quattro. 1992. “Analysis of Molecular Variance Inferred From Metric Distances Among DNA Haplotaypes: Application to Human Mitochondrial DNA Restriction Data.” *Genetics* 131: 479–91.

Figel, Joe J., Elvira Duran, and David Barton Bray. 2011. “Conservation of the Jaguar Panthera Onca in a Community-Dominated Landscape in Montane Forests in Oaxaca, Mexico.” *Oryx* 45 (4): 554–60.

Gomez-Irving, Hernandez, Ellis Edward A., and Gallo Gomez-Cesar A. 2011. “Deforestacion y deterioro de las slevas tropicales en la region Uxpanapa, Veracruz.” Xalapa, Veracruz, Mexico: Centro de Investigaciones Tropicales CITRO, Universidad Veracruzana.

Goslee, S.C., and D.L. Urban. 2007. “The Ecodist Package for Dissimilarity-Based Analysis of Ecological Data.” *Journal of Statistical Software* 22 (7): 1–19.

Hedrick, Philip W. 2005. “A Standardized Genetic Differentiation Measure.” *Evolution* 59 (8): 1633–38.

Iacchei, Matthew, Tal Ben-Horin, Kimberly A. Selkoe, Christopher E. Bird, Francisco J. García-Rodríguez, and Robert J. Toonen. 2013. “Combined Analyses of Kinship and FST Suggest Potential Drivers of Chaotic Genetic Patchiness in High Gene-Flow Populations.” *Molecular Ecology* 22 (13): 3476–94.

Jombart, Thibaut. 2008. “Adegenet: A R Package for the Multivariate Analysis of Genetic Markers.” *Bioinformatics* 24 (11): 1403–5.

Jombart, Thibaut, Sébastien Devillard, and François Balloux. 2010. “Discriminant Analysis of Principal Components: A New Method for the Analysis of Genetically Structured Populations.” *BMC Genetics* 11 (1): 94.

Jost, Lou. 2008. “GST and Its Relatives Do Not Measure Differentiation.” *Molecular Ecology* 17 (18): 4015–26.

Kalinowski, Steven T., Mark L. Taper, and Tristan C. Marshall. 2007. “Revising How the Computer Program Cervus Accommodates Genotyping Error Increases Success in Paternity Assignment.” *Molecular Ecology* 16 (5): 1099–1106.

Kamvar, Zhian N., Jonah C. Brooks, and Niklaus J. Grünwald. 2015. “Novel R Tools for Analysis of Genome-Wide Population Genetic Data with Emphasis on Clonality.” *Plant Genetics and Genomics* 6: 208.

Kamvar, Zhian N., Javier F. Tabima, and Niklaus J. Grünwald. 2014. “Poppr: An R Package for Genetic Analysis of Populations with Clonal, Partially Clonal, And/or Sexual Reproduction.” *PeerJ*.

Keenan, Kevin, Philip McGinnity, Tom F. Cross, Walter W. Crozier, and Paulo A. Prodöhl. 2013. “diveRsity: An R Package for the Estimation and Exploration of Population Genetics Parameters and Their Associated Errors.” *Methods in Ecology and Evolution* 4 (8): 782–88.

Landguth, E. L., S. A. Cushman, M. K. Schwartz, K. S. McKelvey, M. Murphy, and G. Luikart. 2010. “Quantifying the Lag Time to Detect Barriers in Landscape Genetics.” *Molecular Ecology* 19 (19): 4179–91.

Li, C.C., D.E. Weeks, and A. Chakravarti. 1993. “Similarity of DNA Fingerprints Due to Chance and Relatedness.” *Human Heredity* 43 (1): 45–52.

Lira-Noriega, Andrés, and Joseph D. Manthey. 2014. “Relationship of Genetic Diversity and Niche Centrality: A Survey and Analysis.” *Evolution* 68 (4): 1082–93.

McRae, Brad H. 2006. “Isolation by Resistance.” *Evolution* 60 (8): 1551–61.

McRae, Brad, Viral Shah, and Tanmay Mohapatra. 2013. *Circuitscape 4 Users Guide* (version 4.0). The Nature Conservancy. http://www.circuitscape.org.

Menotti-Raymond, Marilyn, Victor A. David, Leslie A. Lyons, Alejandro A. Schäffer, James F. Tomlin, Michelle K. Hutton, and Stephen J. O’Brien. 1999. “A Genetic Linkage Map of Microsatellites in the Domestic Cat (Felis Catus).” *Genomics* 57 (1): 9–23.

Michalski, Fernanda, Fernanda Pedone Valdez, Darren Norris, Chris Zieminski, Cyntia Kayo Kashivakura, Cristine S. Trinca, Heath B. Smith, et al. 2011. “Successful Carnivore Identification with Faecal DNA across a Fragmented Amazonian Landscape.” *Molecular Ecology Resources* 11 (5): 862–71.

Milligan, Brook G. 2003. “Maximum-Likelihood Estimation of Relatedness.” *Genetics* 163 (3): 1153–67.

Myers, Norman, Russell A. Mittermeier, Cristina G. Mittermeier, Gustavo A. B. da Fonseca, and Jennifer Kent. 2000. “Biodiversity Hotspots for Conservation Priorities.” *Nature* 403 (6772): 853–58.

Nei, M., and R. K. Chesser. 1983. “Estimation of Fixation Indices and Gene Diversities.” *Annals of Human Genetics* 47 (3): 253–59.

Paradis, Emmanuel. 2010. “Pegas: An R Package for Population Genetics with an Integrated–modular Approach.” *Bioinformatics* 26 (3): 419–20.

Pew, Jack, Jinliang Wang, Paul Muir, and Tim Frasier. 2016. *Related: An R Package for Analyzing Pairwise Relatedness Data Based on Codominant Molecular Markers.* (version R package version 1.0). Accessed October 30.

Pritchard, Jonathan K., Matthew Stephens, and Peter Donnelly. 2000. “Inference of Population Structure Using Multilocus Genotype Data.” *Genetics* 155 (2): 945–59.

Pritchard, Jonathan K., Xiaoquan Wen, and Daniel Falush. 2010. “Documentation for Structure Software: Version 2.3.”

Queller, David C., and Keith F. Goodnight. 1989. “Estimating Relatedness Using Genetic Markers.” *Evolution* 43 (2): 258–75.

Rabinowitz, Alan, and Kathy A. Zeller. 2010. “A Range-Wide Model of Landscape Connectivity and Conservation for the Jaguar, Panthera Onca.” *Biological Conservation* 143 (4): 939–45.

R Core Team. 2016. *R: A Language and Environment for Statistical Computing.* Vienna, Austria: R Foundation for Statistical Computing. http://www.R-project.org/.

Roffler, Gretchen H., Michael K. Schwartz, Kristy L. Pilgrim, Sandra L. Talbot, George K. Sage, Layne G. Adams, and Gordon Luikart. 2016. “Identification of Landscape Features Influencing Gene Flow: How Useful Are Habitat Selection Models?” *Evolutionary Applications* 9 (6): 805–17.

Sanderson, Eric W., Kent H. Redford, Cheryl-Lesley B. Chetkiewicz, Rodrigo A. Medellin, Alan R. Rabinowitz, John G. Robinson, and Andrew B. Taber. 2002. “Planning to Save a Species: The Jaguar as a Model.” *Conservation Biology* 16 (1): 58–72.

Sandoval-Mendoza, Juana B., Anibal F. Ramirez-Soto, Ixchel M. Shesena-Hernandez, Carlo Sormani, Fortunato Ruiz-DeLaMerced, Daniel Jarvio-Arellano, and Eder Farid-Mora. 2007. “Evaluacion Del Estado de Conservacion de Los Ecosistemas Forestales de La Region Denominada Uxpanapa 2006-2007.” SEDARPA & ProNatura asociacion civil.

Sunquist, Fiona, and Mel Sunquist. 2002. *Wild Cats of the World*. 1 edition. Chicago: University of Chicago Press.

Van De Casteele, T., P. Galbusera, and E. Matthysen. 2001. “A Comparison of Microsatellite-Based Pairwise Relatedness Estimators.” *Molecular Ecology* 10 (6): 1539–49.

Van Oosterhout, Cock, William F. Hutchinson, Derek P. M. Wills, and Peter Shipley. 2004. “Micro-Checker: Software for Identifying and Correcting Genotyping Errors in Microsatellite Data.” *Molecular Ecology Notes* 4 (3): 535–38.

Wang, Jinliang. 2002. “An Estimator for Pairwise Relatedness Using Molecular Markers.” *Genetics* 160 (3): 1203–15.

Weir, B. S., and C. Clark Cockerham. 1984. “Estimating F-Statistics for the Analysis of Population Structure.” *Evolution* 38 (6): 1358–70.

White, Jennifer Mae. 2010. *Development of Noninvasive Genetic Techniques to Monitor Elusive Carnivores*. Master’s Thesis, Michigan State University, Department of Fisheries and Wildlife.

Wultsch, Claudia, Anthony Caragiulo, Isabela Dias-Freedman, Howard Quigley, Salisa Rabinowitz, and George Amato. 2016. “Genetic Diversity and Population Structure of Mesoamerican Jaguars (Panthera Onca): Implications for Conservation and Management.” *PLOS ONE* 11 (10): e0162377.

Wultsch, Claudia, Lisette P. Waits, and Marcella J. Kelly. 2016. “A Comparative Analysis of Genetic Diversity and Structure in Jaguars (Panthera Onca), Pumas (Puma Concolor), and Ocelots (Leopardus Pardalis) in Fragmented Landscapes of a Critical Mesoamerican Linkage Zone.” *PLOS ONE* 11 (3): e0151043.

Zanin, Marina, Begoña Adrados, Noa González, Severine Roques, Daniel Brito, Cuauhtemoc Chávez, Yamel Rubio, and Francisco Palomares. 2016. “Gene Flow and Genetic Structure of the Puma and Jaguar in Mexico.” *European Journal of Wildlife Research*, May, 1–9.

Zeller, Kathy. 2007. “Jaguars in the New Millennium. Data Set Update: The State of the Jaguar in 2006. WCS Report.” *Wildlife Conservation Society, New York*, 1–82.

APPENDIX - TABLES:

Table S1. Microsatellite Loci and Primer Sequences

Locus Name	Primer Sequence
FCA026_F	5' - AGC CCT TAG AGT CAT GCA - 3'
FCA026_R	5' - GTTTCTT TGT ACA CGC ACC AAA AAC AA - 3'
FCA090_F	5' - ATC AAA AGT CTT GAA GAG CAT GG - 3'
FCA090_R	5' - GTTTCTT TGT TAG CTC ATG TTC ATG TGT CC - 3'
FCA132_F	5' - ATC AAG GCC AAC TGT CCG - 3
FCA132_R	5' - GTTTCTT GAT GCC TCA TTA GAA AAA TGG C - 3'
FCA008_F	5' - ACT GTA AAT TTC TGA GCT GGC C - 3'
FCA008_R	5' - GTTTCTT TGA CAG ACT GTT CTG GGT ATG G - 3'
FCA043_F	5' - GAG CCA CCC TAG CAC ATA TAC C - 3'
FCA043_R	5' - GTTTCTT AGA CGG GAT TGC ATG AAA AG - 3'
FCA096_F	5' - CAC GCC AAA CTC TAT GCT GA - 3'
FCA096_R	5' - GTTTCTT CAA TGT GCC GTC CAA GAA C - 3'
FCA035_F	5' - CTT GCC TCT GAA AAA TGT AAA ATG - 3'
FCA035_R	5' - GTTTCTT AAA CGT AGG TGG GGT TAG TGG - 3'
FCA082_F	5' - TCC CTT GGG ACT AAC CTG TG - 3'
FCA082_R	5' - GTTTCTT AAG GTG TGA AGC TTC CGA AA - 3'
FCA275_F	5' - TTG GCT GCC CAG TTT TAG TT - 3'
FCA275_R	5' - GTTTCTT ACG AAG GGG CAG GAC TAT CT - 3'
FCA126_F	5' - GCC CCT GAT ACC CTG AAT G - 3
FCA126_R	5' - GTTTCTT CTA TCC TTG CTG GCT GAA GG - 3'
FCA057_F	5' - AAG TGT GGG ATT GGG TGA AA - 3'
FCA057_R	5' - GTTTCTT CCA TAA GAG GCT CTT AAA AAC TGA - 3'

*Menotti-Raymond et al. 1999

** Reverse primers modified from original published squence through the addition of "GTTTCTT" to encourage adenylation (addition of +a)

Table S2. Multiple Regression on Distance Models. Two relatedness estimates of relatedness (Dyadic Likelihood and Queller-Goodnight) as independent variables and resistance distances based on geographic layers as independent variables, including species-specific Resource Selection Functions (RSPF) from Day et al. 2016 this dissertation. *P-value calculated from 100 permutations.*

	Model ID	Dyadic Likelihood	R2	p-value	Queller Goodnight	R2	p-value
JAGUAR	Jnull	dyadml~EuclidDist	0.0866	0.340	quellergt~EuclidDist	0.0345	0.530
	J01	dyadml~RSPF	0.0966	0.250	quellergt~RSPF	0.0444	0.380
	J02	dyadml~EuclidDist*RSPF	0.0967	0.610	quellergt~EuclidDist*RSPF	0.0477	0.640
	J03	dyadml~EuclidDist+ITIBigRough	0.1896	0.261	quellergt~EuclidDist+ITIBigRough	0.0398	0.777
	J04	dyadml~EuclidDist+VegSmP	0.1884	0.310	quellergt~EuclidDist+VegSmP	0.1780	0.135
	J05	dyadml~EuclidDist+VegSmTF	0.1191	0.480	quellergt~EuclidDist+VegSmTF	0.0382	0.756
	J06	dyadml~EuclidDist+VegSimpH	0.1530	0.365	quellergt~EuclidDist+VegSimpH	0.0584	0.683
	J07	dyadml~LogEuclidDist	0.0493	0.464	quellergt~LogEuclidDist	0.0268	0.549
	J08	dyadml~EuclidDist+VillagesGiant	0.1593	0.361	quellergt~EuclidDist+VillagesGiant	0.1099	0.450
	J09	dyadml~EuclidDist+RdSmOne	0.1626	0.344	quellergt~EuclidDist+RdSmOne	0.0982	0.460
	J10	dyadml~EuclidDist+RdMed100	0.1636	0.362	quellergt~EuclidDist+RdMed100	0.1036	0.431
	J11	dyadml~EuclidDist+VegSmTF+RdSmOne	0.1630	0.597	quellergt~EuclidDist+VegSmTF+RdSmOne	0.1262	0.661
	J12	dyadml~VegSmTF	0.0426	0.508	quellergt~VegSmTF	0.0224	0.578
	J13	dyadml~VegSmP	0.0549	0.460	quellergt~VegSmP	0.1021	0.219
	J14	dyadml~VegSimpH	0.1287	0.252	quellergt~VegSimpH	0.0502	0.412
	J15	dyadml~VegSimpH+VegSmTF	0.2487	0.100	quellergt~VegSimpH+VegSmTF	0.0755	0.643
PUMA	Pnull	dyadml~EuclidDist	0.0062	0.770	quellergt~EuclidDist	0.0204	0.580
	P01	dyadml~RSPF	0.0123	0.640	quellergt~RSPF	0.0036	0.930
	P02	dyadml~EuclidDist+RSPF	0.0756	0.610	quellergt~EuclidDist+RSPF	0.2601	0.820
	P03	dyadml~EuclidDist+ITImedMod	0.0584	0.741	quellergt~EuclidDist+ITImedMod	0.0267	0.819
	P04	dyadml~EuclidDist+ITIsmMod	0.0696	0.670	quellergt~EuclidDist+ITIsmMod	0.0298	0.779
	P05	dyadml~EuclidDist+RdMed100	0.0065	0.967	quellergt~EuclidDist+RdMed100	0.0484	0.707
	P06	dyadml~EuclidDist+RdSmOne	0.0445	0.809	quellergt~EuclidDist+RdSmOne	0.0271	0.847
	P07	dyadml~LogEuclidDist	0.0147	0.657	quellergt~LogEuclidDist	0.0096	0.683
	P08	dyadml~EuclidDist+RiosBig	0.0527	0.706	quellergt~EuclidDist+RiosBig	0.0786	0.570
	P09	dyadml~EuclidDist+RiosGiant	0.0076	0.942	quellergt~EuclidDist+RiosGiant	0.1368	0.345
	P10	dyadml~RiosBig	0.0237	0.594	quellergt~RiosBig	0.0215	0.591
	P11	dyadml~ITImedMod	0.0085	0.776	quellergt~ITImedMod	0.0029	0.838
	P12	dyadml~RdMed100	0.0036	0.845	quellergt~RdMed100	0.0018	0.848
	P13	dyadml~ITImedMod+RdMed100+RiosBig	0.1805	0.608	quellergt~ITImedMod+RdMed100+RiosBig	0.0333	0.899
	P14	dyadml~ITIsmMod+RdSmOne+RiosGiant	0.2472	0.459	quellergt~ITIsmMod+RdSmOne+RiosGiant	0.0426	0.874

Table S3. Genotypes for Jaguar and Puma using 10 nuclear microsatellite loci. Samples were collected from two locations, Uxpanapa (UX) and northern Quintana Roo (QR). A subset of Uxpanapa samples were used for analysis of Individual Relatedness (x=used, - =unused due to missing data or lack of geographic location). Matching genotypes are clusterd and indicated with a single "X".

Location	Species	SampleID	Individual Relatedness	Location Comparison	FCA008	FCA008	FCA043	FCA043	FCA096	FCA096	FCA126	FCA126	FCA026	FCA026	FCA090	FCA090	FCA132	FCA132	FCA082	FCA082	FCA275	FCA275	FCA056	FCA056	Confirmed Alleles (20)	Confirmed Genoytpe (10)
UX	JAGUAR	U10JJ21	-	x	-99	-99	120	122	198	-99	-99	161	-99	154	114	-99	-99	-99	263	263	140	140	154	-99	9	4
UX	JAGUAR	U10JJ51	x	x	122	132	120	120	190	190	157	161	154	156	114	116	178	178	263	263	130	140	156	158	20	10
UX	JAGUAR	U10JJ60	x	x	122	132	122	122	184	200	157	161	154	154	118	120	178	178	263	263	130	140	158	158	20	10
UX	JAGUAR	U10JJ63			122	132	122	122	184	200	157	161	154	154	118	120	178	178	263	265	130	140	158	158		
UX	JAGUAR	U11JJ09	x	x	116	122	122	124	-99	206	161	161	156	156	116	118	178	178	263	-99	140	140	154	160	18	8
UX	JAGUAR	U11JJ20	-	x	120	122	-99	122	184	200	157	159	152	154	116	120	178	180	263	265	130	140	158	160	19	9
UX	JAGUAR	U11JJ51	x	x	116	122	120	122	190	206	159	161	154	154	120	120	180	182	263	263	136	140	152	158	20	10
UX	JAGUAR	U11JJ52			116	122	120	122	190	206	159	161	154	154	118	120	180	182	-99	263	136	140	-99	158		
UX	JAGUAR	U11JJ57	x	x	122	132	120	120	190	204	159	161	154	156	114	114	182	182	-99	263	130	140	160	160	19	9
UX	JAGUAR	U11JJ59	-	x	116	122	120	122	190	-99	159	161	-99	154	120	-99	-99	-99	-99	-99	136	140	158	-99	12	5
UX	JAGUAR	U11JJ64	x	x	114	116	120	122	200	202	157	161	154	154	114	116	178	180	263	263	130	140	160	164	20	10
QR	JAGUAR	Y08EDEN3		x	122	132	122	122	-99	-99	159	-99	-99	156	-99	118	-99	-99	-99	-99	130	140	-99	-99	9	3
QR	JAGUAR	Y08S22			122	122	122	*124*	190	206	-99	-99	154	154	114	114	178	178	263	-99	128	130	-99	160		
QR	JAGUAR	Y08S23		x	122	122	120	122	190	206	159	165	154	154	114	114	178	178	261	263	128	130	158	160	20	10
QR	JAGUAR	Y08S25			122	122	120	122	190	206	159	165	154	-99	114	114	178	178	263	-99	130	130	158	160		
QR	JAGUAR	Y08S40		x	132	132	122	122	-99	200	161	161	154	156	114	120	178	178	263	-99	140	140	158	160	18	8
QR	JAGUAR	Y08S54		x	116	122	120	120	190	206	161	161	154	154	116	116	178	178	263	263	130	136	160	160	20	10
QR	JAGUAR	Y08S55			116	122	120	120	190	206	161	161	154	154	116	116	178	178	263	263	130	136	-99	160		
QR	JAGUAR	Y08S60		x	122	122	-99	-99	190	-99	159	161	152	154	-99	118	178	-99	263	-99	140	-99	160	160	13	4
QR	JAGUAR	Y08S89		x	130	132	120	120	190	200	161	165	154	156	114	114	178	-99	-99	263	130	140	-99	160	17	7
QR	JAGUAR	Y08S93		x	132	-99	120	120	-99	-99	-99	165	154	156	114	114	-99	-99	263	-99	130	140	160	160	13	5
UX	PUMA	U10JJ12	x	x	154	172	138	140	198	212	140	140	146	156	116	116	182	186	249	249	136	140	156	158	20	10
UX	PUMA	U11JJ06	x	x	154	172	128	136	196	198	136	140	140	146	116	116	176	176	249	-99	136	146	156	158	19	9
UX	PUMA	U11JJ21	x	x	154	172	128	138	198	216	136	138	140	146	112	116	176	184	249	255	142	146	152	158	20	10
UX	PUMA	U11JJ43	x	x	154	156	128	138	202	202	140	140	146	146	108	116	176	186	249	251	140	142	152	152	20	10
UX	PUMA	U11JJ44	x	x	154	172	128	138	196	214	136	140	146	156	104	120	176	186	249	257	142	142	152	156	20	10
UX	PUMA	U11JJ47	x	x	154	172	138	142	198	216	140	140	140	146	114	116	178	178	249	255	142	146	152	156	20	10
QR	PUMA	Y08S15		x	154	154	130	-99	208	208	134	140	140	146	116	118	176	182	251	257	142	142	152	158	19	9
QR	PUMA	Y08S18			154	154	-99	130	208	208	134	140	140	146	116	118	-99	-99	251	-99	142	142	152	158		
QR	PUMA	Y08S31		x	154	154	138	140	208	-99	140	140	-99	-99	108	116	176	176	251	255	142	142	-99	160	20	10
QR	PUMA	Y08S34			154	154	138	140	208	208	140	140	146	158	108	116	176	176	251	255	142	142	158	160		
QR	PUMA	Y08S47		x	154	154	128	130	-99	208	140	140	146	154	108	116	182	182	-99	-99	146	150	156	160	20	10
QR	PUMA	Y08S49			154	154	128	130	208	208	140	140	146	154	108	116	182	182	251	253	146	150	156	160		
QR	PUMA	Y08S51		x	152	154	128	130	208	208	140	140	146	154	108	116	182	182	251	253	146	150	156	160	20	10
QR	PUMA	Y08S66		x	154	154	130	138	198	216	140	140	146	158	-99	116	178	-99	249	249	140	146	148	158	18	8

Table S4. Tests for departures from Hardy-Weinberg equilibrium by locus for all samples (Overall), or by location (UX = Uxpanapa, QR = Quintana Roo).

JAGUAR	Locus	Overall (*n=16*)				UX (*n=9*)	QR (*n=7*)
		chi^2	df	Pr(chi^2 >)	Pr.exact	Pr.exact	Pr.exact
	FCA008	21.2263	15	0.129753427	0.028	0.02	0.161
	FCA043	22.21895	6	0.001105068	0.036	0.535	0.207
	FCA096	36.07545	28	0.140686532	0.046	0.001	0.566
	FCA126	13.06485	10	0.220068578	0.234	0.268	0.949
	FCA026	1.65155	6	0.948800099	0.837	1	1
	FCA090	17.1307	10	0.071521547	0.013	1	0.001
	FCA132	24.84771	6	0.000364348	0	0.262	1
	FCA082	1.819226	6	0.93555087	0.819	0.428	0.186
	FCA275	6.685264	10	0.754786188	0.709	0.165	1
	FCA056	9.709366	21	0.98244419	0.844	0.566	0.469
PUMA	Locus	Overall (*n=11*)				UX (*n=6*)	QR (*n=5*)
		chi^2	df	Pr(chi^2 >)	Pr.exact	Pr.exact	Pr.exact
	FCA008	1.983471	10	0.99646527	1	0.001	1
	FCA043	28.0102	21	0.139862171	0.079	0.331	0.17
	FCA096	57.79882	28	0.00077207	0.001	0.09	0.001
	FCA126	18.67769	10	0.044552773	0.071	0.187	1
	FCA026	16.6	15	0.343333012	0.321	0.733	1
	FCA090	43.4	28	0.031826883	0.166	0.001	0.001
	FCA132	25.72917	15	0.040967615	0.002	0.001	0.001
	FCA082	12.5713	15	0.63537273	0.591	1	0.132
	FCA275	23.09277	15	0.0821899	0.02	1	0.001
	FCA056	18.06122	15	0.259460489	0.339	1	0.001

APPENDIX- FIGURES:

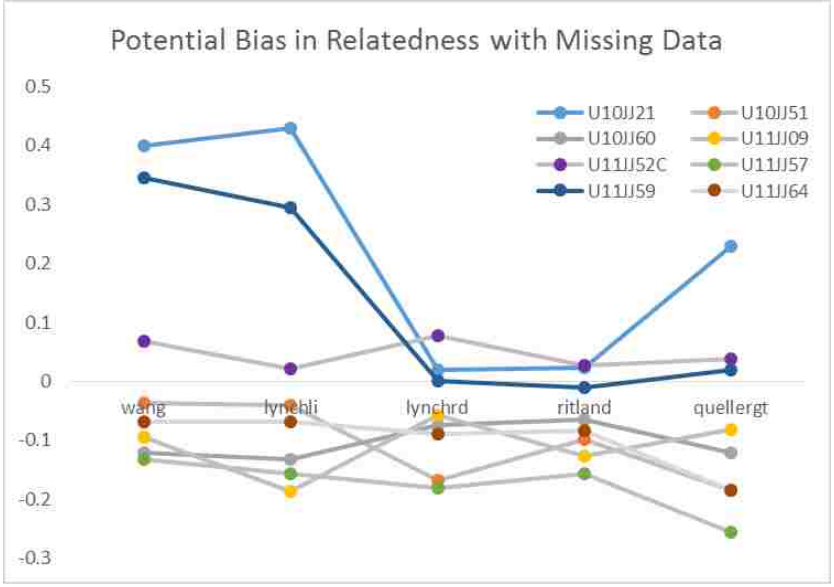

Figure S1. Potential Bias in Relatedness estimation (y-axis) with missing genotype data across multiple estimators (x-axis categories). Blue lines indicate the two samples with more missing data than the other samples.

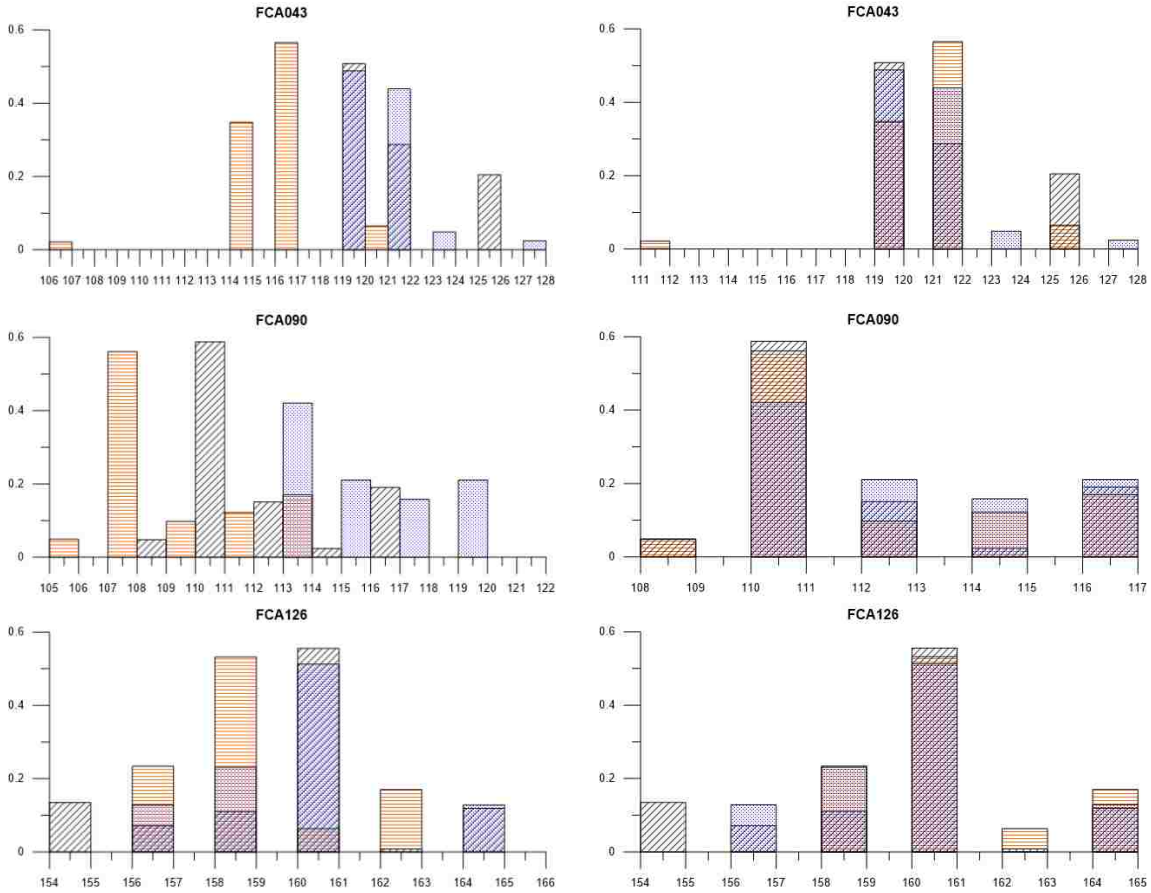

Figure S2. Visual adjustment of three microsatellite allele frequencies from three jaguar research groups. LEFT: Original distribution of alleles for each study. RIGHT: Maximum concordance of allele sizes achieved by adding or subtracting integers.

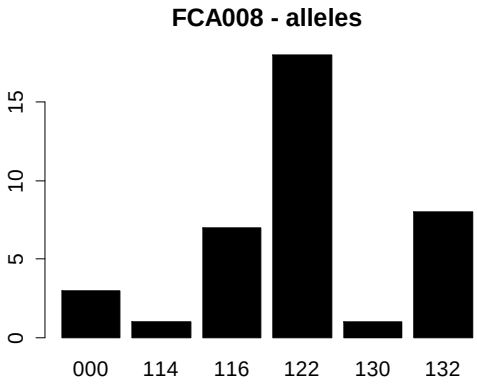
FCA008 - alleles
0
5
10
15
000
114
116
122
130
132

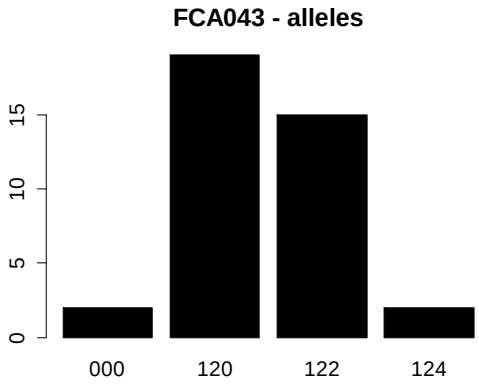
FCA043 - alleles
0
5
10
15
000
120
122
124

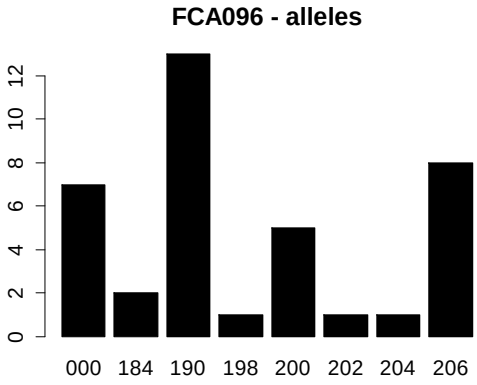
FCA096 - alleles
0
2
4
6
8
10
12
000
184
190
198
200
202
204
206

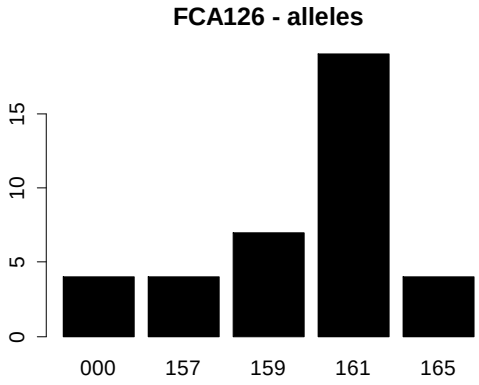
FCA126 - alleles
0
5
10
15
000
157
159
161
165

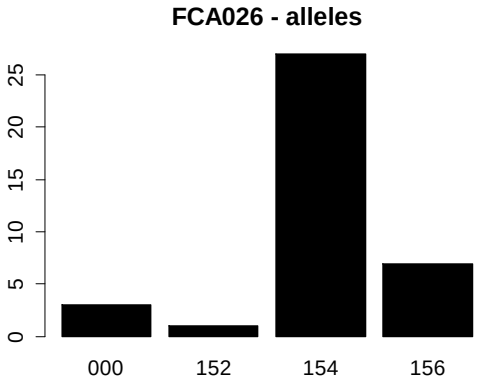
FCA026 - alleles
0
5
10
15
20
25
000
152
154
156

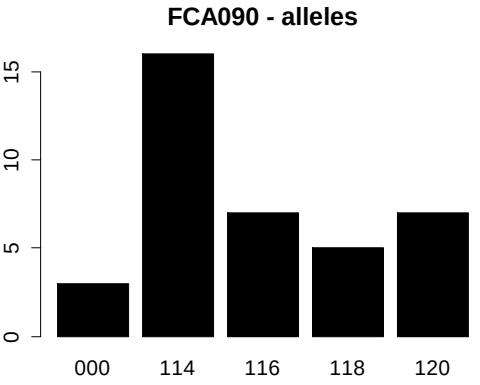
FCA090 - alleles
0
5
10
15
000
114
116
118
120

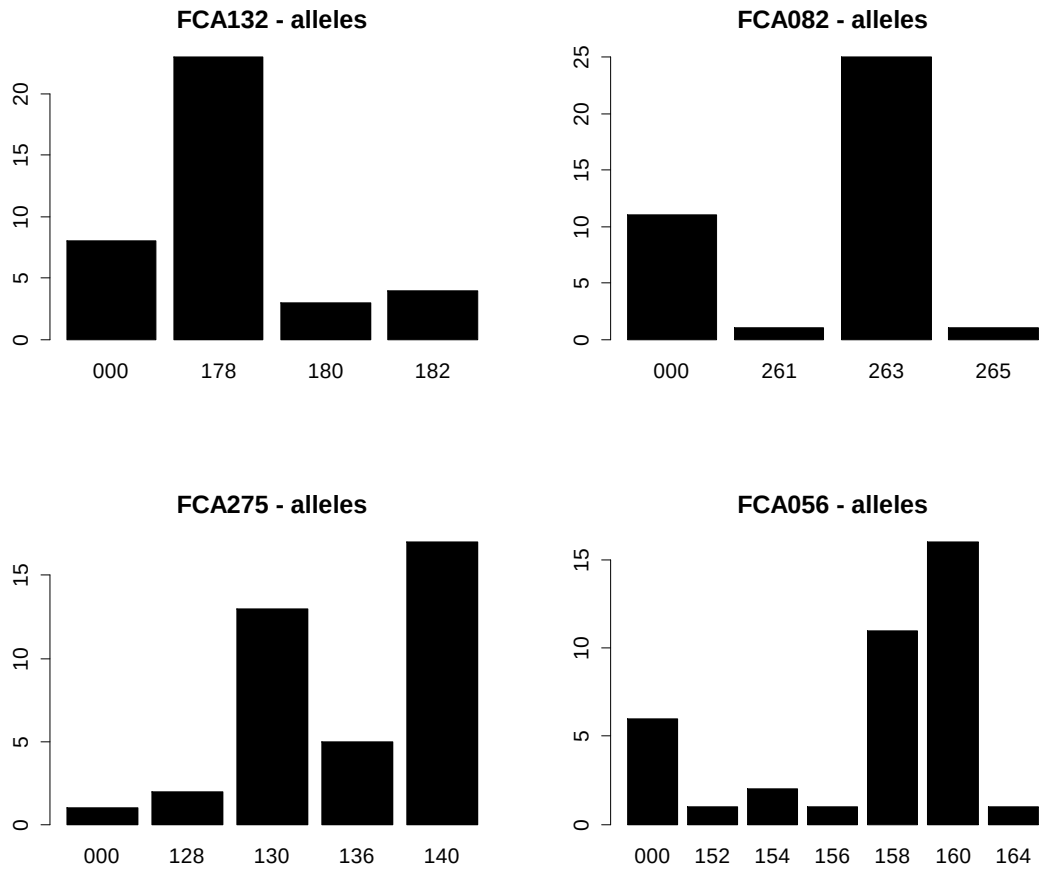

Figure S3. Jaguar allele frequencies

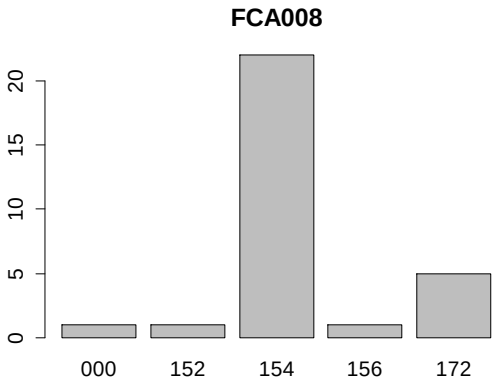
FCA008
0
5
10
15
20
000
152
154
156
172

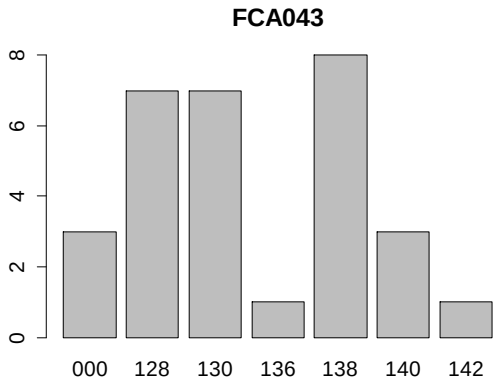
FCA043
0
2
4
6
8
000
128
130
136
138
140
142

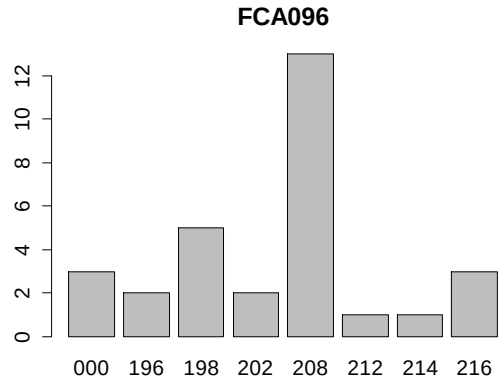
FCA096
0
2
4
6
8
10
12
000
196
198
202
208
212
214
216

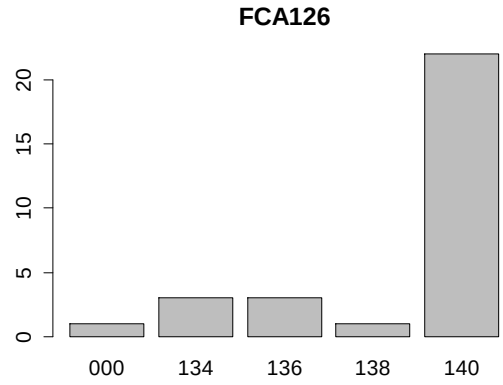
FCA126
0
5
10
15
20
000
134
136
138
140

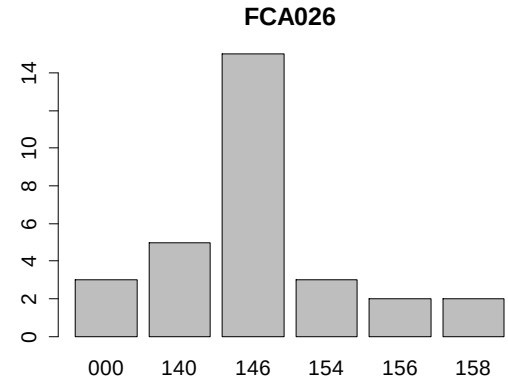
FCA026
0
2
4
6
8
10
14
000
140
146
154
156
158

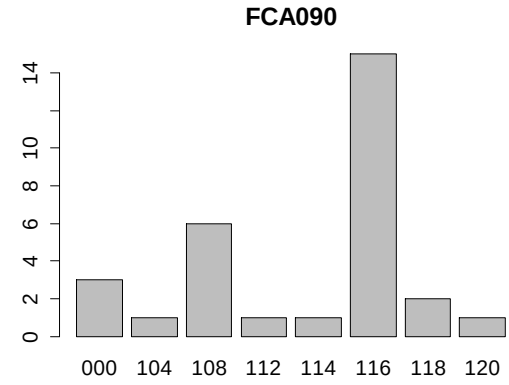
FCA090
0
2
4
6
8
10
14
000
104
108
112
114
116
118
120

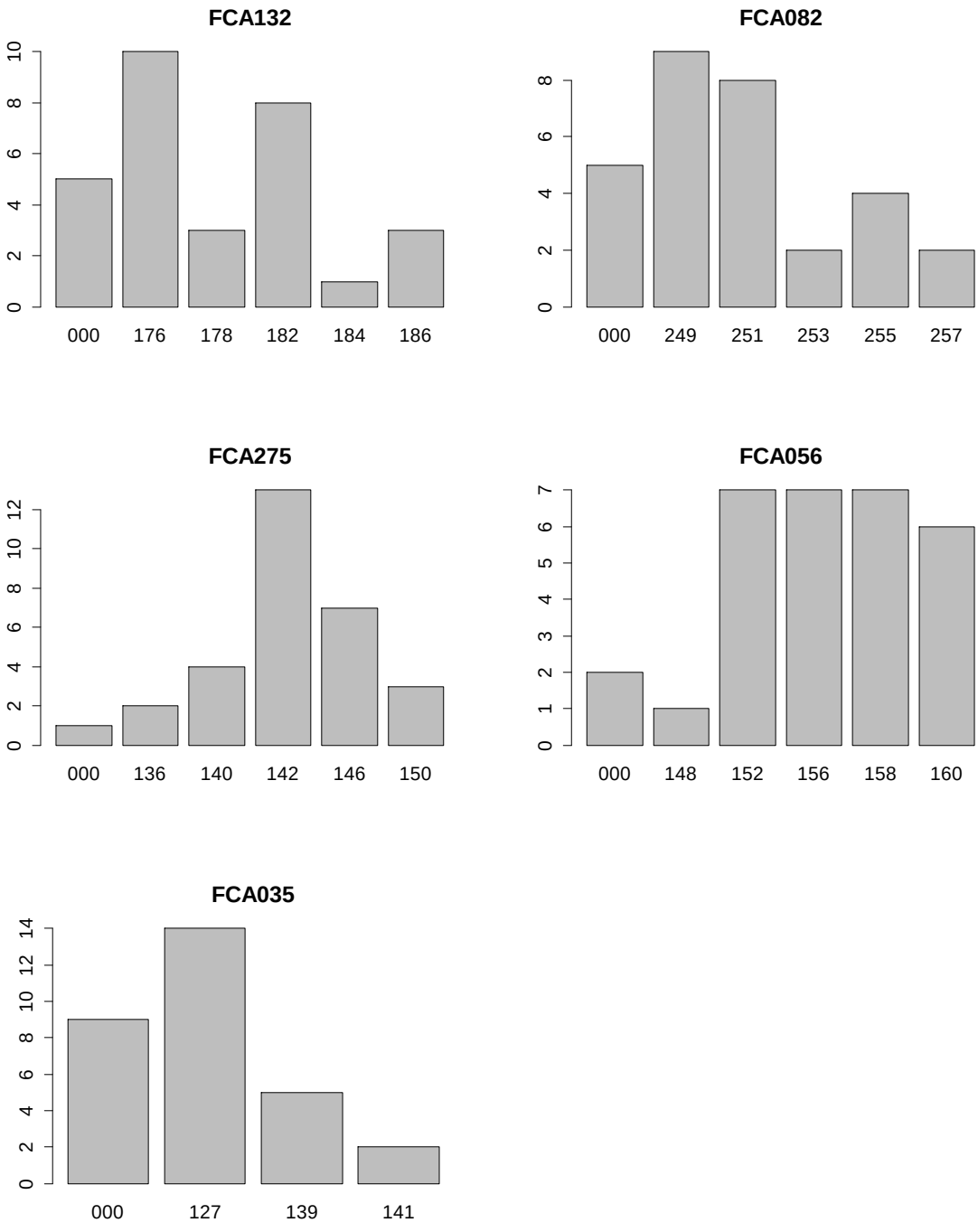

Figure S4. Puma allele frequencies

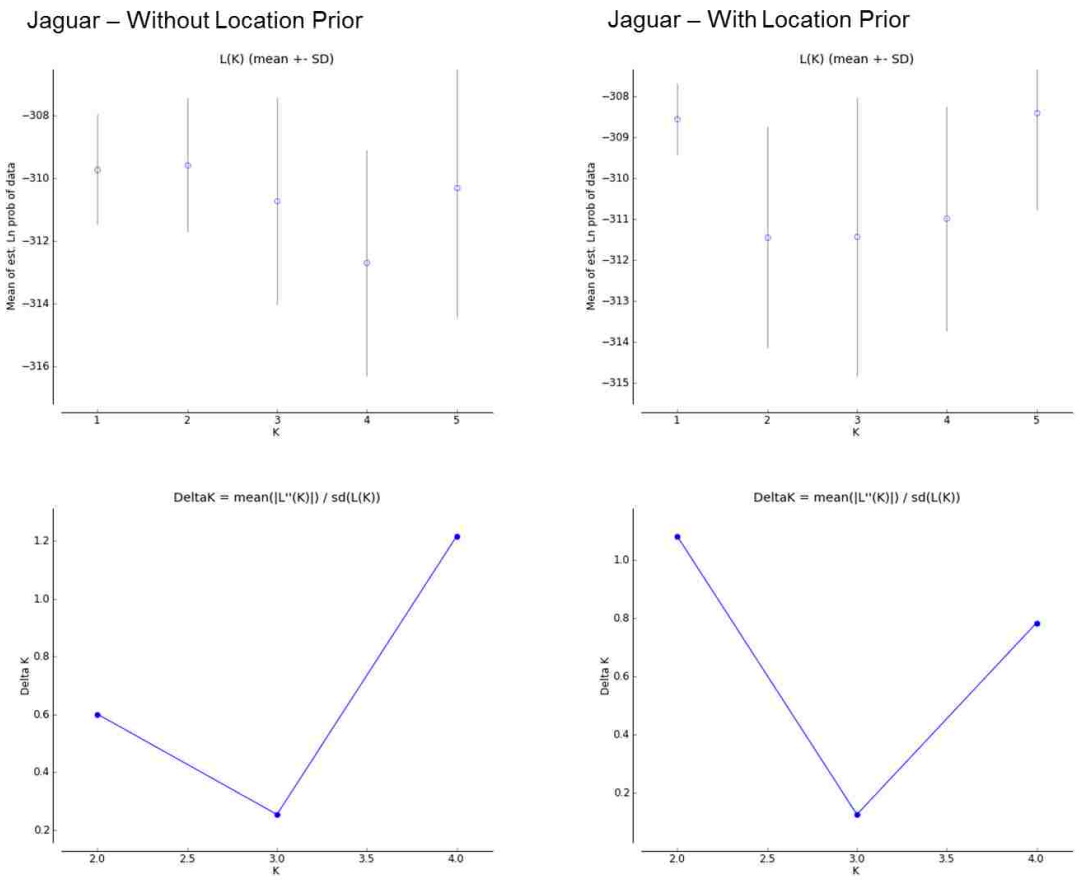

Figure S5. Support for number of Bayesian clusters for Jaguar, either with or without using location as a prior.

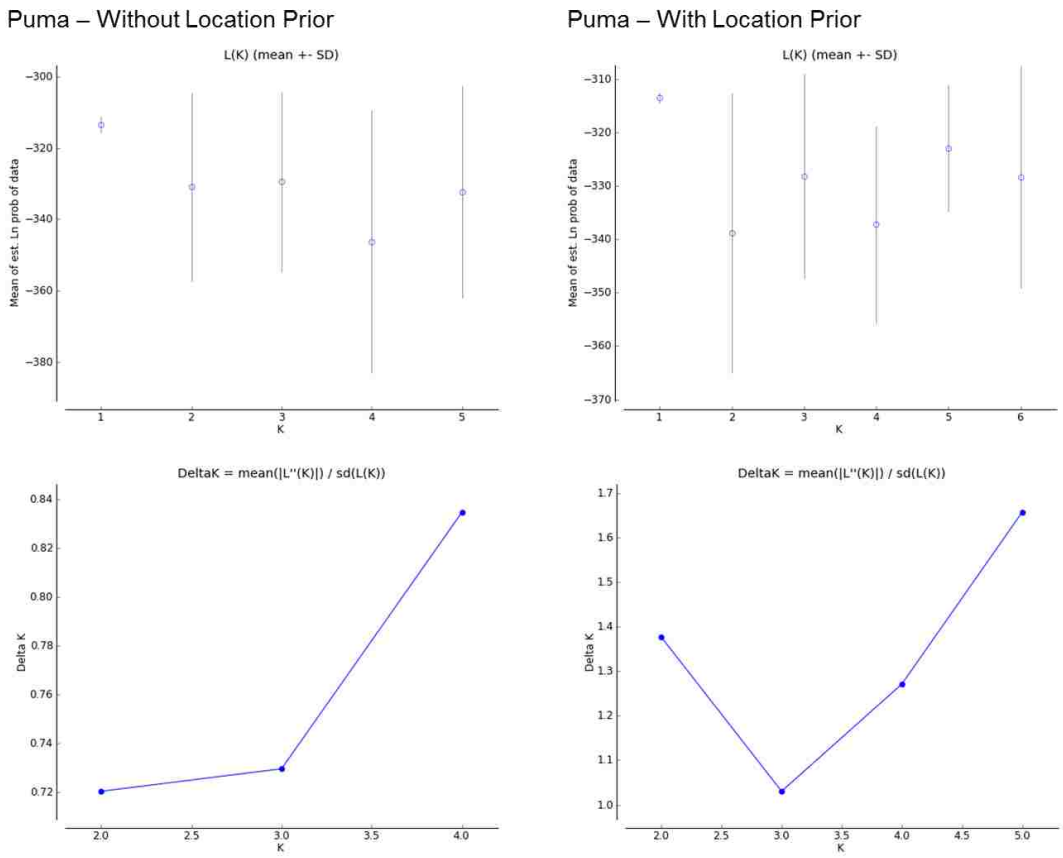

Figure S6. Support for number of Bayesian clusters for puma, either with or without using location as a prior

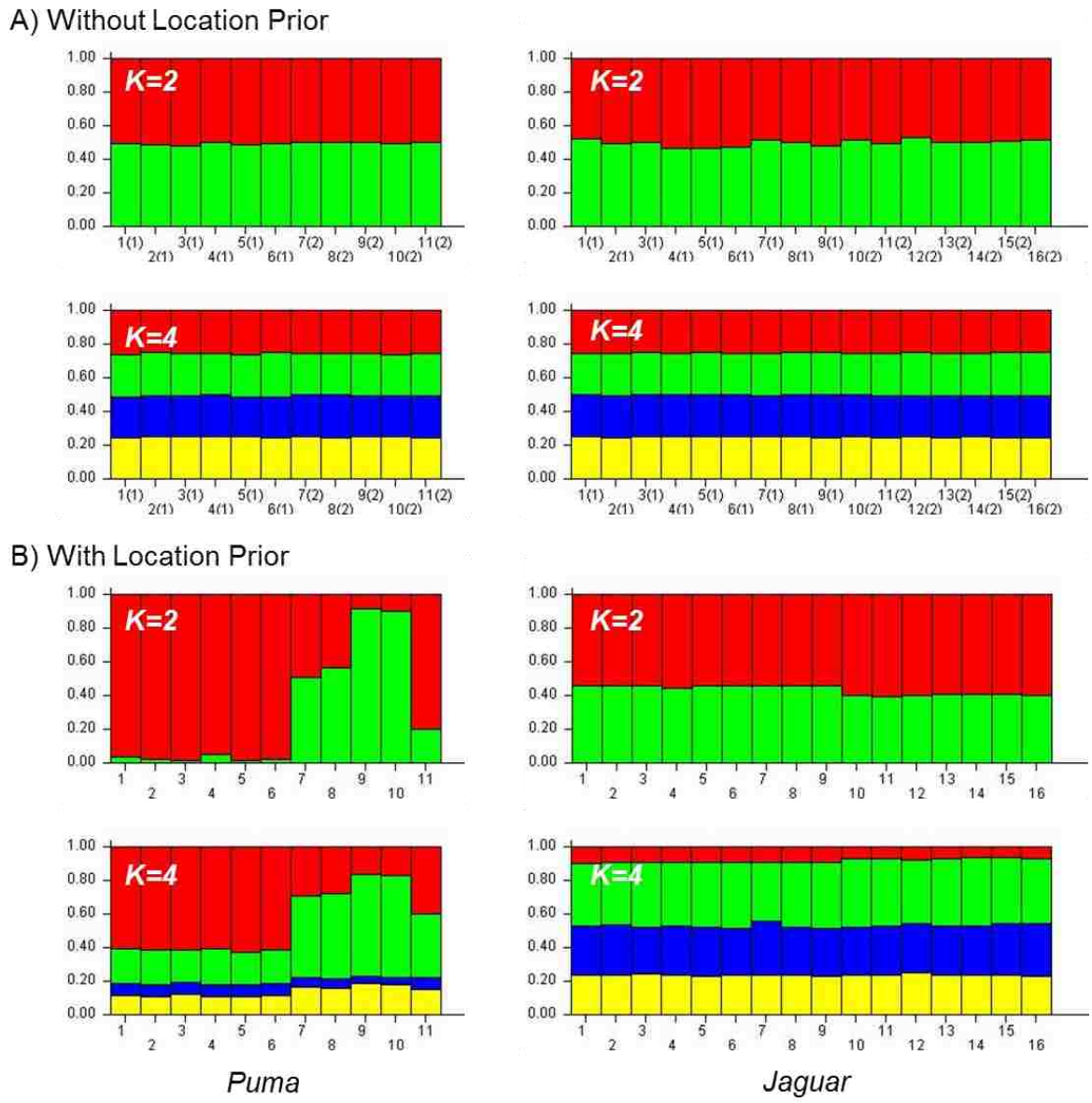

Figure S7. Representative assignment bar plots for two (K=2) or four (K=4) genetic clusters for jaguar and puma, either without (A) or with (B) using location as a prior.

CHAPTER 3: HexSim with Genetics Toolkit: An Individual-based Spatially-explicit Eco-evo Modeling Platform for Integrating Population Dynamics, Movement Ecology, and Evolutionary Processes.

Jennifer M.W. Day[1]*, Nathan Schumaker[2]

[1] Center for Conservation Biology, Department of Biology, University of Washington, Seattle, USA

[2] U.S. Environmental Protection Agency, Western Ecology Division, Corvallis, OR, USA

ABSTRACT

The inherent complexity of eco-evolutionary (hereafter eco-evo) dynamics make the development of both theory and applications challenging, thus increasing researchers' reliance on computer simulations. This manuscript begins with an introduction to eco-evo dynamics, highlighting specific challenges to eco-evo modeling within four focal disciplines (1) Landscape Genetics, (2) Population Genetics, (3) Conservation Biology, and (4) Evolutionary Ecology. We then describe a theoretical model within the platform, HexSim, that explores how spatial pattern can drive eco-evo dynamics.

HexSim has the capacity for integrating complex movement ecology and demographics while also including flexible genetic traits. The purpose of this manuscript is twofold: (1) Illustrate the platform's ability to recapitulate expectations from theory, here referred to as "core concepts", in each focal discipline, thereby demonstrating the platform's reliability. (2) Provide simple examples of how the platform's capacity for biological realism may be used to address methodological challenges in each discipline.

Our theoretical model was designed to illustrate gene flow, drift, and selection on populations inhabiting a spatially-subdivided landscape. The simulation model treatments include two levels of landscape permeability, two types of dispersal behavior, and two rules governing the strength of selection acting on locally adaptive alleles. Our results exhibit plausible patterns of isolation by distance, genetic drift, extinction probabilities, and population growth in response to landscape pattern and model treatment. We highlight results that overcome some of the existing methodological challenges to eco-evo modeling, such as reliance on resistance surfaces as a proxy for past gene flow, and the treatment of migration-rates as a model input rather than a synthetic emergent model output.

Future applications of HexSim may include investigating how eco-evo dynamics are affected by complex movement ecology such as territoriality, herd-movement, or natal affinities. Other potential applications include examining the driving force of landscape pattern in eco-evo dynamics, with either theoretical, geographically explicit, or dynamic landscapes. The flexible genetic traits of HexSim allow for linkage, polymorphic loci, multiple mutation models and more. The platform tracks demo-genetic output simultaneously. Future applications may use the demographic and genetic output to complete the eco-evo feedback loop, with genetic traits dynamically impacting ecological traits. The work described here is an exploration of new methods that capture some of the biological realism that researchers have long agreed drives ecology and evolution, but which are difficult to incorporate into theories, models, and policies.

Keywords: individual-based modeling, conservation genetics, population genetics, landscape genetics, evolutionary ecology

INTRODUCTION

Eco-evolutionary dynamics include unidirectional and reciprocal interactions between biological forces at both the ecological and evolutionary ends of the spatio-temporal spectrum (Figure S1). Eco-evolutionary (hereafter "eco-evo") dynamics include the classic unidirectional eco-evo dynamic, natural selection, in which ecological change affects the evolution of allele frequencies within a population. While reciprocal feedbacks have been theorized for a long time, the longer time scales at which evolutionary forces operate has generally been viewed as too slow to influence observable ecological responses. This perception of temporal disparity, as well as past methodological limitations in tracking the molecular genetics of selection, slowed the development of research into eco-evolutionary dynamics until recently. With advances in molecular genetics, the time scales between evolutionary and ecological forces have been shown to be sufficiently coincident (Kinnison and Hendry 2001) and feedbacks from rapid-evolution impinging on ecological processes have been directly observed in an increasing number of natural systems (Thompson 1998; Hairston et al. 2005; Fanie Pelletier et al. 2007; Sinervo, Svensson, and Comendant 2000; Laland, Odling-Smee, and Feldman 1999; Yoshida et al. 2003). This has accelerated the resurgence of research into eco-evolutionary dynamics (F. Pelletier, Garant, and Hendry 2009; Ezard, Côté, and Pelletier 2009; Saccheri and Hanski 2006; Fussmann, Loreau, and Abrams 2007; Carroll et al. 2007), with recent work including observational (Palkovacs and Post 2008; Hanski and Saccheri 2006), experimental (Sinervo, Svensson, and Comendant 2000; Yoshida et al. 2003), and theoretical approaches (Laland, Odling-Smee, and Feldman 1999).

Eco-evo dynamics are shaped by landscape spatial pattern and thus mediated by movement (Figure S1). The influence of spatial pattern on eco-evo dynamics spans all spatio-temporal scales and many scientific disciplines, from cancer development within spatially structured populations of somatic cells (Martens et al. 2011) to ecosystem responses to climate change [*reviewed in* (Walther et al. 2002). The eco-evo responses of interest vary by discipline, yet again are all influenced by spatial pattern and

movement. For example, evolutionary geneticists may follow the evolution of heritable traits responding to spatially heterogeneous selection pressures, population geneticists may examine changes in allele frequencies influenced by spatially-restricted gene flow, phylogeographers may investigate coalescent timing across glaciations, and conservation biologists may explore links between genetic diversity and resilience in spatially isolated populations. As the rate of anthropogenic landscape change increases, determining how spatial pattern influences eco-evo dynamics becomes a more crucial component of predicting biotic resilience.

Here, we illustrate how the simulation platform, HexSim can model spatial drivers of eco-evo dynamics. We propose that this linkage might be used to better explore and communicate eco-evo dynamics within four focal disciplines; 1. Landscape Genetics, 2. Population Genetics, 3. Conservation Biology, and 4. Evolutionary Ecology. Spatially-explicit individual-based simulation models capable of linking both ecological and evolutionary processes are growing in number and improving in quality (Hoban, Bertorelle, and Gaggiotti 2012; Epperson et al. 2010). However, HexSim is capable of modeling a full complement of genetic and demographic sophistication. HexSim differs from other available platforms in several aspects relevant to the study of eco-evo dynamics. First, life history processes are directly linked to static or dynamic landscape maps, and multiple spatial drivers can simultaneously influence different parts of the same simulation. Further, movement responses to landscape structure are not constrained by a reliance on resistance surfaces, patch-mosaic structures, stepping stones, or the use of graph-theoretic networks – all simplifications that are frequently employed to speed model development or improve tractability, but at a cost to biological realism.

Below, we briefly discuss the methodological challenges currently limiting simulation approaches within each of four focal disciplines. Descriptions of each discipline below are simplified for the sake of brevity.

(1) Landscape Genetics seeks to understand how landscape pattern influences gene flow. A standard approach is to compare inter-individual genetic distance to metrics of landscape structure, often quantified as distance cost across a resistance surface. Currently available landscape genetics modeling platforms have been limited in either spatial, demographic, or behavior sophistication (Balkenhol, Waits, and Dezzani 2009). While these constraints may not pose issues for many studies, some species of interest will require a full complement of complexity to realistically model gene flow. Additionally, most platforms cannot simultaneously simulate multiple interacting eco-evo drivers of gene flow, such as local adaptation along with source-sink demographics (Hoban, Bertorelle, and Gaggiotti 2012).

(2) Population Genetics investigates the causes and consequences of population genetic structure. Biological forces such as selection and mutation rates can be spatially patterned by landscape structure, yet are often assumed to be spatially uniform for simplicity. Additionally, in classic population genetic models, spatial complexity is reduced to discrete populations, and migration processes are characterized by a single univariate input parameter, '*m*'. These simplifications have facilitated the generation of a wealth of theory; but, a lack of biological realism and/or spatial complexity limits application of this theory to systems in which space is continuous and dynamic (e.g. successional forest under a disturbance regime), or cases where gene flow is governed by complex movement and mating behavior (e.g. stage-specific movement behavior and territoriality).

(3) Conservation Biology is a broadly defined discipline, but at its core investigates forces affecting population viability. Landscape pattern drives population viability through its influence on ecological and evolutionary processes. The relative importance of demography versus genetics is actively debated in the conservation literature (Lande 1988; Frankham 2005). Some forecasting tools can simulate inbreeding rates and incorporate them into probabilities of extinction (e.g. *Vortex*), but existing models simplify the linkages between ecological and evolutionary processes, which limits the

applied utility of such forecasts. For example, a platform capable of simulating complex interacting demographic and genetic traits is necessary to forecast the consequences of landscape changes that will alter an organism's habitat quality and pattern (eco), while simultaneously impacting its mate-finding or natural selection processes (evo).

(4) Evolutionary Ecology explicitly explores the interactions and feedbacks between ecological and evolutionary forces that subsequently affect demographic and genetic traits. As addressed above, landscape pattern shapes the myriad feedbacks through which biological forces influence population and community demo-genetic traits. A resurgence of interest in these processes has underscored the need for biologically sophisticated, mechanistic simulation platforms capable of explicitly modeling dynamic eco-evo feedbacks in a spatially-realistic setting.

Here, we demonstrate how the explicit inclusion of spatial pattern and movement ecology can advance eco-evo theory and its applications to the four focal fields listed above, using a theoretical model built within the HexSim platform. Our model individuals have a simple life-cycle with density dependent reproduction, juvenile dispersal, probabilistic mortality, and local adaptation during part of the simulation. Biological forces (e.g. migration rates and genetic drift) and observable demographic and genetic responses (e.g. population size and allele frequencies) emerge mechanistically from changes to landscape structure. Our model landscape consists of adjoining habitat patches of three sizes, and the connectivity between those patches varies through the simulation. For each discipline, we highlight results that (a) illustrate *a priori* expectations of an eco-evo dynamic fundamental to the discipline, here referred to as "core concepts", and that (b) illustrate how adding biological and spatial complexity can enhance modeling applications (Table 1).

Table 1. How landscape spatial pattern and biological realism are important to four focal disciplines. For each discipline we illustrate one core concept, and one advancement our work brings to eco-evo investigations.

Discipline	Research Question	Topics of Highlighted Results	
		Core Concept	*Advancement*
LANDSCAPE GENETICS	How is gene flow controlled by the landscape?	Isolation by Distance is a function of dispersal behavior.	Replacing resistance surfaces and cost-distance matrices with measures of genetic distance arising from eco-evo processes and species-landscape interactions.
POPULATIONS GENETICS	How is genetic structure controlled by the landscape?	Genetic structure is influenced by IBD & demographics.	Allowing migration rates between populations to emerge mechanistically from the interplay between dispersal behavior and landscape structure.
CONSERVATION BIOLOGY	How are inbreeding and population viability controlled by the landscape?	Homozygosity and stochastic extinction are consequences of demographic processes.	Insuring that forecasts of genetic degradation are driven by spatially-realistic movement models and incorporate pre-existing genetic structure and diversity.
EVOLUTIONARY ECOLOGY	How are feedbacks between ecological and heritable traits controlled by the landscape?	Population size is an ecological response to the evolutionary force of selection.	Creating eco-evo feedback loops between local selection for specific alleles and counteracting asymmetric migration stemming from source-sink dynamics in heterogeneous landscapes.

MATERIALS AND METHODS

Our study was built around a theoretical simulation that is relatively simple compared to the ecological complexity capable within the HexSim modeling platform (Schumaker 2016). HexSim is a windows-based platform with graphical user interface. Originally designed for population viability analysis, HexSim itself has evolved, and the platform now contains a large collection of features for developing demographic models, includes a thoroughly-integrated genetics toolkit, and can track multiple demographic and genetic outputs simultaneously.

Landscape Structure: HexSim spatial data (maps) are assembled from a space-filling arrays of hexagonal cells. Our landscape was composed of six adjacent habitat patches (2 of each small, medium, and large patches) built up from multiple hexagonal cells (each of equal quality), embedded in a non-habitat "matrix", without gradients (Fig 1) (Text S1 for more detail). A set of movement barriers was, at times, used to isolate the six patches from each other. At other times, small semi-permeable openings in the movement barriers allowed limited dispersal between neighboring patches. These barrier openings were identical in size, and assigned equal transmission probabilities (within any given simulation).

Ecological Characteristics: Our simulations ran for a series of "time steps" (implicitly defined in HexSim, but corresponding here to a year), with a sequence of life history events and species-landscape interactions being performed at each step. In brief, the life cycle consisted of (a) resource acquisition, (b) pair formation, (c) reproduction, (d) juvenile dispersal, and (e) survival (Figure S2). The individuals making up our simulated population included both sexes and two age classes (juvenile and adults). Females were allowed to reproduce only if they could pair with a male within a circular neighborhood. Reproductive rates were normally distributed with mean values based on the amount of resource individuals were able to acquire, which introduced a density-dependent feedback that was further modified by the requirement for pair-formation. Individuals acquired their resources from a roughly-circular neighborhood of 37 hexagonal cells, and these resources were shared equally among all individuals attempting to utilize them (scramble competition). Juveniles dispersed from their natal site in the year of their birth, and transitioned to adults at the start of the subsequent year (there was no neonatal mortality). Adults did not move in our simulations. Dispersal within HexSim can be intricately parameterized, but our simulated movement behavior was simple. Dispersal path lengths were drawn

from one of two uniform distributions, either "short" (1-5 hexagon steps) or "long" (5-25 hexagon steps). Dispersal paths were moderately auto-correlated, but otherwise random. Individual dispersers took a series of steps from hexagon to adjacent hexagon, and stopped when their path length had been reached. Yearly survival probability was determined on the basis of stage class (juvenile = 0.5, adult = 0.885), but individuals with less than 20% of their resource goal experienced an additional 10% probability of mortality. Our simulations included a period in which survival decisions were also based on genetic adaptation. In these cases, mortality rates that were previously determined by stage class became jointly determined by stage class, location, and genotype (see below).

Evolutionary Characteristics: Our simulation agents were diploid with ten loci and zero linkage between loci. The starting population was assigned alleles drawn randomly from a collection of five per locus, labeled A1-A5, based upon locus-specific initial allele frequencies of our choosing (Table S1). The initial allele frequencies were not spatially stratified, and we did not simulate mutation. Offspring genotypes were assembled by drawing a single allele from each parent at each locus, without linkage. Individuals possessed five purely neutral loci (L1-L5), and five loci (L6-L10) containing at least one allele capable of conferring a fitness advantage. These locally adaptive alleles imparted a survival gain to juveniles when they were in the habitat type (type "A" vs. type "B") to which they were genetically pre-adapted (Table S1). The survival gain (S) per adaptive allele was either strong (S = 0.10) or weak (S = 0.01). Selection, modeled this way, was a predictable process because genotype dictated the mean juvenile survival probability. Selection was initiated at time-step 3000. All ten loci were used for all genetic analyses described below, with the exception of adaptation, for which only L6-L10 were used.

Progression of Landscape Change: Our initial landscape was continuous, of uniform quality, and free from movement barriers. This landscape persisted for the first 1000 simulation time steps,

hereafter referred to as the *Continuous* epoch (Fig 1). We anticipated that Isolation by Distance (IBD) would be the predominant evolutionary force in this landscape. To simulate the effect of drift alone, we then imposed absolute movement barriers that isolated sub-populations from each other within landscape patches for the subsequent 1000 simulation time steps. We refer to this epoch as *Isolated Patches*. Six separate patches were delineated by the movement barriers, with two patches each of three different sizes. Following patch isolation, we created small gaps in the movement barriers between patches, allowing infrequent migration between the previously isolated sub-populations. Barrier gaps varied in permeability (high = 0.70 transmission probability per encounter, low = 0.02 transmission probability per encounter), affecting the likelihood that agents would cross the barrier when they encountered a gap during dispersal. We refer to this third epoch of 1000 time-steps as *Semi-connected*. During the final 1000 time steps, the landscape patches were each assigned one of two "habitat types" that conferred increased fitness to juveniles with specific genotypes, as previously described. We refer to this landscape as *Semi-connected with Local Selection*.

Treatments and Observable Responses: Agent dispersal behavior (long vs. short), strength of selection (strong vs. weak), and barrier gap permeability (low vs. high) together formed eight treatment combinations. Each treatment was repeated in ten replicates. For each treatment, we tracked individual genotypes, per-capita homozygosity, per-patch population size, and the number of dispersers moving between the patches. We did not track individual pedigree information. Upon completion of the simulations, we used HexSim's report generator to create files suitable for input to the genetic

software package STRUCTURE (Pritchard, Stephens, and Donnelly 2000). See S2 Text for processing time and computational requirements.

Analysis: Generation time was not an input parameter in our model, but instead was calculated from simulation results. The female agents in our model could reproduce beginning in their second time-step, and could continue to do so in each time step until their death, thereby producing overlapping generations. We measured generation time as the observed average age of reproducing females (Hamilton 1966).

Migration rates between patches were calculated using the recorded number of patch transitions during the *Semi-connected* epoch. To qualify as a migrant, individuals had to both cross through a barrier gap connecting two patches, and subsequently reproduce somewhere other than their natal patch. Collected this way, our migration data intentionally excluded non-breeders (mostly those who died as juveniles), and individuals that reproduced in their natal patch after making a temporary excursion elsewhere. For the purpose of computing the average number of migrants per generation, each barrier crossing location (barrier gap) was treated as an independent sample, thus migration is reported at the scale of the landscape patch.

The four highlighted disciplines differ not only in their central research questions, as described above, but also in their genetic analytical approaches. We analyzed the results of our simulations with an eye to each of these approaches:

Landscape Genetics: Isolation by distance (IBD) produced by dispersal limitations (Wright 1943) is a core concept in landscape genetics. We used results from the *Continuous* epoch to illustrate the degree of IBD for our short and long-distance dispersal treatment groups. We constructed dispersal kernels by plotting the frequency of observed dispersal distances for all individuals in all replicates from time step 1 to 1000. We visually assessed the degree of IBD using correlograms generated by the

application *Alleles in Space* (Miller 2005), where the average genetic distance between individuals is plotted for varying distance classes. We also plotted the frequency of observations for each distance class, to ensure that the inter-individual genetic distances were not due to underlying distribution of individuals on the landscape.

We calculated inter-individual genetic-distances resulting cumulatively from each landscape history. For ease of illustration, we subset our results as follows: For each treatment group, we randomly selected a single replicate simulation. From the selected replicate, we extracted genotype reports from the last time step of each of the four landscape epochs. From those reports, we randomly selected 25 individuals from each of the six patch locations. For those 150 individuals, we calculated a simple metric of pairwise genetic distance (number loci for which alleles differ between individuals / total number loci) using the "*ape"* R (v3.2.2) package "*dist.gene"* function with "*percentage"* method (R Core Team 2013; Paradis, Claude, and Strimmer 2004). We visualized the 150x150 pairwise genetic distances as triangular matrices.

Population Genetics: We used a Bayesian clustering method, implemented by the program STRUCTURE (v 2.3.4), to analyze population genetic structure (Pritchard, Stephens, and Donnelly 2000). At the end of each landscape epoch, we collected genotype information stratified by putative population (patch), and imported these data into STRUCTURE. Unequal sample sizes (small patches ≈ 25 individuals, large patches ≈ 1000) interfered with the assessment of the number of subpopulations and assignment probabilities (data not shown). This known limitation of the software (Pritchard, Wen, and Falush 2010) was overcome by randomly drawing a fixed number of individuals (n=25) from each patch for analysis. In cases where there were fewer than 25 individuals extant in a given patch, genotypes were randomly selected for inclusion with replacement until each patch had a sample of 25, for 150 total individuals. This created an analogous sampling scheme to that common in noninvasive genetic

sampling, where a small fraction of large populations are sampled, and small populations are sampled thoroughly, potentially repeatedly sampling the same individual.

We expect the number of unique genetic clusters (commonly referred to as "K") to vary from 1 to 6 based on landscape structure. Therefore, following convention, we tested possible values of K ranging from 1 to 20. All STRUCTURE analyses were run with a burn-in period of 10,000 iterations, with an additional 10,000 analysis iterations. We performed 20 replicate trials for each possible K value using the default settings of the admixture model and correlated allele frequencies. Each individual was given a "sample location" based on patch location, regardless of whether the landscape was continuous or patchy at that time ("sample location" was *not* used to aid in determination of the number of subpopulations). The best supported *K* values were identified using two methods: 1) plotting the replicate average *Ln P(D|K)*, and visually determining the minimum *K* of the curve's asymptote (Pritchard, Wen, and Falush 2010), and 2) using Evanno's Δ*K* method (Evanno, Regnaut, and Goudet 2005). If there were close ties between supported *K* values, using either method, we considered them all for individual assignment analyses. Assignment plots were generated for the 150 individuals, organized by patch location.

Conservation Biology: We used a separate series of model simulations to finely manipulate barrier gap permeability and carefully examine the effect of landscape connectivity on the amelioration of accumulated homozygosity. We calculated *Per-capita Homozygosity* as the percent of homozygous genotypes across all alleles and individuals within a given landscape patch. Large values of *Per-capita Homozygosity* could result from a few highly inbred individuals or from many slightly inbred individuals. These separate simulations were otherwise identical to the primary models described above.
We used the primary set of 80 simulations (8 treatments, 10 replicates each) to examine the effect of patch isolation on allele frequencies. We extracted genotype results from each replicate for two time steps, the ends of the *Continuous* and *Isolated Patches* epochs. We calculated three metrics of genetic

degradation for each locus in each sub-population using output from the "'*diveRsity"* R package "*divBasic"* function (Keenan et al. 2013), as described below:

(1) *Allelic richness* = the number of unique alleles per locus. All ten loci began with 5 alleles each.

(2) *Allelic evenness* = $\sum(p_i Ln(p_i))/Ln(5)$, where p_i is the frequency of the i^{th} allele within each locus, and $Ln(5)$ is the maximum evenness in each locus, given that all were initiated with 5 alleles. (This expression for allelic evenness is analogous to the Shannon-Weaver biodiversity metric.) The starting population had different initial allele frequencies corresponding to allelic evenness values of 1.0 = "Equal", 0.96 = "Unequal", and 0.72 = "Rare" (Table S1).

(3) *Heterozygosity deficit* = $H_{obs} - H_{exp}$, where observed heterozygosity (H_{obs}) is the number of observed heterozygous genotypes and expected heterozygosity is calculated as: $H_{exp} = 1 - \sum_{i=1}^{n}(q_i)^2$ where n = number of alleles and q_i is the frequency of the i^{th} of n alleles at a locus. Note that H_{exp} is calculated based on the number extant alleles at a locus, and will fluctuate dramatically as alleles are lost from a population. Therefore, unlike Allelic richness or Allelic evenness, this metric has a shifting baseline.

For each metric, we calculated mean and standard deviation across all replicates within the same patch size (small, medium, or large) and of the same initial allele frequency (equal, unequal, or rare) for each of the two time points of interest (at the end of the *Continuous* and *Isolated Patches* epochs).

Evolutionary Ecology: Population size was tracked for each patch across all time steps to facilitate measuring the response to adaptation. Additionally, we computed the change in frequency of adaptive alleles within each landscape patch during the *Semi-Connected with Selection* epoch. L6 contained two adaptive alleles and 3 neutral, while L7-through L10 each contained one adaptive allele and 4 neutral. L7-A5 and L9-A1 were adaptive in habitat type A, while L8-A5 and L10-A1 were adaptive

in habitat type B. Within L6, A2 was adaptive in habitat type A, and A4 was adaptive in habitat type B. Tracking adaptive allele frequencies in L6 allowed us to examine the effect of local adaptation on allele frequency in combination with asymmetric migration from adjacent patches, where the opposite allele was advantageous.

RESULTS

The age-class structure that arose from our model resulted in an average age of reproducing females of 8.7 years (time-steps). Therefore, each landscape epoch of 1000 simulation time steps spanned approximately 115 generations (Fig 1). During the *Semi-Connected* epoch, migration rate between semi-connected patches varied with dispersal distance, barrier gap permeability, and patch size (Fig 2). The vast majority of individuals remained in their natal patch regardless of dispersal ability, barrier permeability, or natal patch size. As anticipated, we observed higher migration rates when agents were assigned the long-distance dispersal behavior and the barrier gaps were highly permeable. Migration was asymmetric, with small patches generating proportionately large numbers of emigrants, and large patches experiencing proportionately high numbers of immigrants.

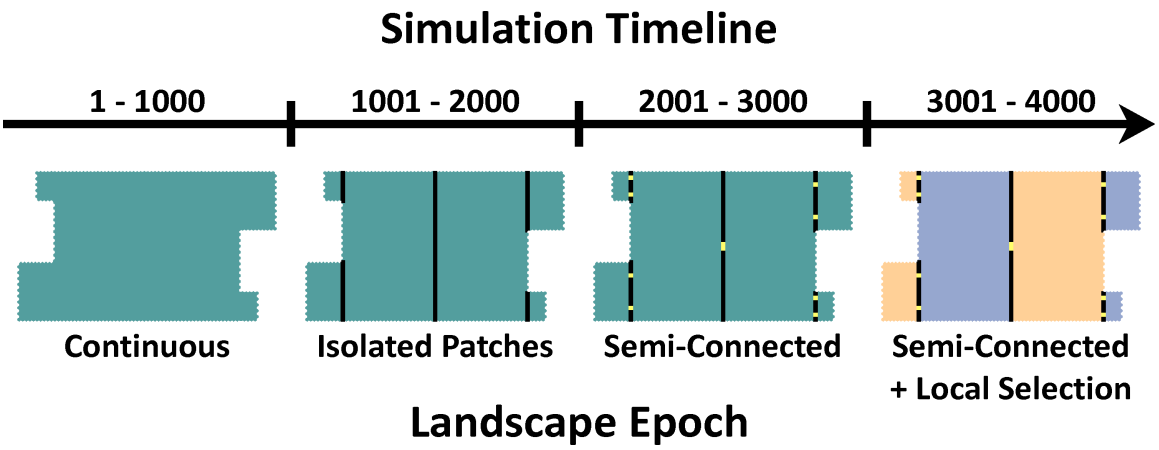

Fig 1. Progression of landscape epochs over 4000 time steps. *Barriers to movement are reflective, shown here as black lines. Landscape edges are also reflective. Gaps in the barriers, shown in yellow and introduced at time step 2000, are of the same total length for each barrier. Gaps vary in permeability (either high or low), determining the chance of an agent passing through the barrier when the gap is encountered during dispersal. At time step 3000, the landscape is assigned two habitat types (shown in blue and orange) that confer genotype-specific adaptive advantage to juvenile survival (See, Agent Evolutionary Characteristics).*

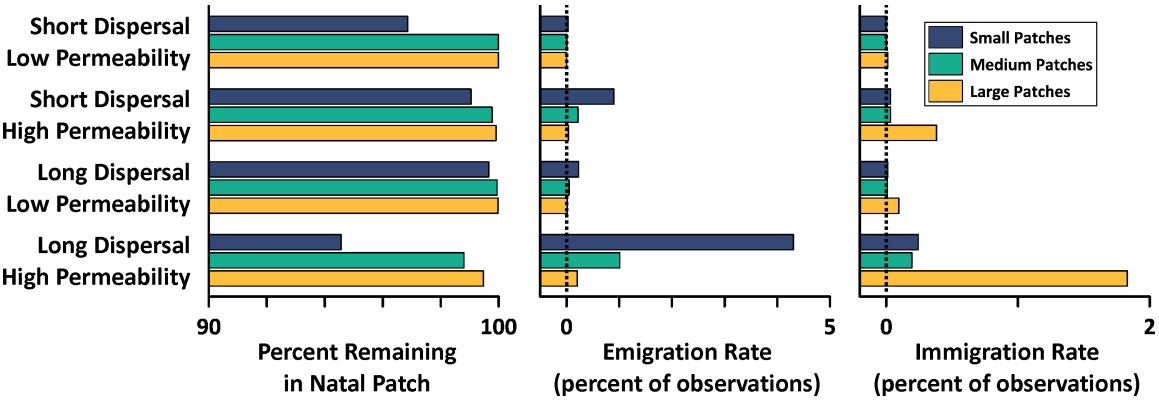

Fig 2. Observed migration rates of long or short-dispersing individuals across barriers of varying permeability during the Semi-Connected epoch. *Left: Percent of the population that is born and reproduces in the same patch. Middle: Emigration rates, sorted by size of sending patch. Right: Immigration rates, sorted by size of receiving patch.*

Landscape Genetics: The short and long distance dispersal behaviors, measured during the *Continuous* landscape epoch, produced notably different dispersal kernels (Fig 3 *left*). IBD was evident in the relationship between geographic distance and genetic distance when dispersal distances were short, but

not when dispersal distances were long (Fig 3 *right*). We did not observe any change in population spatial distribution associated with dispersal ability, therefore, the observed IBD was not due to a patchy distribution of individuals.

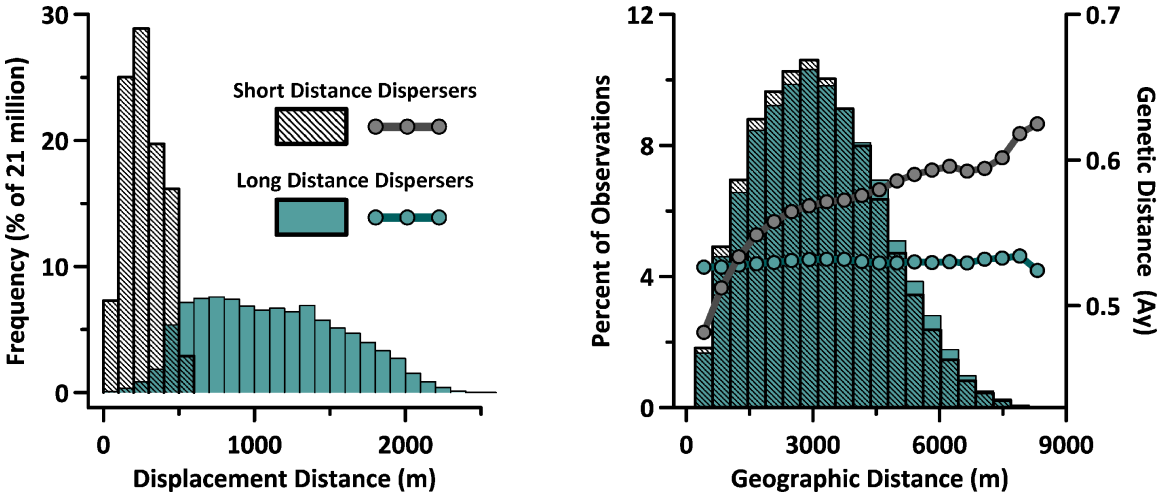

Fig 3. Landscape Genetics Core Concept. *In a spatially-continuous landscape, the observed dispersal kernels reflected juvenile dispersal ability (left), but no discernable difference in the population spatial distribution (right, bar plots). Genetic IBD was evident when dispersal path lengths were short, but not with longer dispersal ability (right, line plots). These data were gathered at the end of the Continuous landscape epoch, after 115 generations of unobstructed movement.*

We treated the series of four landscape epochs as four nested hypothetical landscape histories: H0, H1, H2, H3. Genetic distance matrices observed at the conclusion of each epoch illustrate the effectiveness of gene flow at mixing the subpopulations, given the landscape history and dispersal behavior (Fig 4). Additionally, barrier gap permeability affects gene flow in H2 &H3, and selection strength affects gene flow in H3.

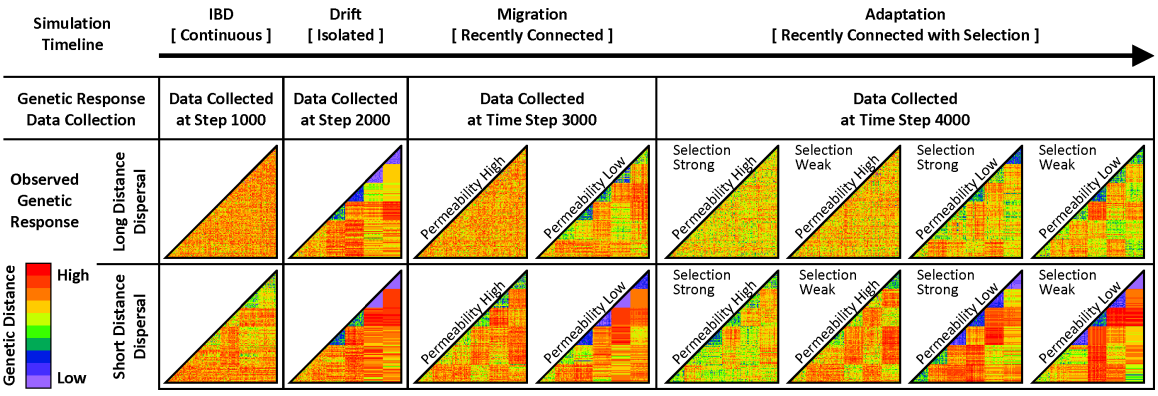

Fig 4. Landscape Genetics Advancement. *Modeling gene flow for four landscape histories, beginning with IBD only, and building to a complex history of sequential epochs of IBD, drift, migration, and finally, local selection. The resulting pairwise genetic distance matrices (colored triangles) illustrate the strength of gene flow within a given landscape history, where increasing contrast in the geometric patterns visible within the matrices results from reduced gene flow between landscape patches. Data collected at time step 4000 illustrate the interacting effects of gene flow and local adaptation on genetic-distance.*

Population Genetics: For each supported K value, we plotted the assignment probability for each of 150 sampled individuals (Fig 5). Individuals are represented by vertical lines, and the distribution of colors within a line indicates the assignment probability to each distinct genetic cluster. Accordingly, a monochromatic line indicates that an individual has been assigned with certainty to a single genetic cluster. Solid blocks of color in a given sample location indicate that all individuals at that location have been confidently assigned to a unique genetic cluster. The assignment of individuals to multiple clusters (i.e. multi-colored vertical lines) can result from biological phenomenon such as retained genetic diversity in large populations or recent migration events. But importantly, when many individuals are assigned to multiple clusters, this may indicate that the inferred *K* value is inaccurate.

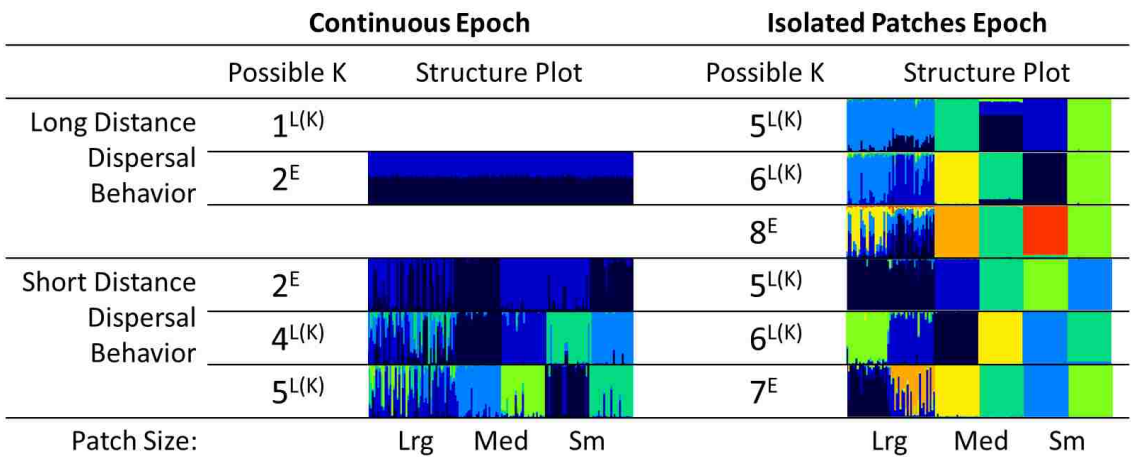

Fig 5. Population Genetics Core Concept. *The inferred number of genetic subpopulations (Possible K value) resulting from either the visual interpretation of likelihood probabilities (denoted by L(K)) or from Evanno's ΔK method (denoted by E), presented as a function of dispersal distance. The corresponding assignment probability plots, obtained from program STRUCTURE, are displayed in color, with individuals (small vertical bars) sorted by patch. When a single method produced multiple equally-supported estimates of K, then all values were included in the table.*

We know that, in the *Continuous* epoch, there is a single biological population present on the landscape. But without the benefit (inherent in modeling) of knowing the true population dynamics, genetic analysis can easily lead to a conclusion that there are several distinct populations present on the landscape. For example, in our simulations, short distance dispersal and resulting IBD led to the inference of multiple genetic clusters (Fig 5). When dispersers moved longer distances, and IBD was therefore absent, the L(*K*) method produced the expected result: a single population.

We know that in the *Isolated Patches* epoch, there are 6 distinct populations isolated by absolute barriers. By the end of the epoch, 5-8 unique genetic clusters were identified by our genetic analyses, regardless of dispersal behavior. Evanno's method tended to produce inflated estimates of *K* that exceeded the true number of 6 genetic subpopulations. The STRUCTURE plots indicate clearly that the 4 smaller patches were each home to a single genetic cluster, made unique by drift. The two large

patches housed either one or two genetic clusters, due to a weak effect of drift in these larger populations.

The population genetic structure produced by drift during the *Isolated Patches* epoch was mitigated by the limited inter-patch migration that characterized the subsequent *Semi-Connected* epoch (Fig 6). The differing numbers of migrants per generation produced varying degrees of genetic mixing over the course of these 115 generations. The observed 15.46 migrants per generation resulting from long distance dispersal and high barrier gap permeability produced sufficient genetic mixing to return to panmixia, while the other treatments failed to do so. Long-distance dispersal with low barrier permeability resulted in 0.76 migrants per generation, and this migration rate was insufficient to return the population to panmixia within the 115 generations of the epoch. A return to panmixia by the end of the *Semi-Connected* epoch was not expected in simulations employing a short dispersal distance, and no such outcome was observed.

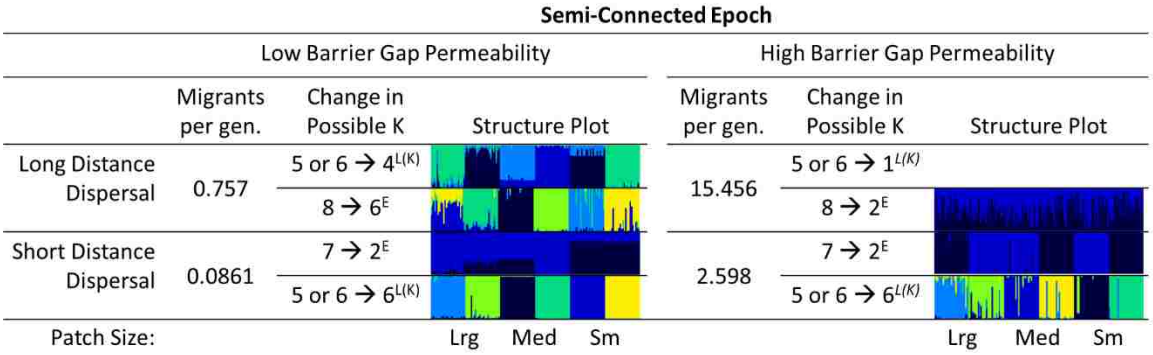

Fig 6. Population Genetics Advancement. *The average (across replicates) of observed migrants per generation, presented as a function of dispersal distance and barrier gap permeability. Population genetic structure (Change in Possible K) at the end of the Semi-Connected epoch declined from where it began in the prior Isolated Patches epoch. The corresponding assignment probability plots, obtained from program STRUCTURE, are displayed in color*.

Conservation Biology: As described in the *Methods*, we used a separate series of otherwise identical model simulations to finely manipulate barrier gap permeability, with the goal of examining the effect of

landscape connectivity on population homozygosity. We calculated *Per-capita Homozygosity* as the percent of homozygous genotypes across all alleles and individuals within a given landscape patch. High *Per-capita Homozygosity* could result from a few highly inbred individuals or many slightly inbred individuals. This analysis included the *Continuous*, *Isolated Patches*, and *Semi-Connected* epochs only.

Per-capita homozygostiy varied dramatically with landscape epoch, and fluctuated more in the small patches than the large ones (Fig 7). While we observed little accumulation of homozygosity during the *Continuous* epoch, this changed when migration between patches was limited by dispersal barriers. During the *Isolated Patches* epoch, homozygosity increased rapidly, but this general trend was strongly influenced by patch size. Both patch size and barrier gap permeability affected the amount of "genetic rescue" resulting from migration during the *Semi-connected* epoch.

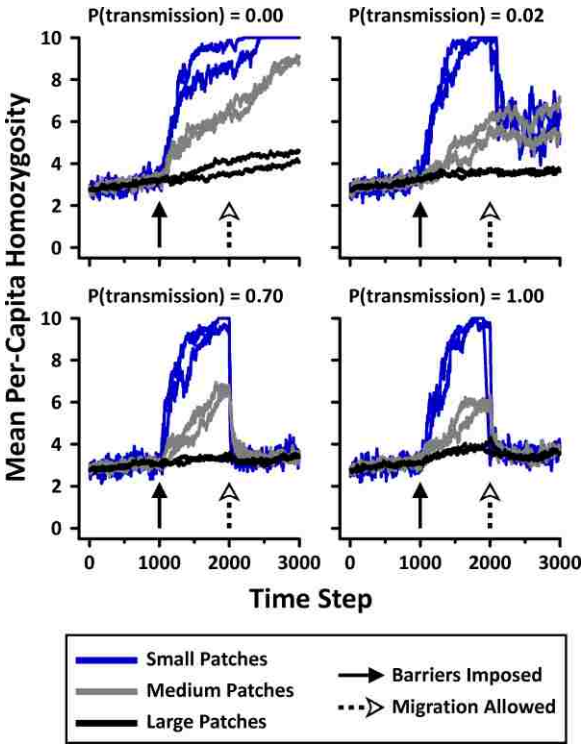

Fig 7. Conservation Biology Core Concept. *Per-capita homozygosity across simulation time steps spanning the Continuous, Isolated Patches, and Semi-Connected landscape epochs, displayed by patch size. The degree of genetic rescue, attributable to migration, changed depending on barrier gap permeability during the Semi-Connected epoch. Our simulated low and high barrier crossing probabilities corresponded to P(transmission) values of 0.02 and 0.70, respectively.*

Changes in allele frequencies observed during the *Continuous* and *Isolated Patches* epochs were affected by patch size, locus-specific initial allele frequencies, and dispersal distance (Fig 8). Even during the *Continuous* epoch, prior to patch isolation, rare alleles were lost due to drift. As anticipated, this process became more pronounced when dispersal was limited by impermeable barriers (the *Isolated Patches* epoch). The loss of allelic richness and evenness during patch isolation was most pronounced in the small patches, and least severe in the large patches. Short-distance dispersal also influenced loss of allelic richness and evenness in both epochs, but only in medium and small patches. A heterozygosity deficit was observed when dispersal distances were short, but only in large and medium patches.

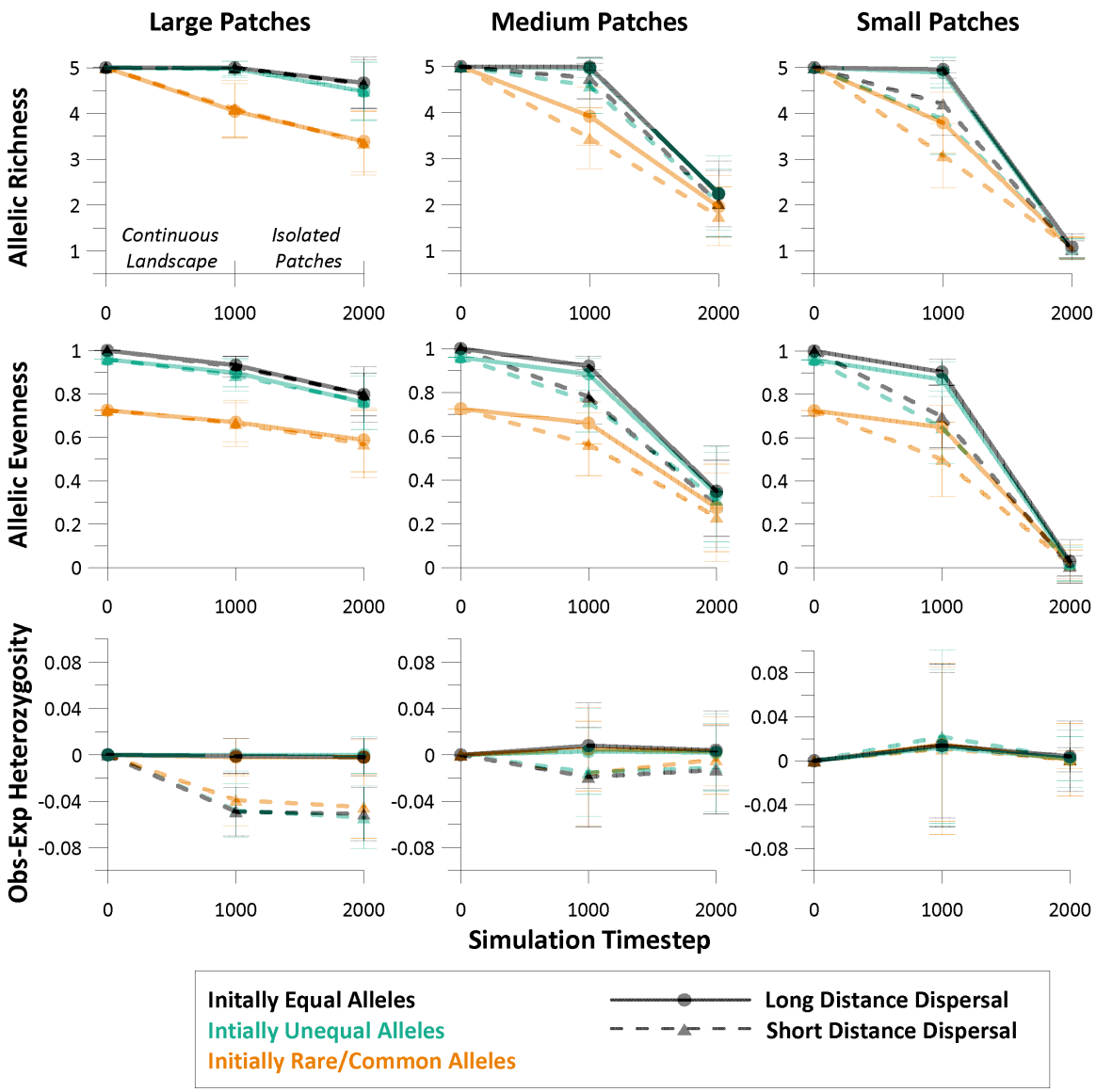

Fig 8. Conservation Biology Advancement. *Mean and standard deviation of three genetic degradation metrics derived from allele frequencies (rows) sorted by patch size (columns). Allele frequencies fluctuated over the Continuous and Isolated Patches epochs shown here, and vary by initial allele frequencies and dispersal distance.*

Evolutionary Ecology: Selection pressure was initiated at the beginning of the final landscape epoch, at time step 3000. Carrying capacity and population sizes emerged mechanistically from our model. Population size was most stochastic in the smaller patches, and most stable in the large patches (Fig 9). A non-zero probability of extinction was observed only for the small patches, and was greatest when the

dispersal distances were short and movement barriers were present. We observed that adaptation to local conditions effectively increased patch carrying capacity. These effects of adaptation were more pronounced when selection pressure was strong.

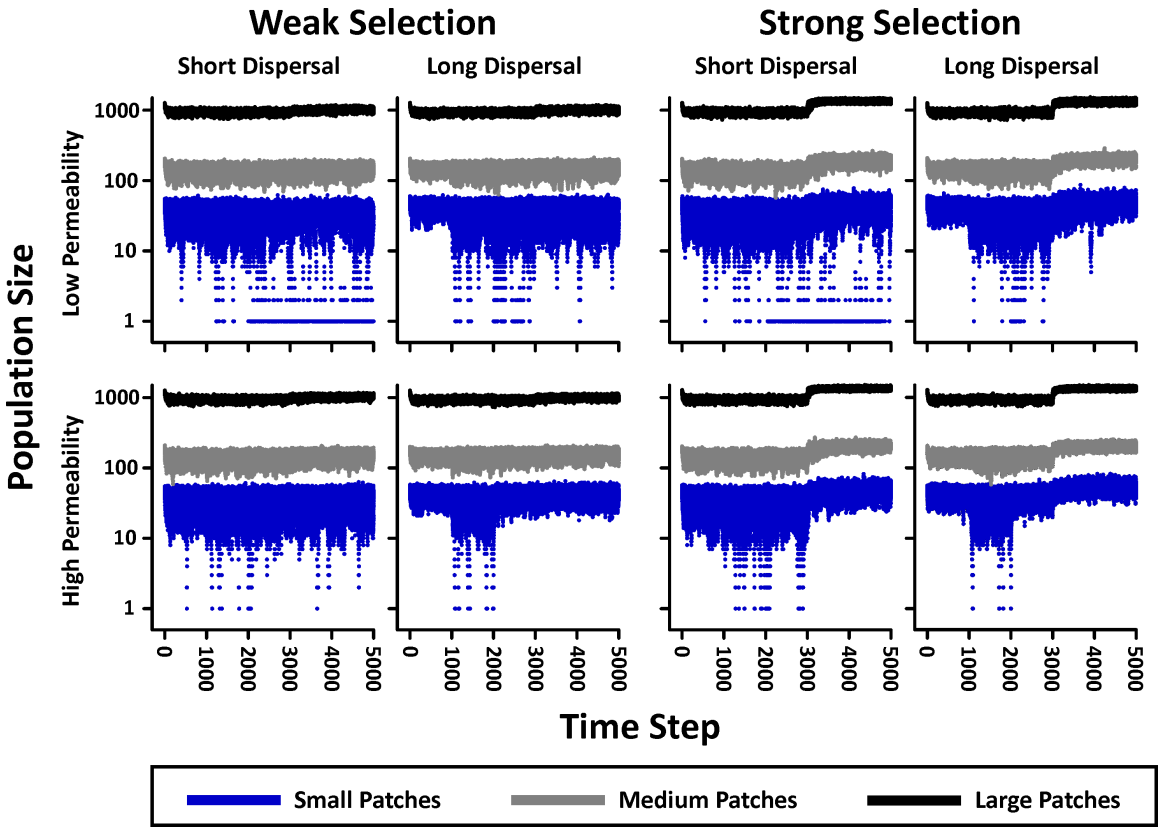

Fig 9. Evolutionary Ecology Core Concept. *Observed trends in population size stratified by patch size. Results from all ten simulation replicates are shown. Data were collected for an additional 1000 time steps during the final landscape epoch in order to better visualize the long-term population response to selection pressure. Carrying capacity was effectively increased by local adaptation, but the magnitude of this effect depended on the strength of selection. Extinction events can be inferred from occasional very low population sizes observed for the small patches.*

Loci L7-L10 had one each of five alleles that was locally adaptive during the *Semi-connected with Selection* epoch. The frequency of the adaptive alleles increased globally across all subpopulations as selection acted locally and migration moved the adaptive alleles across the landscape. Locus L6 had two adaptive alleles that each conferred a survival advantages in a different habitat type. The effect of local

selection increasing the frequency of locally adaptive alleles was counteracted by asymmetric migration (see Fig 2) between adjacent patches of different habitat types. L6-A2 was under local selection in half of the patches, and L6-A4 was under local selection in the other half (Fig 10). In small patches, local selection was almost always swamped by migration from the neighboring large patches, except when selection was strong, dispersal distance was short, and gap permeability was low. In the small and medium patches of the remaining treatments, the extent to which selection was swamped by migration varied more continuously based on the strength of selection, barrier gap permeability, and dispersal distance. In large patches, selection was often able to act effectively regardless of selection strength or migration rate, except when selection was weak and dispersal distance was long.

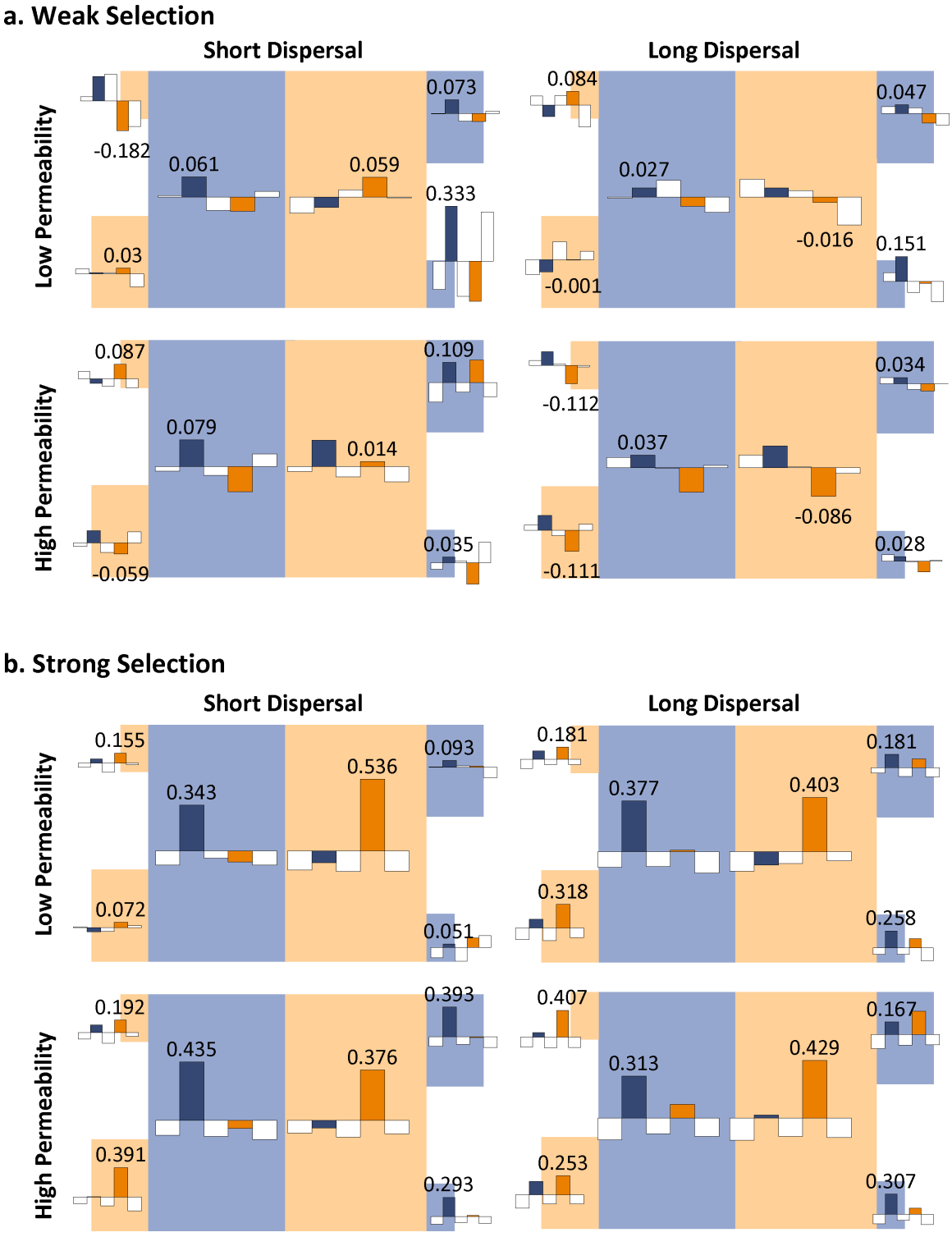

Fig 10. Evolutionary Ecology Advancement. *Average change in allele frequencies at a single locus (L6) across all replicates in response to selection during the Semi-connected with Selection epoch. Each bar plot displays the patch-specific change in frequency of all 5 of L6's alleles. Allele A2 (blue bars) conferred an increase in juvenile survival if an individual was located in a blue patch, and allele A4 (orange bars) does so in the orange patches.*

DISCUSSION

We purposefully developed a simple individual-based model to clearly illustrate how spatial structure drives eco-evo dynamics and demonstrate the ability of HexSim to recapitulate core-concepts in each focal discipline. By imposing landscape change on functionally-static eco-evolutionary models, we were able to alter key emergent forces, such as gene flow, genetic drift, and adaptive selection, as well as demo-genetic responses such as population size, probability of extinction, and allele frequencies. Our model also demonstrated how critical demo-genetic traits, including generation time and migration rate, can arise from a parsimonious mechanistic model, rather than being specified *a priori*.

A common approach in landscape genetics is to assume that current genetic pattern is a result of landscape pattern (with some lag-time) represented by resistance surfaces. Hypothetical "resistance distances" between individuals are compared to actual genetic distances between sampled individuals or groups, and tests are performed to infer which elements in the landscape most strongly influence gene flow. But complex movement behavior and dynamic landscape histories are not always easily captured by resistance surfaces, and this in turn limits the ability to infer past gene flow. We demonstrated how the cumulative effects of gene flow, genetic drift, and selection can be simulated over several hypothetical landscape histories. The resulting inter-individual genetic distance matrices simultaneously captured the influences of dynamic landscape structure, dispersal behavior, and demography.

An ongoing challenge for empirical population geneticists and phylogeneticists has been determining the number of populations represented within a given sample. Our model corroborates previous work demonstrating that small amounts of IBD inflate inferences, made by program STRUCTURE and using Evanno's ΔK method, demonstrating the utility of our simulation approach as a tool for investigating disconnects between statistical theory and empirical practice. One of the biggest advances of our approach for population genetics is the ability to parameterize movement based on

biological mechanisms, and to then let migration rates emerge from species-landscape interactions. For example, theory meets practice when it becomes necessary to increase the connectivity between isolated subpopulations because the benefit that landscape changes will have on gene flow cannot be known in advance. Our model demonstrates how a simple spatially-explicit landscape and movement process produces departures from the "one-migrant-per-generation" theoretically-derived guideline for re-establishing genetic panmixia between subdivided populations within a reasonable timeframe (over 100 generations in our model). Our approach illustrates how researchers might elucidate the landscape conditions necessary, given a specific eco-evo history, for recovering genetic panmixia within a target number of generations.

Forecasting genetic degradation in small populations facing extinction is a challenging task that should ideally acknowledge the influences of both demographic and genetic processes. Our simple theoretical model exhibited nuanced differences in the rate and severity of genetic degradation, suggesting that complex demo-genetic feedbacks are likely ubiquitous in practice, given real-world complexity. Although our theoretical model is simple, our results highlight how HexSim may be used in future studies to improve understanding of inbreeding and outbreeding depression, and explore the relative importance of genetic versus demographic components of population or species viability.

The complexity inherent in evolutionary ecology necessitates simulation toolkits containing dynamic feedbacks linking evolutionary and ecological forces. The HexSim modeling platform provides such an integration. Our model captured one such feedback, namely, the counteracting forces of local selection and asymmetric migration from spatially proximal sub-populations. The interplay between local selection and asymmetric migration that we found in our smaller patches are likely to be observed as species ranges expand due to climate change.

Future applications of this approach may benefit from the modeling platform's ability to include both theoretical and geographically explicit (e.g. imported from GIS) landscapes, as well as the ability to

include dynamic landscapes (e.g. herbaceous ground cover in response to herbivore population density) within the model itself. HexSim models can incorporate empirically-derived life history information, multiple-species interactions, or multiple-disturbances. While our model included only simple genotypes without mutation, we anticipate future projects investigating how mode of inheritance, linkage between alleles, initial geographic distributions of allele frequencies, and multiple mutation regimes (e.g. stepwise, infinite alleles, or two-phase models) interact with landscape spatial pattern and movement. For example, conservation geneticists may use HexSim to simulate mutation rates based on exposure to spatially-distributed chemical mutagens encountered during dispersal and mitigated by selection against deleterious alleles. Rates and patterns of gene flow may be investigated within the context of nuanced, biologically-realistic movement behaviors, including rare long-distance dispersal events, site fidelity and memory, attraction and avoidance, or sex-specific behaviors, to name a few. In addition to the four disciplines highlighted here, our methods may have applications in the fields of phylogenetics, phylogeography, medical science, and evolutionary theory. For example, phylogeneticists could use HexSim to simulate past species range shifts, model incomplete lineage sorting, or ask how linkage affects coalescent metrics. Phylogeographers could use the platform to explore the stability of admixtures zones over time, or improve the demarcation of evolutionary significant units.

CONCLUSIONS

As is true with science in general, ecologists often make use of simplifying assumptions in order to keep model development tractable. The cost of these simplifications has been that theory often lacks grounding in the very biological detail that we know governs species' interactions with their

environments, and with each other. HexSim allows us to improve modeling applications by challenging the assumptions upon which they have been constructed and show how the details matter.

ACKNOWLEDGMENTS: Allen Brookes developed the source code for HexSim and has been an invaluable member of our research team. David Beck at the University of Washington eScience Institute aided in data management and processing. This work was funded in part by the WRF-Hall Graduate Student Fellowship from the University of Washington, Department of Biology. The information in this document has been funded in part by the U.S. Environmental Protection Agency. It has been subjected to review by the National Health and Environmental Effects Research Laboratory's Western Ecology Division and approved for publication. Approval does not signify that the contents reflect the views of the Agency, nor does mention of trade names or commercial products constitute endorsement or recommendation for use.

REFERENCES

Balkenhol, Niko, Lisette P. Waits, and Raymond J. Dezzani. 2009. “Statistical Approaches in Landscape Genetics: An Evaluation of Methods for Linking Landscape and Genetic Data.” *Ecography* 32 (5): 818–30.

Carroll, S. P., A. P. Hendry, D. N. Reznick, and C. W. Fox. 2007. “Evolution on Ecological Time-Scales.” *Functional Ecology* 21 (3): 387–93.

Epperson, Bryan K., Brad H. Mcrae, Kim Scribner, Samuel A. Cushman, Michael S. Rosenberg, Marie-Josée Fortin, Patrick M. A. James, et al. 2010. “Utility of Computer Simulations in Landscape Genetics.” *Molecular Ecology* 19 (17): 3549–64.

Evanno, G., S. Regnaut, and J. Goudet. 2005. “Detecting the Number of Clusters of Individuals Using the Software Structure: A Simulation Study.” *Molecular Ecology* 14 (8): 2611–20.

Ezard, Thomas H. G., Steeve D. Côté, and Fanie Pelletier. 2009. “Eco-Evolutionary Dynamics: Disentangling Phenotypic, Environmental and Population Fluctuations.” *Philosophical Transactions of the Royal Society of London B: Biological Sciences* 364 (1523): 1491–98.

Frankham, Richard. 2005. “Genetics and Extinction.” *Biological Conservation* 126 (2): 131–40.

Fussmann, G. F., M. Loreau, and P. A. Abrams. 2007. “Eco-Evolutionary Dynamics of Communities and Ecosystems.” *Functional Ecology* 21 (3): 465–77.

Hairston, Nelson G., Stephen P. Ellner, Monica A. Geber, Takehito Yoshida, and Jennifer A. Fox. 2005. “Rapid Evolution and the Convergence of Ecological and Evolutionary Time.” *Ecology Letters* 8 (10): 1114–27.

Hamilton, W. D. 1966. “The Moulding of Senescence by Natural Selection.” *Journal of Theoretical Biology* 12 (1): 12–45.

Hanski, Ilkka, and Ilik Saccheri. 2006. “Molecular-Level Variation Affects Population Growth in a Butterfly Metapopulation.” *PLOS Biol* 4 (5): e129.

Hendry, Andrew P., and Michael T. Kinnison. 1999. “Perspective: The Pace of Modern Life: Measuring Rates of Contemporary Microevolution.” *Evolution* 53 (6): 1637–53.

Hoban, Sean, Giorgio Bertorelle, and Oscar E. Gaggiotti. 2012. “Computer Simulations: Tools for Population and Evolutionary Genetics.” *Nature Reviews Genetics* 13 (2): 110–22.

Keenan, Kevin, Philip McGinnity, Tom F. Cross, Walter W. Crozier, and Paulo A. Prodöhl. 2013. “diveRsity: An R Package for the Estimation and Exploration of Population Genetics Parameters and Their Associated Errors.” *Methods in Ecology and Evolution* 4 (8): 782–88.

Kinnison, Michael T., and Andrew P. Hendry. 2001. “The Pace of Modern Life II: From Rates of Contemporary Microevolution to Pattern and Process.” In *Microevolution Rate, Pattern, Process*, edited by A. P. Hendry and M. T. Kinnison, 145–64. Contemporary Issues in Genetics and Evolution 8. Springer, Netherlands.

Laland, K. N., F. J. Odling-Smee, and M. W. Feldman. 1999. “Evolutionary Consequences of Niche Construction and Their Implications for Ecology.” *Proceedings of the National Academy of Sciences* 96 (18): 10242–47.

Lande, R. 1988. “Genetics and Demography in Biological Conservation.” *Science* 241 (4872): 1455–60.

Martens, Erik A., Rumen Kostadinov, Carlo C. Maley, and Oskar Hallatschek. 2011. “Spatial Structure Increases the Waiting Time for Cancer.” *New Journal of Physics* 13 (11): 115014.

Miller, M. P. 2005. “Alleles In Space (AIS): Computer Software for the Joint Analysis of Interindividual Spatial and Genetic Information.” *Journal of Heredity* 96 (6): 722–24.

Palkovacs, Eric P., and David M. Post. 2008. “Eco-Evolutionary Interactions between Predators and Prey: Can Predator-Induced Changes to Prey Communities Feed back to Shape Predator Foraging Traits?” *Evolutionary Ecology Research* 10 (5): 699–720.

Paradis, Emmanuel, Julien Claude, and Korbinian Strimmer. 2004. “APE: Analyses of Phylogenetics and Evolution in R Language.” *Bioinformatics* 20 (2): 289–90.

Pelletier, F., D. Garant, and A.P. Hendry. 2009. “Eco-Evolutionary Dynamics.” *Philosophical Transactions of the Royal Society of London B: Biological Sciences* 364 (1523): 1483–89.

Pelletier, Fanie, Tim Clutton-Brock, Josephine Pemberton, Shripad Tuljapurkar, and Tim Coulson. 2007. “The Evolutionary Demography of Ecological Change: Linking Trait Variation and Population Growth.” *Science* 315 (5818): 1571–74.

Pritchard, Jonathan K., Matthew Stephens, and Peter Donnelly. 2000. “Inference of Population Structure Using Multilocus Genotype Data.” *Genetics* 155 (2): 945–59.

Pritchard, Jonathan K., Xiaoquan Wen, and Daniel Falush. 2010. “Documentation for Structure Software: Version 2.3.”

R Core Team. 2013. *R: A Language and Environment for Statistical Computing.* Vienna, Austria: R Foundation for Statistical Computing. http://www.R-project.org/.

Saccheri, Ilik, and Ilkka Hanski. 2006. “Natural Selection and Population Dynamics.” *Trends in Ecology & Evolution*, Twenty years of TREE - part I, 21 (6): 341–47.

Schumaker, NH. 2016. *HexSim* (version 4.0). Corvallis, Oregon, USA: U.S. Environmental Protection Agency, Environmental Research Laboratory.

Sinervo, Barry, Erik Svensson, and Tosha Comendant. 2000. "Density Cycles and an Offspring Quantity and Quality Game Driven by Natural Selection." *Nature* 406 (6799): 985–88.

Thompson, John N. 1998. "Rapid Evolution as an Ecological Process." *Trends in Ecology & Evolution* 13 (8): 329–32.

Walther, Gian-Reto, Eric Post, Peter Convey, Annette Menzel, Camille Parmesan, Trevor J. C. Beebee, Jean-Marc Fromentin, Ove Hoegh-Guldberg, and Franz Bairlein. 2002. "Ecological Responses to Recent Climate Change." *Nature* 416 (6879): 389–95.

Waples, Robin S., and Oscar Gaggiotti. 2006. "INVITED REVIEW: What Is a Population? An Empirical Evaluation of Some Genetic Methods for Identifying the Number of Gene Pools and Their Degree of Connectivity." *Molecular Ecology* 15 (6): 1419–39.

Wright, Sewall. 1943. "Isolation by Distance." *Genetics* 28 (2): 114–38.

Yoshida, Takehito, Laura E. Jones, Stephen P. Ellner, Gregor F. Fussmann, and Nelson G. Hairston. 2003. "Rapid Evolution Drives Ecological Dynamics in a Predator–prey System." *Nature* 424 (6946): 303–6.

SUPPLEMENTARY MATERIAL:

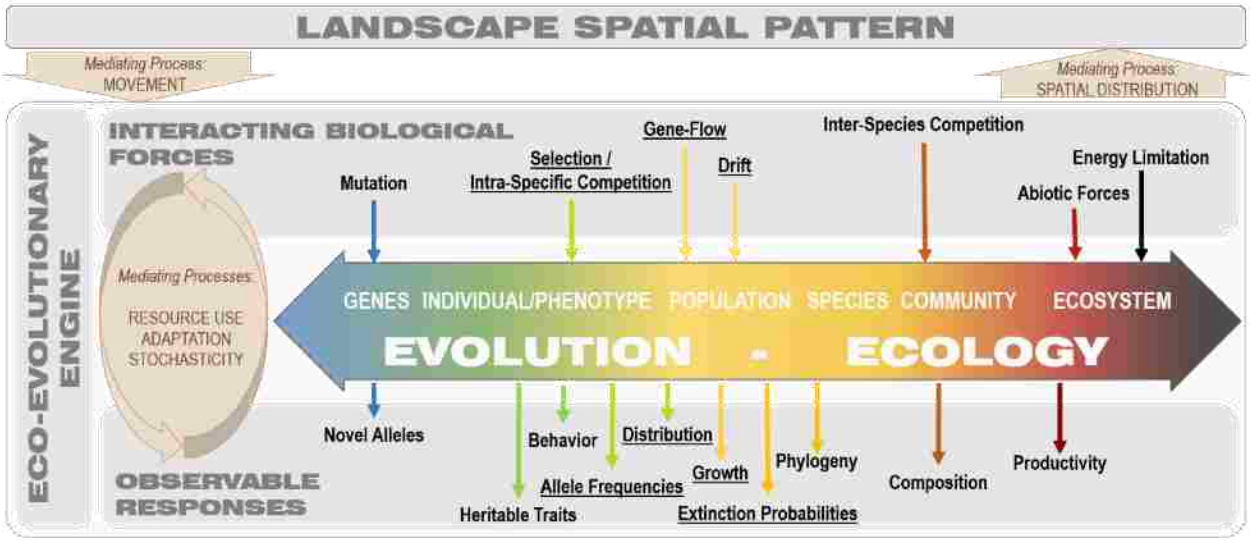

Figure S1. Conceptual Framework of Spatially-explicit Eco-evolutionary Dynamics*. This framework presents eco-evolutionary dynamics as a feedback loop between interacting biological forces and observable responses operating along a pseudo-hierarchical spectrum. Feedback between observable responses and biological forces is mediated by processes such as resource use and adaptation, and modified by stochasticity. Landscape spatial pattern (extent, arrangement, and connectivity) shapes and constrains eco-evolutionary dynamics. Movement (of genes, individuals, nutrients, etc.) is the mediating process through which eco-evolutionary dynamics are affected by spatial pattern. Changes in the spatial distribution of eco-evolutionary dynamics can, in-turn, change the landscape spatial pattern. This framework assumes significant overlap in the rate at which "ecological" and "evolutionary" forces produce responses. Vertical linear arrows approximate where biological forces operate and at what level we typically observe responses (those underlined are highlighted in this study).*

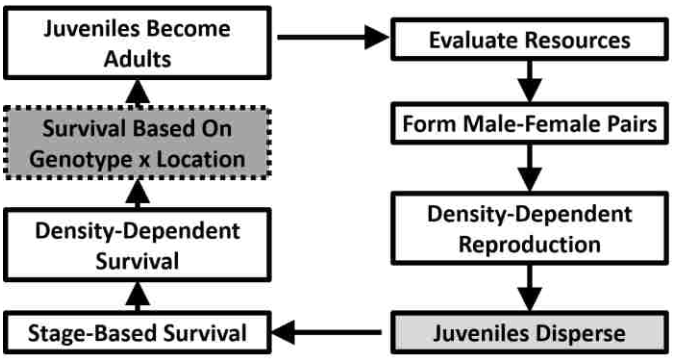

Figure S2. Agent lifecycle for each time-step. *Starting in the upper right, adults evaluate resources within an "explored zone" around their location. Resources (pixels) are divided by the number of individuals that have a given pixel within their explored zone. Males and female adults form pairs and females reproduce probabilistically based on their resources within their explored zone. New juveniles disperse from their natal location with either short or long-distance dispersal behavior. Survival is determined by both life stage (juvenile survival < adult survival) and amount of resources within their explored zone (sub-optimal resource acquisition < resource goal satiated). Survival probability based on genotype and location is initiated at time step 3000. At the end of the time step, juveniles become adults and do not disperse again in their lifetime.*

LOCUS	ALLELE	INITIAL ALLELE FREQUENCY	LOCAL ADAPTATION TO HABIAT TYPE
1	1-5	0.20, 0.20, 0.20, 0.20, 0.20	Neutral
2	1-5	0.30, 0.25, 0.20, 0.15, 0.10	Neutral
3	1-5	0.10, 0.15, 0.20, 0.25, 0.30	Neutral
4	1-5	0.01, 0.04, 0.15, 0.30, 0.50	Neutral
5	1-5	0.50, 0.30, 0.15, 0.04, 0.01	Neutral
6	1	0.20	Neutral
	2	0.20	Locally Adapted - Habitat Type A
	3	0.20	Neutral
	4	0.20	Locally Adapted - Habitat Type B
	5	0.20	Neutral
7	1	0.30	Neutral
	2	0.25	Neutral
	3	0.20	Neutral
	4	0.15	Neutral
	5	0.10	Locally Adapted - Habitat Type A
8	1	0.10	Neutral
	2	0.15	Neutral
	3	0.20	Neutral
	4	0.25	Neutral
	5	0.30	Locally Adapted - Habitat Type B
9	1	0.01	Locally Adapted - Habitat Type A
	2	0.04	Neutral
	3	0.15	Neutral
	4	0.30	Neutral
	5	0.50	Neutral
10	1	0.50	Locally Adapted - Habitat Type B
	2	0.30	Neutral
	3	0.15	Neutral
	4	0.04	Neutral
	5	0.01	Neutral

Table S1. *Initial Allele-Frequency Conditions for 10-Locus Genotypes*

Text S1: *Landscape Structure Details*

Our maps contained 72 columns and 51 rows, and thus 3672 hexagons total. Two large adjoining patches were each assembled from 1326 separate hexagons. Two medium-sized patches (200 hexagons each) and two small patches (50 hexagons each) abutted the large patches, but not each other. Patch dimensions expressed as columns x rows, were 26x51, 10x20, and 5x10. The total habitat area was 72x51 hexagons in extent, but this region contained 520 matrix hexagons. Our simulated individuals were never allowed to leave the habitat patches and enter the non-habitat matrix.

Text S2: *Processing Time and Computational Requirements*

All 80 simulations were run on a Dell PowerEdge R820 server. Individual model runs took roughly four hours of processing time to complete. Our simulations could be replicated at a similar speed on a modern desktop or laptop computer, and use of the server simply made it possible to run all 80 simulations at the same time. Two subsequent computationally-intensive post-processing steps added many additional hours of computer time. These involved (1) combining the raw output files (over 4 Gbytes per file) from each of the 8 collections of 10 replicate simulations into a single multi-replicate output file, and (2) producing HexSim report files from the 80 simulations. These steps are simple to perform in HexSim, but the file sizes involved were large; the total size of all raw output files reached 1/3 Terabyte. The collection of reports from which we derive our results totaled about 13 Gbytes in size.

Chapter 4: Exploring Movement Ecology Drivers of Gene Flow in Large Neotropical Felids through Mexico, Guatemala, and Belize via Spatially-Explicit Eco-Evo Simulations

Jennifer M.W. Day[1]*, Samuel K. Wasser[1], Nathan Schumaker[2]

[1] Center for Conservation Biology, Department of Biology, University of Washington, Seattle, USA

[2] U.S. Environmental Protection Agency, Western Ecology Division, Corvallis, OR, USA

ABSTRACT:

The mechanistic relationship between resource selection at fine scales and gene flow at broader spatial scales is poorly understood. There are several components of movement ecology that may influence realized dispersal, including intrinsic dispersal capability, sensitivity to the landscape during movement, and criteria for territory establishment. This study aims to investigate how sensitivity to the landscape and territorial behavior impact gene flow in the large Neotropical felids of Mesoamerica.

The primary goal of this study is to develop a spatially-explicit individual-based model (SIBM) that captures the complex movement ecology of Neotropical felids, and tracks gene flow across generations. The secondary goal is to conduct a pilot-simulation to test behavioral drivers of gene flow in this system. Specifically, we model the effect of (A) increased land-cover selectivity in territory establishment and (B) increased dispersal sensitivity to land-cover, on gene flow. Gene flow is assessed by genetic-distances between proposed Jaguar Conservation Units (JCU). The landscape of our model has a 25 hectare (0.25 km^2) resolution, a biologically relevant spatial scale for modeling resource selection behavior. The geographically-explicit extent of the landscape includes Mexico, Guatemala, and Belize, a spatial extent appropriate for observing gene flow for highly vagile Neotropical felids.

Our results demonstrate male-competition for territories, resource-driven landscape carrying-capacity, and sex-specific dispersal patterns. Preliminary results from our experimental treatments suggest that selectivity for territory establishment and dispersal sensitivity to the landscape have antagonistic effects on gene flow. However, additional model years are required to determine if these behavioral influences on gene flow persist over many generations. Specific JCUs were found to be particularly sensitive to our experimental treatments, highlighting these locations for further study. Our model provides a powerful tool for investigating movement ecology drivers of gene flow in these behaviorally-complex species. The spatial scale (extent and grain) of our model landscape allows us to make empirically-relevant predictions regarding gene flow and movement, and maximizes the potential

for conservation applications. The preliminary results from our pilot experiments take the first step toward understanding the behavioral mechanics driving realized dispersal and gene flow of Neotropical felids.

INTRODUCTION:

Gene flow within and among populations is controlled by a combination of intrinsic (biology, physiology, and behavior) and extrinsic (landscape patterns and quality) factors (Bender and Fahrig 2005; Nathan et al. 2008). Human alteration of wildlife habitat, both quality and pattern, has affected the spatial genetic patterns of organisms across the planet. Our study is motivated by a need to predict how landscape degradation affects gene flow, as well as how proposed conservation actions may help ameliorate those effects. Predicting gene flow is especially challenging when species are highly vagile and behaviorally complex, such as in the case of large carnivores. The large carnivores of Mesoamerica face increasing habitat loss and degradation due to forest conversion to pasture and agriculture, along with habitat fragmentation due to road expansion. The goal of this study is to investigate possible drivers of gene flow of large felids in Mesoamerica. Our study takes the first step toward reconciling the apparent contradiction between the greater resource selectivity by jaguars (*Panthera onca*) relative to pumas (*Puma concolor*), and yet greater genetic differentiation within pumas (indicating higher gene flow through Mesoamerica) relative to jaguars.

Our study aims to investigate how fine-scale movement ecology dynamics scale up to produce broader-scale patterns of gene flow. We use spatially-explicit individual-based simulations (SIBM) designed to capture the complexity of movement ecology of large felids, including male-competition for home range territory, sex-specific home range size and dispersal distances, and selection/avoidance of landscape features at a fine spatial grain. We chose to build our model within the HexSim platform (Schumaker 2016), due its ecological flexibility. Our model includes the behavioral complexity we deemed necessary to capture the spatial dynamics of these territorial species, while maintaining as much model simplicity as possible. We implement our model over a 25 hectare (0.25 km^2) resolution landscape covering Mexico, Guatemala, and Belize (MGB). We track demographic (e.g. carrying capacity and sex-ratio) and spatial output (e.g. dispersal distance, territory size) across the entire study area, and

monitor gene flow using genotypic data from five polymorphic loci, sampled from within the 16 proposed Jaguar Conservation Units (JCUs) in our study area (Sanderson et al. 2002; Zeller 2007). This is principally a study in methods development, and as such is focused primarily on model description and parameter justification.

The quality and heterogeneity of the non-habitat matrix has been shown to impact the functional connectivity between wild felid populations, in addition to the effects of intrinsic dispersal ability (Revilla et al. 2004). However, the behavioral mechanisms underlying realized dispersal remain largely unknown. We use our model to conduct a pilot-simulation of two experimental treatments to investigate the effect of two aspects of movement ecology on gene flow, while holding intrinsic dispersal capacity constant: (1) selectivity toward land-cover types for the establishment of home range territory, and (2) strength of selection/avoidance of land-cover types during dispersal movements. Our baseline model includes all of the movement complexity we deemed necessary to create a realistic rate of gene flow between JCUs, and is then modified to address the following two research questions:

Question 1: How does selectivity in territorial requirements interact with the Mexico, Guatemala, and Belize (MGB) landscape to influence gene flow?

Experimental Treatment: Lower the resource quality of non-forested land-cover for the establishment of territories.

- H0: Specialization in territorial requirements does not influence gene flow

  Prediction: Gene flow between JCUs does not change from baseline conditions
- H1: Territorial requirements influence gene flow by impacting the probability of newly established territories being near to forested natal sites.

  Prediction: Gene flow is reduced between JCUs

- H2: Territorial requirements influences gene flow by impacting the search duration for suitable territory.

  Predictions: Gene flow is increased between JCUs

Question 2: How does more sensitivity (higher attraction and stronger avoidance) toward landscape features interact with MGB landscape pattern during juvenile dispersal to impact gene flow?

Experimental Treatment: Alter movement behavior by increasing attraction to forest land-cover and strengthen repulsion from human-dominated land-cover.

- H0: Dispersal behavior sensitivity does not influence gene flow

  Prediction: Gene flow between JCUs does not change from baseline conditions

- H1: Dispersal behavior sensitivity limits realized dispersal.

  Prediction: Gene flow is reduced between JCUs

- H2: Dispersal behavior sensitivity produces rare, long-distance realized dispersal

  Predictions: Gene flow is increased between JCUs

For each of these two experimental treatments we will monitor the change in gene flow from our baseline model, as assessed by genetic distance between JCUs. Our larger goal is to build a large felid model with enough biological realism to enable future studies to explore how ecological and evolutionary dynamics are affected by territorial behavior, mating behaviors, barriers such as roads and rivers, climate-change, inter-species competition, genetic mutational models, genotype-phenotype feedbacks, habitat loss, poaching pressure, and more.

MODEL DESCRIPTION:

Evolutionary characteristics: Each individual within the model carries a diploid genotype for five polymorphic loci modeled after empirical estimates of number of unique alleles and allele frequencies for microsatellite loci commonly used in felid genetics studies (Table 1). Loci are neutral and unlinked. Alleles are inherited bi-parentally with Mendelian segregation. While we have not implemented mutation within this initial model, HexSim has the capacity to model mutation by specifying a matrix of mutation transition probabilities from one allele to another.

Table 4. Initial parameterization of allele frequencies for five loci carried by each individual.

		Allele Frequency at Initialization									
Locus ID	No. Alleles	Allele0	Allele1	Allele2	Allele3	Allele4	Allele5	Allele6	Allele7	Allele8	Allele9
FCA043	10	0.0300	0.0700	0.1000	0.1300	0.1700	0.1700	0.1300	0.1000	0.0700	0.0300
FCA090	5	0.1000	0.1000	0.6000	0.1000	0.1000					
FCA126	6	0.0800	0.1700	0.2500	0.2500	0.1700	0.0800				
FCA056	5	0.2000	0.2000	0.2000	0.2000	0.2000					
FCA096	7	0.0625	0.1250	0.1875	0.2500	0.1875	0.1250	0.0625			

Ecological characteristics: Individuals are either male or female. Individuals are considered juveniles from 1-2 years old, and adults >3 years old (Sunquist and Sunquist 2002). The period where cubs stay with their mother does not contribute to spatial territorial dynamics or gene flow. Therefore, when individuals are "born" into the model, they immediately undergo dispersal from their natal site. In order to simulate the typical pattern of spatial territoriality of wild cats, while minimizing model complexity, we had males form territories that could contain up to 3 females, depending on resources within that territory. The resources available within a male territory depends on both the size of the territory and quality of the landscape (see "**Landscape ecology**; *Resource Quality"* below). Females join male territories if they were not already fully occupied. We have implemented mechanisms within the model so that female site fidelity will remain fairly constant, even if the resident male dies or is outcompeted by other males (see next section). While we recognize this to be a simplification of a biological system

where females maintain independent territories, we feel this is an adequate approximation of the territorial dynamics of these wild felids. Combining male and female territories in this way allowed us to simplify mate-findings and territorial dynamics. Throughout the simulation, if individuals do not have a home range (males) or do not belong to a male group (females) then they are deemed "floaters". Floaters cannot reproduce, and experience additional mortality relative to group members (see next section).

Annual series of events: We begin our description of an annual cycle when an individual is born into the model, ready to disperse from their natal site (✯ in Figure 1). The age at which wild felids disperse away from their mother is not necessarily concurrent with sexual maturity. Dispersal happens between 1-3 years of age, and sexual maturity ranges from 3-5 years of age (Foster 2008; Sunquist and Sunquist 2002; Benson et al. 2016). Therefore, we drew our age at birth randomly from a uniform distribution between 1-3 years. This means that some females will have a probability of reproducing in their first year post dispersal (provided they find a mate), while others will remain juveniles for 1-2 years post-dispersal.

New individuals encounter a landscape that is divided up into male territories, with some areas potentially unclaimed. In the first step of the annual series of events, any males that do not have a territory (first-years and those who did not secure a territory in previous years) will disperse through the landscape (see **Intrinsic Dispersal**) and claim any unoccupied land, as long as it contains the sufficient resources for a single female to join his group (see **Landscape ecology**; *Resource Quality*). Claiming unoccupied territory is not the only way that a wild felid male may obtain a territory. Older males may be displaced from their territory, or forced to contract their range due to competition with other males (Schaller and Crawshaw 1980; A. R. Rabinowitz and Nottingham Jr. 1986; Sunquist and Sunquist 2002). Therefore, in the next step of our annual cycle, males have a chance of losing their hold over their

territory (becoming a temporary floater), with vulnerability increasing with age. Specifically, one year old territory holders have a 4% probability of becoming a floater, and this probability increases linearly to 100% at 25 years of age. However, the only males that this applies to, are those with a male floater (challenger) located within their territory.

Next, all floater males compete in a scramble competition for available territory. To clarify, at this point in the model, there are two ways that a male could be a floater competing for territory: (1) they were unable to find any suitable unoccupied territory during dispersal, or (2) they held territory the previous year but became a floater this year due to the presence of a challenger within their territory (which be more likely for older males). The maximum size of a territory formed during this process is 1/3 smaller than the maximum size possible when claiming unavailable territory. This is intended to simulate naturally occurring range-contraction resulting from competition (Sunquist and Sunquist 2002).

Any females that lost their groups due to male competition, immediately rejoin the newly formed local male groups, before the new female dispersers have left their natal site. We based the order of who rejoins the group by age, with older females going first. This is to ensure that resident females rejoin local groups, rather than a female that failed to secure a home range in the previous cycle, but happens to be nearby. However, if there are resources available for an additional female, then a nearby floater may join a group at this time. This process maintains female site fidelity, a reasonable surrogate for female territoriality. Next, the female floaters disperse through the landscape (see **Intrinsic Dispersal**) and join male groups if there are enough available resources and the group has not met its maximum membership of 3 females.

At this point in the annual cycle, both females and males have either successfully found territories, or were unsuccessful and remained floaters. Next, we increment each individual's age, and also increment a trait tracking of the number of consecutive years that an individual has been a floater. Dispersal is a risky time in the life of a big cat (Sunquist and Sunquist 2002; Crawshaw JR. et al. 2004).

Therefore, probabilistic mortality in the next step is based on both age, and years floating. The age-based survival is modeled to be a Type I survivorship curve, with a maximum lifespan of 25 years (Nowell and Jackson 1996; Caso et al. 2008). The floater-based survival probability drops steeply to mimic the danger of prolonged search for territory (1st year as floater = 0.75, 2nd = 0.50, 3rd = 0.25, 4th = 0.00 survival). Therefore, individuals that have been floating for four consecutive years will die, regardless of age.

When a territorial male dies, neighboring males with sub-optimal territories may expand into recently vacated territory. This is intended to simulate naturally occurring range expansion (Schaller and Crawshaw 1980; A. R. Rabinowitz and Nottingham Jr. 1986; Sunquist and Sunquist 2002). Once again, any females that lose their group due to the death of a male will rejoin the new group right away, with more senior females rejoining first, and nearby floaters joining last. To summarize, there are three ways in which a male can gain home range territory: (1) Claim unoccupied territory, (2) Claim territory through competition with a territory-holding male, (3) Expand an existing sub-optimal range into a neighboring territory of a recently deceased male.

Reproduction is the final step before the model returns to male dispersal. Only female adults (3 years or older) reproduce, mating with the male of their group (all males are capable of being mates, regardless of age). We calculated the mean reproductive output based on the following: 1. Average of 2 cubs per litter (Seymour 1989; Benson et al. 2016), 2. An average inter-birth period of 2 years (Benson et al. 2016; Sunquist and Sunquist 2002), and 3. Cub survival to juvenile dispersal age between 0.3-0.6 (Bernal-Escobar, Payan, and Cordovez 2015). This results in an average of 0.45 cubs per paired female per year. Sex ratio of offspring was 1:1 females to males.

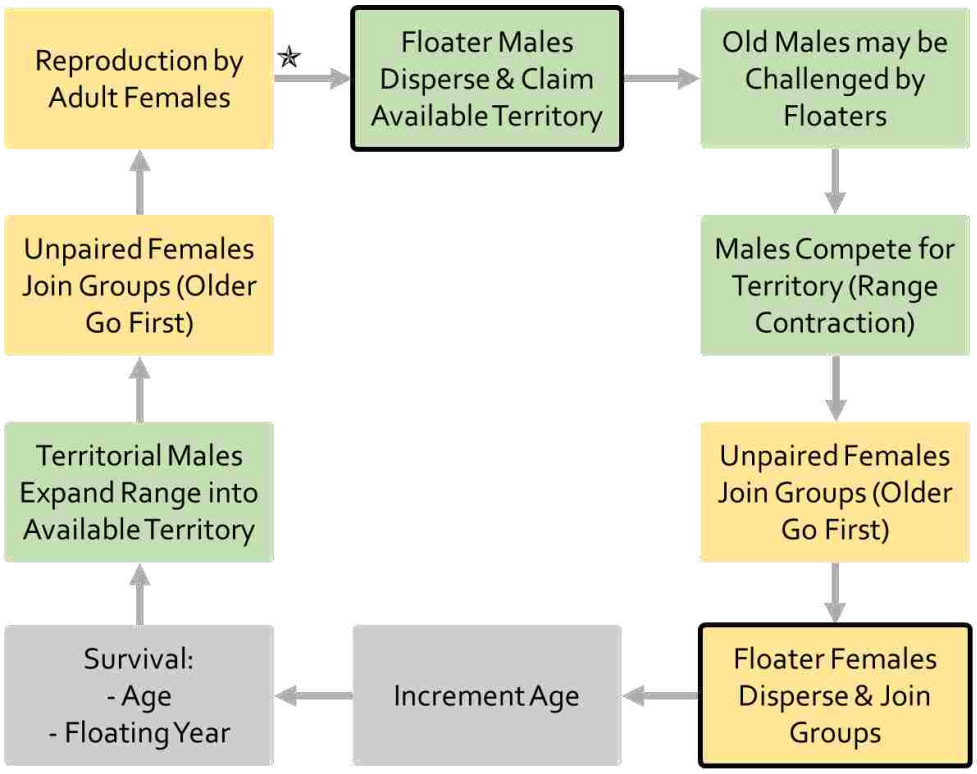

Figure 3. Event sequence of a single year. Star indicates beginning of model description narrative.

Landscape Ecology: A primary goal in building this model, is to enable an exploration of how landscape change (e.g. climate change or forest fragmentation) impacts demographics and genetics. Therefore, we created a landscape of ambitious spatial scale. The spatial extent is from the Mexico/USA border south through Guatemala and Belize. The spatial grain (resolution) of the landscape is 25 hectares (0.25 km^2) per hexagon, for a total of approximately 2,000,000 km^2 area composed of 7,870,267 terrestrial hexagons embedded within >23 million hexagon landscape. There are two principle maps used within the model, 1. *Resource Quality*, and 2. *Dispersal Suitability*. These separate maps give us the flexibility to implement separate movement behaviors for territorial dynamics versus dispersal dynamics. Additionally, we included a geographic *Barriers to Movement* map, containing roads and rivers. Data sources are summarized in appendix Table S1.

Resource Quality: This landscape contains the "resource" data for forming (males) or joining (females) territorial groups. Resource values relate to land-cover type (USGS LandCover 2001-2010), and were assigned based on previous resource selection analyses (Day et al. *this dissertation Chapter 1;* (Crawshaw and Quigley 1991; Schaller and Crawshaw 1980; Monroy-Vilchis et al. 2009; A. R. Rabinowitz and Nottingham Jr. 1986; Aranda 1996), expert opinion (A. Rabinowitz and Zeller 2010; Sanderson et al. 2002), and precedents in large-felid modeling studies (Rodríguez-Soto et al. 2011; Bernal-Escobar, Payan, and Cordovez 2015)(Table 2). In brief, resource values range from 0 (urban or barren) to 100 (forest). The minimum size of a male territory, capable of having one female group member, required a minimum of 6,000 resource units (and an additional 6,000 units for each additional female, up to 3). Therefore, the smallest male territory possible would be composed of completely high quality habitat, and 15 km^2 (1500ha, 60 hexagons). On the upper end, a male territory composed completely of grassland would need to be 300 km^2 (1,200 hexagons) in order to have 3 female group members. Territories will not necessarily be circular; the shape will be dictated by an "adaptive" exploration (see **Intrinsic Dispersal**), which combines the goals of energy conservation (promoting compactness) and resource selection. There is some evidence that these species avoid higher elevation (A. Rabinowitz and Zeller 2010; Rodríguez-Soto et al. 2011; Nowell and Jackson 1996). Therefore, the resource quality values were multiplied by an elevation coefficient (1.0 = 0 – 2,000 m; 0.9 = 2,000 m – 3,000 m; 0.8 = above 3,000 m).

Table 2. Baseline model Landscape Ecology parameters.

USGS LandCover 2001-2010		Neotropical Felid Model			
ID	Landcover	No. Hexagons	% Landscape	Resource Quality	Dispersal Suitability
0	Salt Water	0	0	0	0
15	Snow and Ice	0	0	0	0
13	Urban and Built-Up	28750	0.3653	0	1
16	Barren or Sparsely Vegetated	106921	1.3585	0	2
12	Croplands	658632	8.3686	3	3
17	Fresh Water	25355	0.3222	0	4
14	Cropland/Natural Vegetation Mosaic	829745	10.5428	5	5
7	Open Shrublands	2370147	30.1152	15	6
10	Grasslands	673738	8.5605	15	6
11	Permanent Wetland	53688	0.6822	70	6
9	Savannas	63973	0.8128	30	7
6	Closed Shrublands	9953	0.1265	30	8
8	Woody Savannas	1705231	21.6667	50	8
1	Evergreen Needle leaf Forest	1129	0.0143	100	9
3	Deciduous Needle leaf Forest	357	0.0045	100	9
2	Evergreen Broadleaf Forest	880892	11.1927	100	10
4	Deciduous Broadleaf Forest	175928	2.2353	100	10
5	Mixed Forests	285828	3.6317	100	10

Dispersal Suitability: Dispersal suitability values were also based on land-cover types, and form the basis for the attraction and repulsion movement behavior of dispersing individuals. Assigning values for this landscape is more speculative, due to the paucity of information regarding habitat selection during dispersal. We make the assumption that individuals are able to move through areas that are not suitable for territories (Table 2). The probability of which neighboring hexagon will be chosen for the next step in dispersal movement is the product of both autocorrelation (how strongly we specify forward directionality) and the attraction/repulsion coefficient. The attraction/repulsion coefficient, in turn, is based on the both the *Dispersal Suitability* value and the minimum and maximum attraction/repulsion settings. These settings operate along the continuum of dispersal suitability values (Figure 2). The highest possible value for an attraction coefficient is set to 10 (attraction multiplier), which drives the strength of attraction.

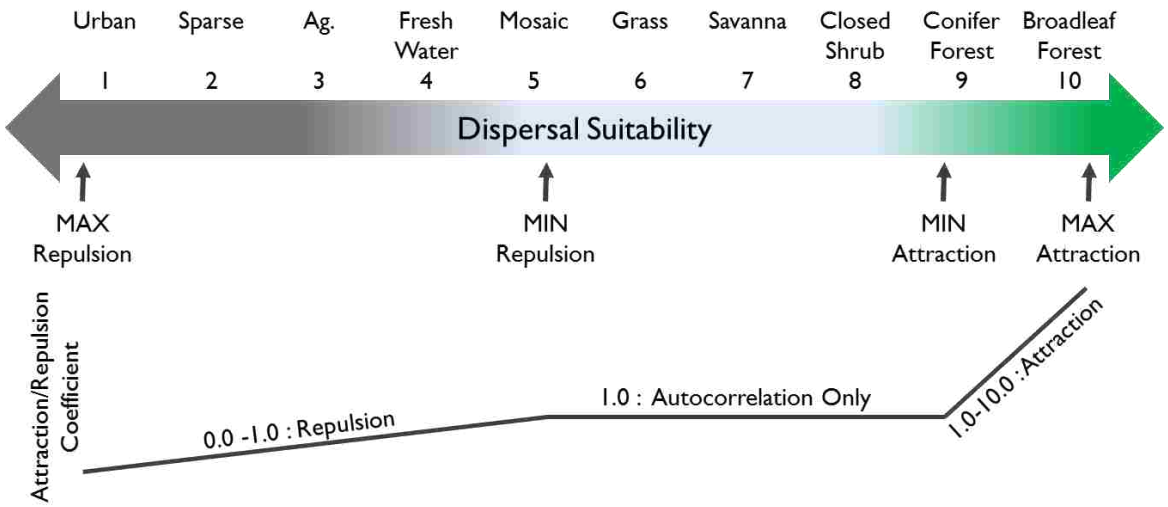

Figure 4. Baseline model attraction and repulsion to land-cover types in the Dispersal Suitability landscape.

Barriers to Movement: The barriers in our model include both major roads and large rivers (appendix Table S1). Territories may span roads or rivers (Mazzolli 2010), therefore, barriers do not impact our simulated territory establishment. However, barriers do influence dispersing individuals, both through direct mortality (Fischer et al. 2003; Miotto et al. 2012) or via avoidance behavior (Day et al. *this dissertation Chapter 1*;(Monroy-Vilchis et al. 2009; Angelieri et al. 2016)). There are three possible outcomes of individuals encountering a barrier in our model; they will either be killed, deflected, or cross (transmission). The roads in our model were assigned an equal 0.10 probability of mortality or deflection, and the remaining 0.80 probability of crossing. The river barriers did not incur any mortality if encountered, but deflected individuals at a 0.10 probability, with a corresponding 0.90 probability of crossing.

Intrinsic Dispersal: The scant data on the juvenile dispersal ability of Neotropical felids suggest that females tend to disperse shorter distances than males, but there is a large range of documented distances (<10 – 370 km) and they overlap across sexes (Crawshaw and Quigley 1991; Stoner et al. 2008;

Crawshaw and Quigley 1984; Crawshaw JR. et al. 2004; Stoner et al. 2013; Weaver, Paquet, and Ruggiero 1996; Sunquist and Sunquist 2002).

A single movement event (during one year) consists of a "dispersal" phase and an "exploration" phase (example Figure 3). During the dispersal phase, individuals move from hexagon to neighboring hexagon with semi-autocorrelated (70%) directionality, meaning that they move predominantly in a "forward" direction. The "forward" direction is determined by the most frequently observed direction over the past 25 movement steps. This allows their movement paths to bend around smaller obstacles (e.g. a small lake) without ricocheting off into a completely new direction, and to gradually change course around larger obstacles (e.g. an urban area). During the exploration phase, individuals explore the surrounding 35,000 hectares. For males, the goal of this exploration is to determine if there is enough available (unclaimed) territory to establish a territory with enough resources to sustain at least one female. For females, the goal of this exploration is to determine if there is a male group with enough available resources for it to join. If the goal is not met, then the individual remains a floater.

We implemented two sex differences in movement behavior. When beginning their movement event, males disperse first and then explore, as described above. Females, however, explore first and then disperse. This simulates the tendency of females to establish territories (join groups in our simulation) close by to their mother's home range (Sunquist and Sunquist 2002; Crawshaw and Quigley 1991; Miotto et al. 2012; Stoner et al. 2013). Additionally, female path lengths during dispersal are 50% shorter, on average, than males. The distance of each dispersal phase is drawn randomly from a log-normal distribution with a mean of 53.7 km (100 hexagons) for males, and 26.9 km (50 hexagons) for females, both with a standard deviation of 2.5 hexagons. The min-max bounds on the length of the dispersal phase are 0 and 537 km (1,000 hexagons) for both males and females. However, the realized dispersal distance, hereafter referred to as "displacement", will depend on both the intrinsic dispersal and interactions with the landscape.

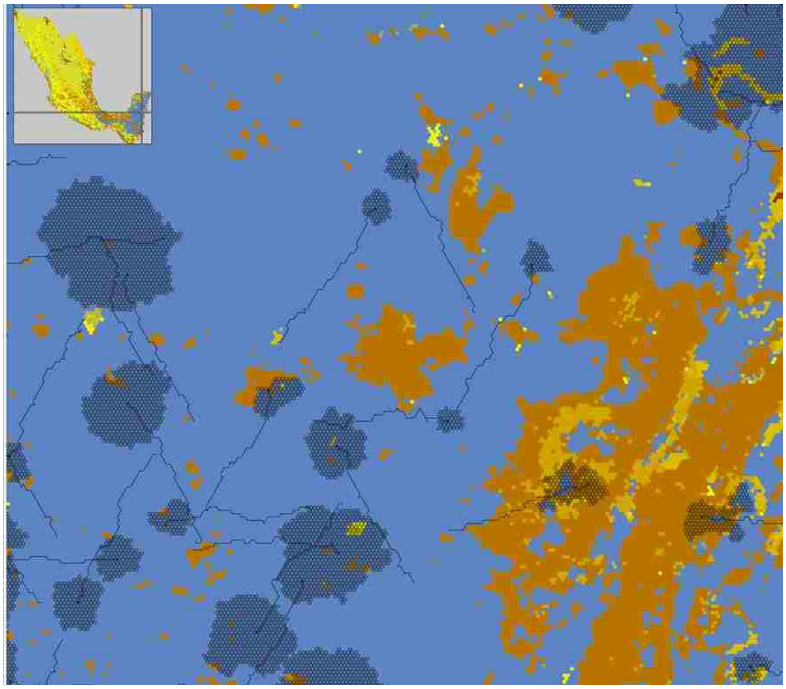

Figure 3. Example of movement from the Baseline model. Thin black lines indicate paths during the Dispersal phase of movement, while the black areas indicate the area evaluated for territories during the Exploration phase. Background colors are land-cover types in the Dispersal Suitability (inset).

Model Initiation: Our models were initialized with 50,000 individuals, randomly located throughout the landscape. Individual genotypes were drawn at random from the initial allele frequencies specified in Table 1, without spatial stratification, thereby initializing a panmictic population. We allowed for a burn-in period of 10 time-steps prior to tracking individual demo-genetic traits.

EXPERIMENTAL TREATMENTS:

Our two research questions were addressed with experimental treatments to our "Baseline" model described above. The first experimental treatment changed the resource quality of land-cover types for establishment of territories during the exploration phase of movement (Table 3). This experimental treatment, hereafter referred to as "Habitat Selectivity", did not change intrinsic dispersal

ability or behavior during the dispersal phase of movement. This treatment directly affected the likelihood and locations of males establishing territories during the exploration phase of movement. It indirectly affected females by changing the spatial arrangement and available resources within groups they were trying to join. This treatment changed the carrying capacity of the landscape, due to the fact that the landscape held less suitable habitat.

Table 3. Experimental treatment of the "Habitat Suitability" for establishing territories. Changes to the Baseline model highlighted in red.

USGS LandCover 2001-2010		Resource Quality	
ID	Landcover	Baseline	Experimental
0	Salt Water	0	0
15	Snow and Ice	0	0
13	Urban and Built-Up	0	0
16	Barren or Sparsely Vegetated	0	0
12	Croplands	3	0
17	Fresh Water	0	0
14	Cropland/Natural Vegetation Mosaic	5	3
7	Open Shrublands	15	5
10	Grasslands	15	5
11	Permanent Wetland	70	70
9	Savannas	30	15
6	Closed Shrublands	30	15
8	Woody Savannas	50	30
1	Evergreen Needle leaf Forest	100	50
3	Deciduous Needle leaf Forest	100	50
2	Evergreen Broadleaf Forest	100	100
4	Deciduous Broadleaf Forest	100	100
5	Mixed Forests	100	100

The second experimental treatment altered behavior during the dispersal phase of movement. A greater range of land-cover types incured movement repulsion, and the degree of attraction to forested land-cover was increased (Figure 4). This treatment is hereafter referred to as "Dispersal Sensitivity".

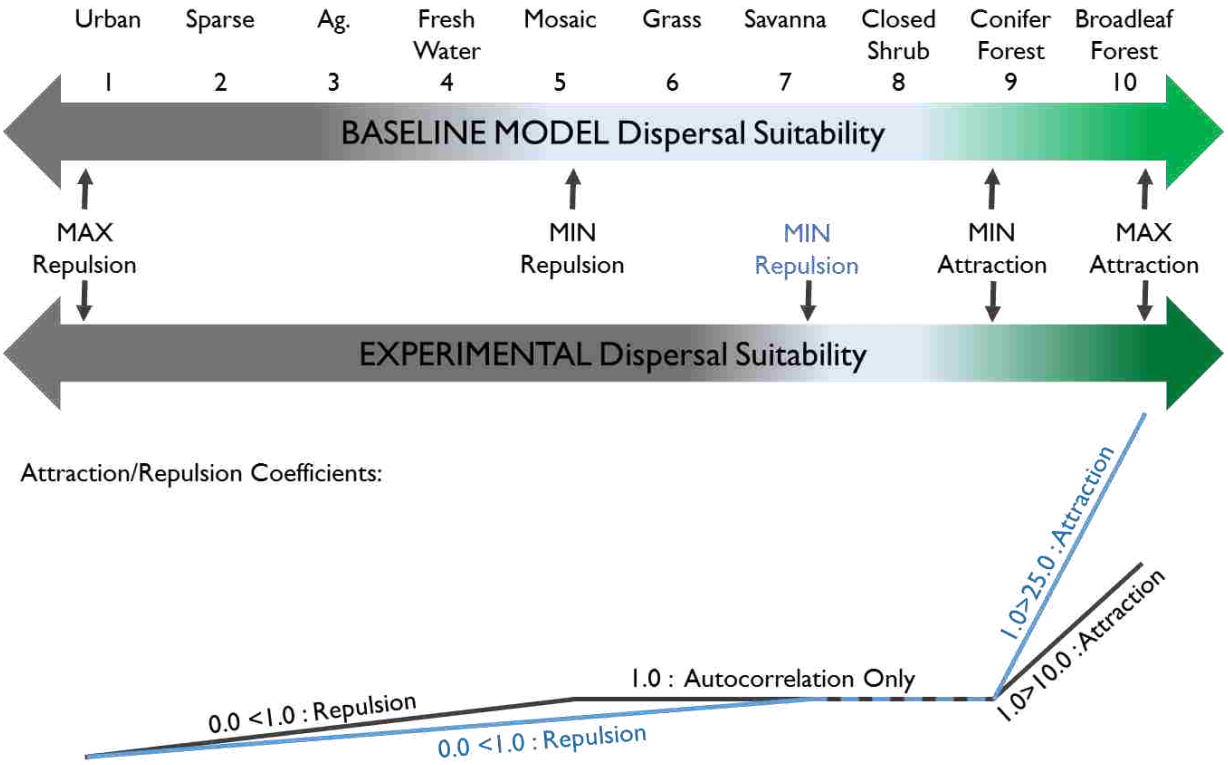

Figure 4. Baseline (black) and experimental "Dispersal Sensitivity" treatment (blue). Experimental treatment includes in higher minimum repulsion (7), and a higher attraction multiplier (25), resulting in avoidance of land-cover ranked 7 or lower, and stronger attraction to land-cover ranked 9 or higher, respectively.

We monitored the effect of these treatments on gene flow by assessing the change in genetic distance between Jaguar Conservation Units (JCUs) using individual genotypes from time-step 35. Our model's complexity and extent caused computational challenges that prevented further time steps from being included in this manuscript. While 35 years may not be a sufficient time period in which to observe statistically significant changes in gene flow, it may give an indication of the direction of change in gene flow given our treatments. Three metrics of genetic distance, Nei's Gst (Nei and Chesser 1983), Jost's D (Jost 2008), and Weir & Cockerham's Fst (Weir and Cockerham 1984) were calculated using the *diveRsity* R-package (Keenan et al. 2013).

RESULTS:

Demographics: Carrying capacity of the entire study area stabilized between 48,000 – 66,000 individuals (Figure 5). While it is not possible to ground-truth this number directly, we can use empirical density estimates to determine biological plausible upper and lower limits. Density estimates for big-cats vary widely from study to study, but average near 3.5 individuals/100km^2 (Ceballos et al. 2002; Núñez, Miller, and Lindzey 2002; Vynne et al. 2011; Payan Garrido 2009; Kelly et al. 2008; Sollmann et al. 2011; Sollmann et al. 2013; Mazzolli 2010; Lindzey et al. 1994; Aranda 1996) Our entire study area is approximately 2,000,000 km^2. If big cats occupied the entire area at this average density, we would anticipate ~71,000 individuals. However, not all of the landscape can support resident populations. There are approximately 335,750 km^2 of forested landscape in our study area. The average density applied to this area would result in ~12,000 individuals. If we consider these to be our upper and lower limits, our steady state population sizes are reasonable.

With increased selectivity in territorial requirements (Habitat Selectivity) a smaller portion of the population exists outside of the Jaguar Conservation Units (JCUs), there being higher concentration of forest habitat within JCUs (Figure 5). The sex ratio that emerged from our model was approximately 2:1 females to males, and was consistent across experimental treatments, even with a smaller population in the Habitat Selectivity treatment (Figure 5).

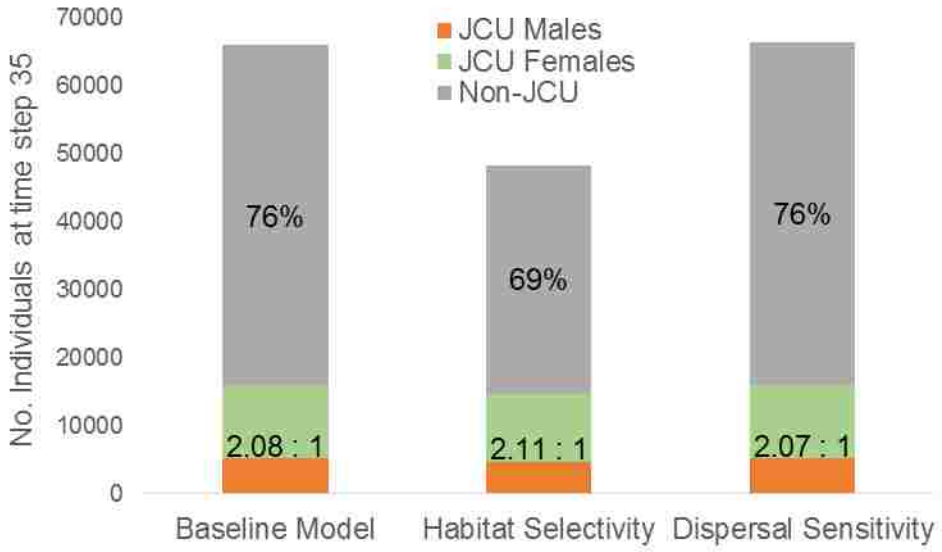

Figure 5. Demographics summary at time step 35 for each model (Baseline, Habitat Selectivity, and Dispersal Sensitivity). Percentages shown are the proportion of the population found outside of Jaguar Conservation Units (JCU). Ratios indicate the sex ratio (females : males) of individuals within JCUs. Total population size is smaller in the Habitat Selectivity model due to reduced carrying capacity of the landscape, caused by our experimental treatment reducing the quality of territorial resources.

Territory Size: We tracked male territory size immediately following each of the shifts in male tenancy: post dispersal/prospecting, competition/range-contraction, and mortality/range-expansion). We observed significantly reduced territory size following range-contraction, and near-optimal territory sizes following range expansion (Figure 6). These results validate the functionality of our modeled territorial dynamics.

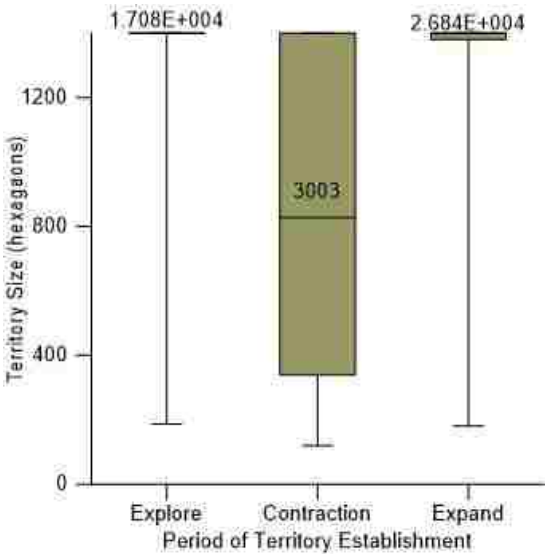

Figure 6. Median with max-min whiskers for male territory size, by period in which the territory was established: during dispersal and exploration (Prospecting), during competition (Contraction), or Expanding into territories vacated due to mortality. Sample sizes above each category indicate the number of individuals over a ten-year period (time step 26-35).

Dispersal Displacement and JCU Fidelity: Intrinsic dispersal capability (path length and degree of autocorrelation) was not changed between experimental treatments. Therefore any change in displacement (realized dispersal distance) between treatments, is due to the interaction of movement behavior (habitat selectivity or dispersal sensitivity) and the landscape. Displacement was not changed by Habitat Specialization, but reduced by Dispersal Sensitivity (Figure 7).

We also examined how our experimental treatments influenced the probability of individuals staying within their natal JCU, versus dispersing into the non-JCU matrix or to another JCU. The increased Habitat Selectivity decreased the probability of transitioning out of a natal JCU into the non-JCU matrix, which has a lower proportion of forested land-cover (Figure 8, A). The Habitat Selectivity treatment increased the probability of staying within the natal JCU, with the exception of JCU10 (Figure 8, A). JCU10, in northern Belize, is predominantly composed of grassland rather than forest, limiting territory establishment in our experimental treatment. Our Dispersal Sensitivity treatment produced the largest change in transition probabilities for JCU4 (Figure 8, B). JCU4 is a small, isolated location in northeast Mexico. Increased Dispersal Sensitivity decreased the probability of staying within JCU4 (JCU4

to JCU4 transition). However, it also decreased the probability of transitioning into the non-JCU matrix, likely due to the dispersal sensitivity behavior preventing leaving the relatively good habitat inside the JCU. The results indicate a high number of perishing floaters in JCU4 under this treatment.

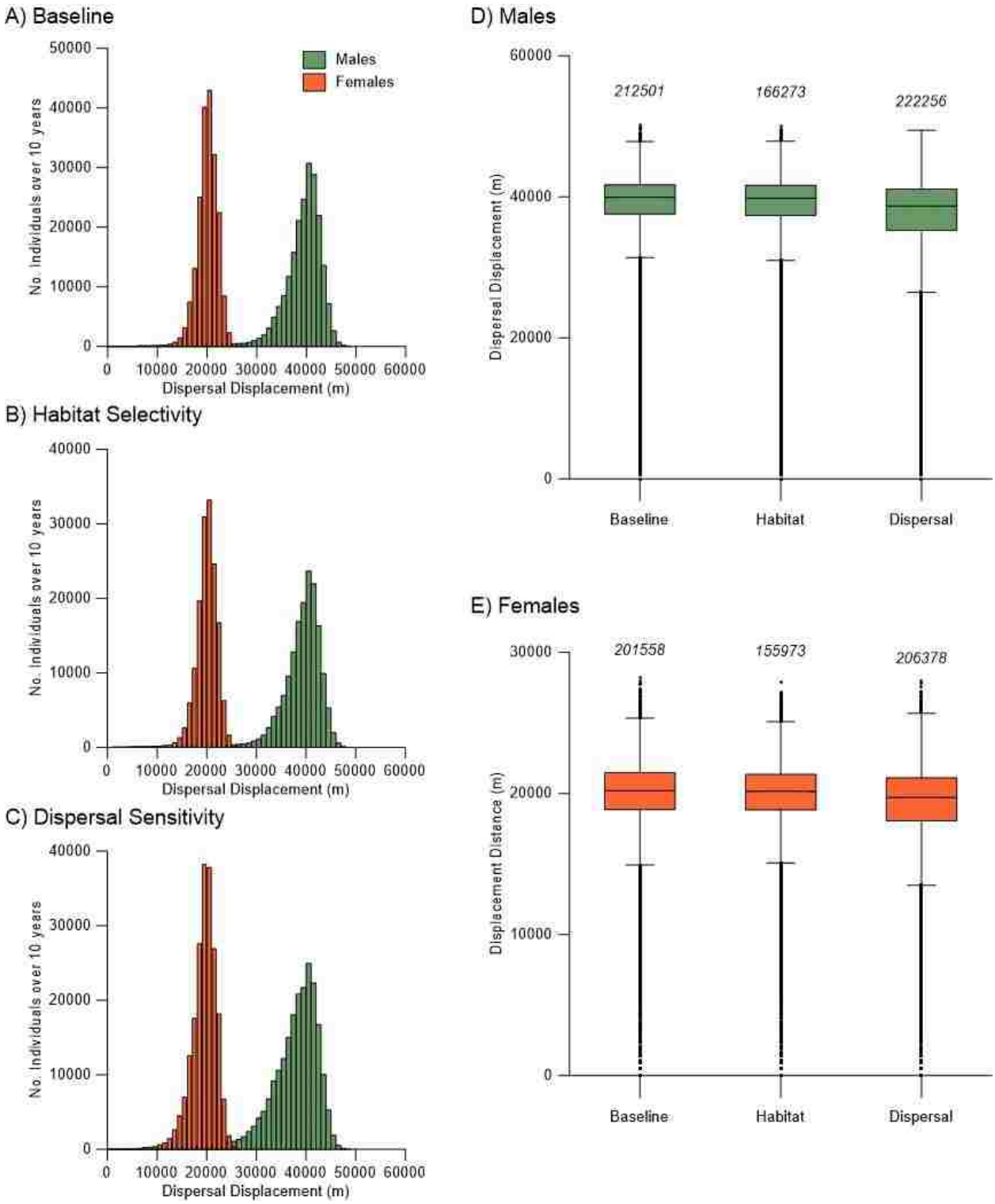

Figure 7. Realized dispersal "displacement" for three models, Baseline (A), Increased Habitat Selectivity (B), and Increased Dispersal Sensitivity (C) over a ten-year period (time-step 26-35). Median-quartile plots for males and females in panels D & E respectively. Sample sizes above each plot indicate the number of individuals over a ten-year period.

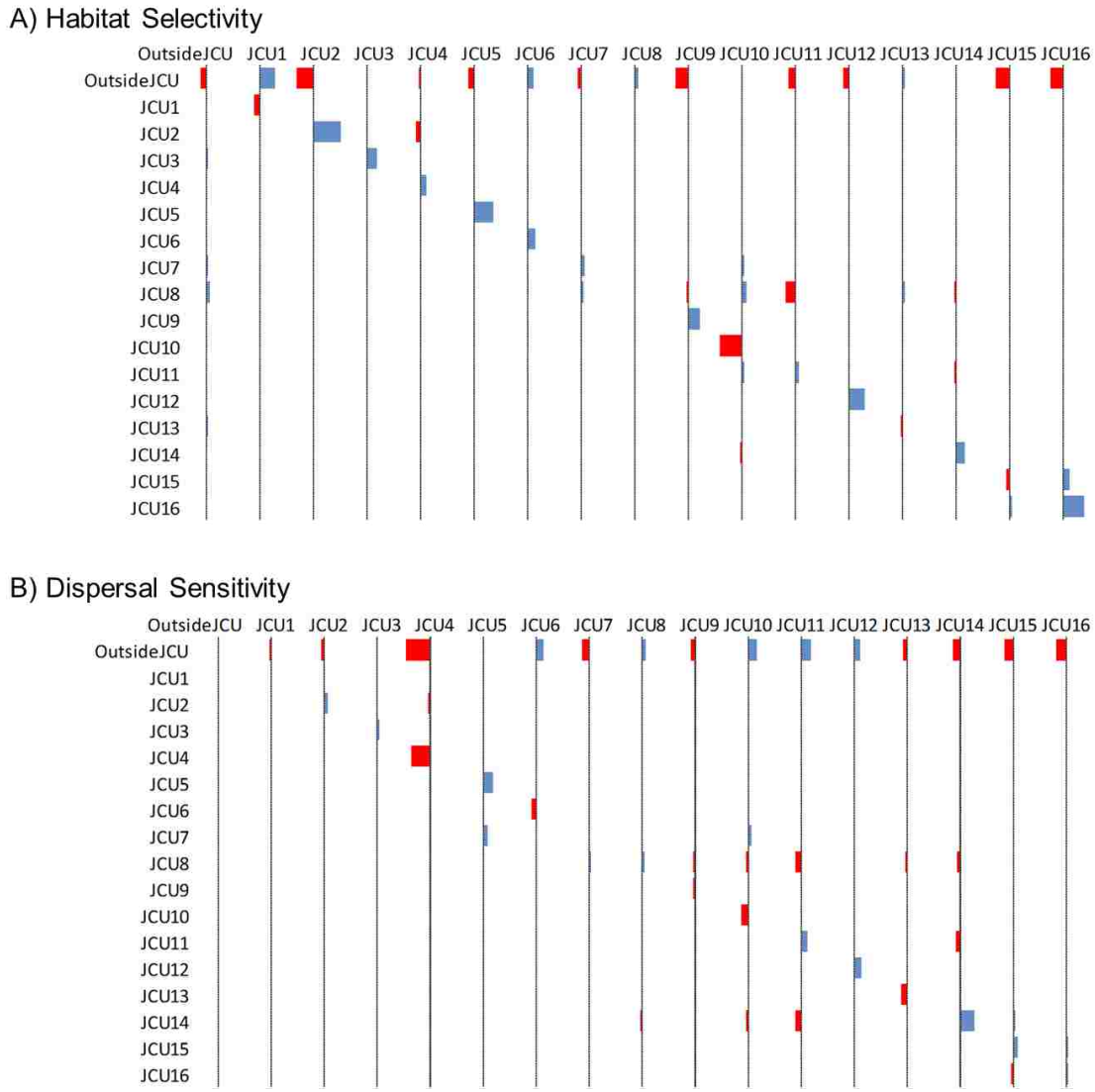

Figure 8. Change in transition probability matrices from the Baseline model to the experimental treatments, increased Habitat Selectivity (A) and increased Dispersal Sensitivity (B). Red flags indicate a lower probability of transition given the experiment treatment, and blue flags indicate a higher probability of transition. The upper row indicates the source, and left column indicates the destination location from one year to the next. Transition probabilities were compiled over 35 years (time step 1-35).

Genetic Distance between JCUs: Overall changes in genetic distances due to experimental treatments were assessed with a paired (by JCU) t-tests. We analyzed the sexes separately to examine how our sex-specific dispersal and territorial dynamics impacted gene flow. Our increased Habitat Selectivity treatment increased genetic distances for both males and females (Figure 9). Conversely, Dispersal Sensitivity decreased genetic distances for males, but had no significant effect for females.

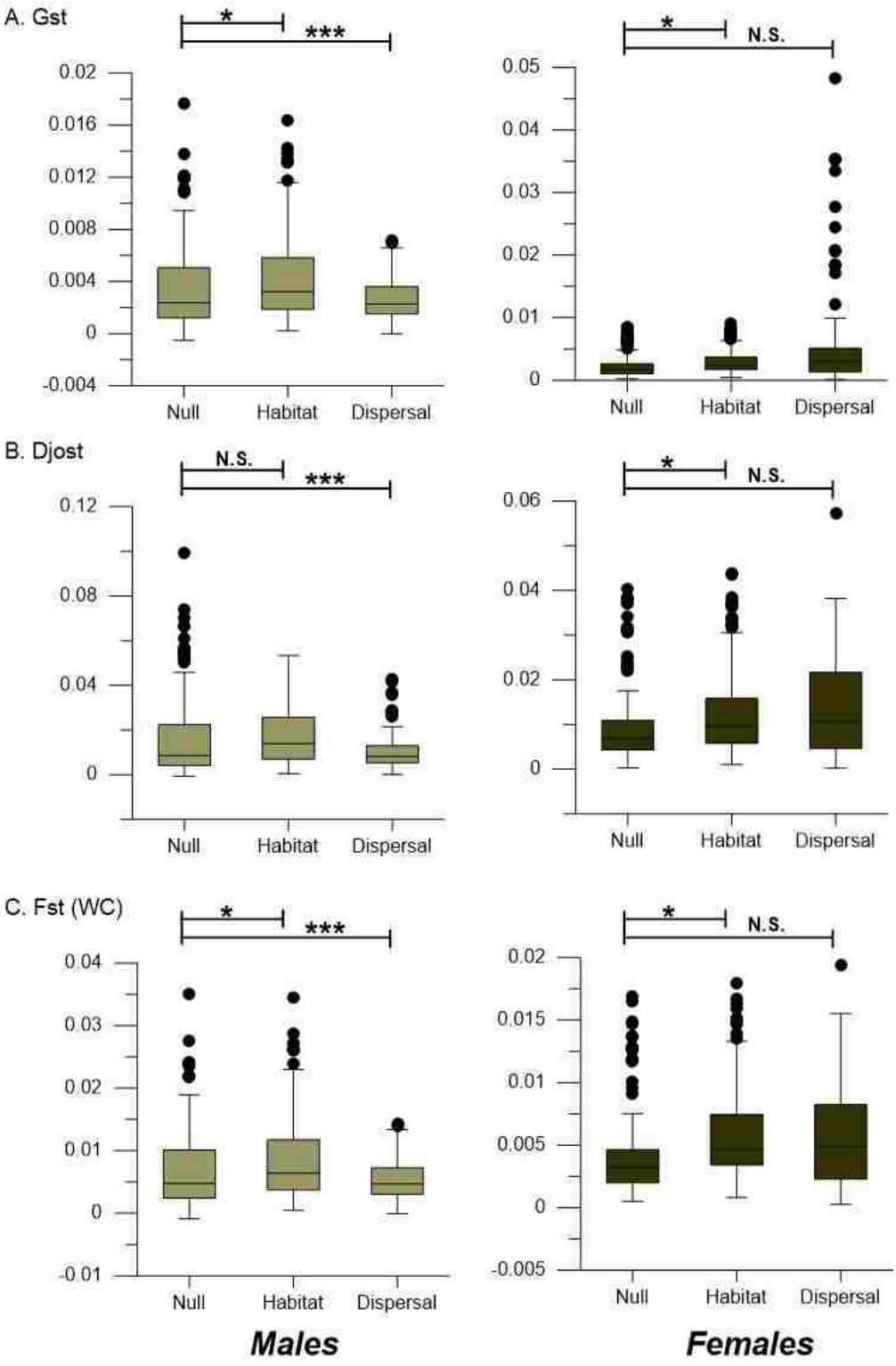

*Figure 9. Median-quartile plots of genetic-distance (Nei's Gst, Jost's D, and Weir & Cockerham's Fst) for three models at time-step 35: Baseline (Null), Habitat Selectivity (Territory), and Dispersal Sensitivity (Dispersal). Non-significant (N.S.), * p<0.05, *** p<0.001.*

In addition to overall patterns in genetic distance, we wanted to determine if there were location-specific changes in gene flow. We plotted each pair-wise genetic-distance (16 JCUs, 120 pair-wise comparisons) to visualize the comparison of our experimental treatments to the Baseline model (Figure 10). For males, there was a cluster of observations from our Habitat Selectivity treatment that fell above the Baseline values of genetic-distance (Figure 10, left, green dots). These observations all involved JCU10 in northern Belize. The transition probability results show that this JCU in particular was impacted by our Habitat Selectivity treatment, causing an increase in emigration due to poor-quality habitat and reduction in population size. The smaller number of individuals remaining within JCU10 under our Habitat Selectivity treatment is the likely cause of the increased genetic-distance to this JCU, due to the random retention of specific genotypes (similar to genetic founder effects).

For both sexes, and across both treatments, there are a greater number of pair-wise estimates that fall below the Baseline values at the upper end of Baseline genetic distance. Several of these below-baseline observations involve JCU4 in northeastern Mexico. Both of our experimental treatments are reducing genetic distance to this small, isolated JCU as compared to our Baseline model. Our transition probability results do not explain this result, as we do not see a greater probability of individuals transitioning to or from JCU4 under our experimental treatments. However, this does not preclude a change in gene flow over generations, despite our limited number of simulation years.

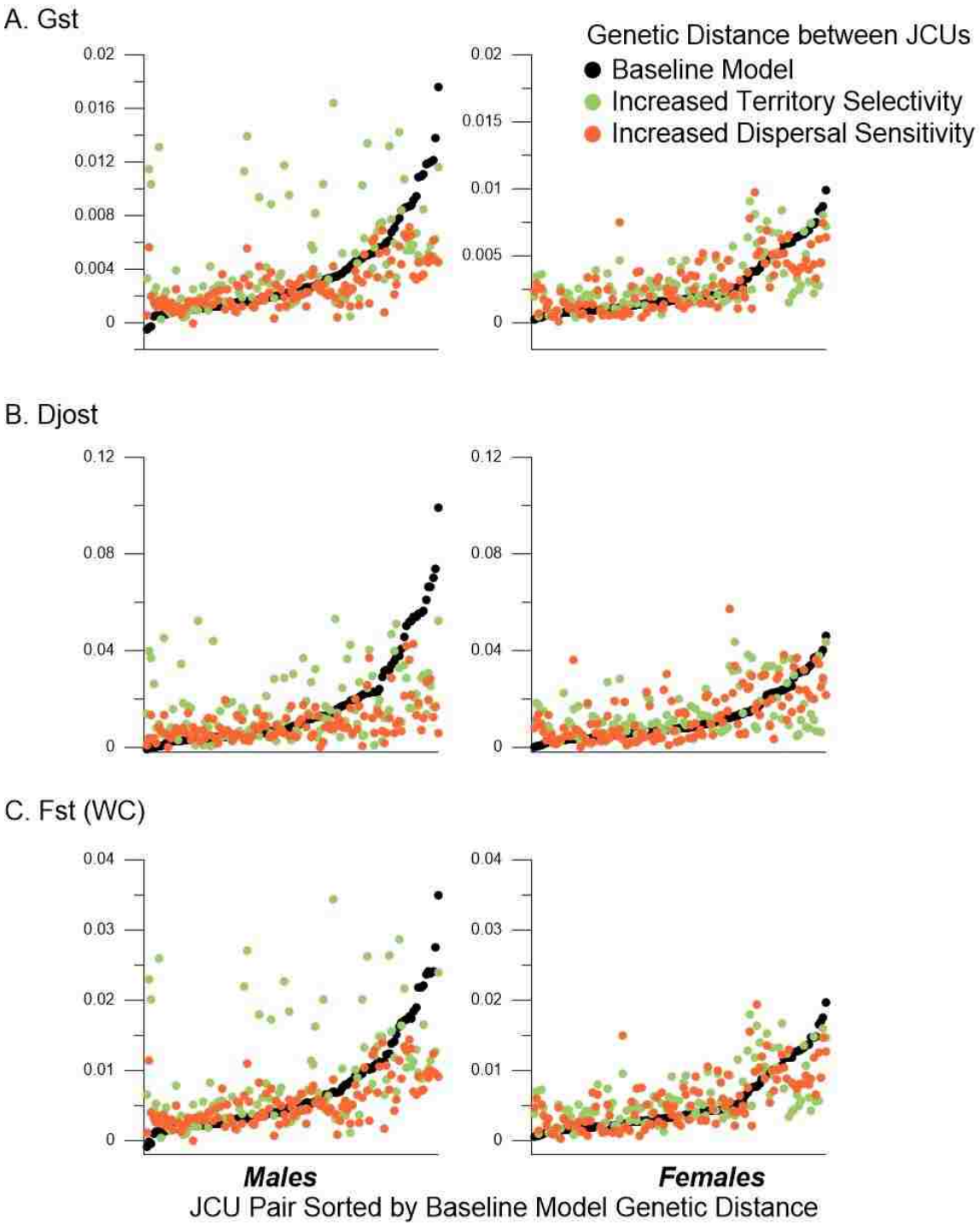

Figure 10. 120 Pair-wise genetic distances between 16 JCUs at time-step 35. Pairs are ordered by ascending genetic distance in Baseline model. Genetic distance metrics are Nei's Gst (A), Jost's D (B), and Wier & Cockerham's Fst (C).

DISCUSSION:

Our model of Neotropical felid spatial dynamics and gene flow provides a powerful new tool for investigating drivers of gene flow in these behaviorally complex species. By including separate behavioral dynamics for dispersal through the landscape, versus establishing territories, we can examine how landscape influences each of these components of movement ecology separately, and track the resulting changes in gene flow. We demonstrated this potential with our experimental treatments. Our model of increased habitat selectivity resulted in decreased gene flow between JCUs, supporting our hypothesis that territorial requirements influence gene flow by impacting the probability of newly established territories being near to forested natal sites. This hypothesized mechanism is supported by an observation of increased JCU fidelity in our Habitat Selectivity treatment. Conversely, our model of increased dispersal sensitivity resulted in increased gene flow. This would seem to support our hypothesis that dispersal behavior sensitivity produces rare, long-distance realized dispersal. We propose that the specific patterns in structural connectivity of the landscape may facilitate gene flow between JCUs without significantly increasing displacement distance. For example, dispersal paths that strictly follow riparian corridors may facilitate locating a suitable territory. It should be kept in mind, however, that our preliminary gene flow results are from time step 35. Therefore, the observed changes in gene flow have taken place over just a few generations at most, and primarily due to first or second-generation migrants. Additional simulation time steps will be needed to determine if these patterns persist over future generations.

Our preliminary results also demonstrate the utility of a geographically-explicit simulation landscape, highlighting JCU4 and JCU10 as particularly sensitive to our experimental treatments. Future investigation of these sites, both via simulations and empirical data, may provide guidance for conservation at these locations. For example, if we hypothesize that territorial habitat selectivity contributes to gene flow in jaguars, then our model predictions suggest that JCU10 is a contentious

place for conservation efforts, as it contains lower quality habitat, yet may contain a genetically-distinct population.

In order to have the highest possible applicability to conservation, the spatial scale (both grain and extent) of an SIBM should match the scales relevant to the organism. This is an especially demanding task when modeling large, highly vagile carnivores. Our model's spatial grain and extent are the most ambitious Neotropical felid modeling effort to date, matching the fine grain of resource selection in these species (Day et al. *this dissertation Chapter 1*), and covering a large enough spatial extent to capture the effects of gene flow (Day et al. *this dissertation, Chapter 2*; Wultsch et al. 2016; Zanin et al. 2016).

Our future applications of this model will include investigating the effect of barriers (rivers and roads) on gene flow, and adding multiple dispersal-exploration phases within a single annual cycle, to allow for multiple territory searches prior to floater-based mortality. Other future applications of our model may include forecasting the effects of specific landscape changes; road construction or climate-induced land-cover change, for example. In short, our eco-evo SIBM model paves the way for generating conservation-relevant predictions of how movement ecology and landscape pattern interact to influence the genetic connectivity of Neotropical felids.

ACKNOWLEDGMENTS: Allen Brookes developed the source code for HexSim and has been an invaluable member of our research team. This work was funded in part by the WRF-Hall Graduate Student Fellowship from the University of Washington, Department of Biology.

LITTERATURE CITED:

Angelieri, Cintia Camila Silva, Christine Adams-Hosking, Katia Maria Paschoaletto Micchi de Barros Ferraz, Marcelo Pereira de Souza, and Clive Alexander McAlpine. 2016. “Using Species Distribution Models to Predict Potential Landscape Restoration Effects on Puma Conservation.” *PLoS ONE* 11 (1): e0145232.

Aranda, Marcelo. 1996. “Distribución y abundancia del jaguar (Panthera onca, Carnivora; Felidae) en el Estado de Chiapas, México.” *Acta Zoológica Mexicana* 68: 45–52.

Bender, Darren J., and Lenore Fahrig. 2005. “Matrix Structure Obscures the Relationship Between Interpatch Movement and Patch Size and Isolation.” *Ecology* 86 (4): 1023–33.

Benson, John F., Peter J. Mahoney, Jeff A. Sikich, Laurel E. K. Serieys, John P. Pollinger, Holly B. Ernest, and Seth P. D. Riley. 2016. “Interactions between Demography, Genetics, and Landscape Connectivity Increase Extinction Probability for a Small Population of Large Carnivores in a Major Metropolitan Area.” *Proc. R. Soc. B* 283 (1837): 20160957.

Bernal-Escobar, Adriana, Esteban Payan, and Juan M. Cordovez. 2015. “Sex Dependent Spatially Explicit Stochastic Dispersal Modeling as a Framework for the Study of Jaguar Conservation and Management in South America.” *Ecological Modelling* 299 (March): 40–50.

Caso, A., C. Lopez-Gonzales, E. Payan, E. Eizirik, T. de Oliveira, R. Leite-Pitman, M. Kelly, and C. Valderrama. 2008. “Panthera Onca: The IUCN Red List of Threatened Species 2008: e.T15953A5327466.” IUCN.

Ceballos, Gerardo, Cuauhtemoc Chávez, Antonio Rivera, Carlos Manterola, and B. Wall. 2002. “Tamaño Poblacional Y Conservación Del Jaguar En La Reserva de La Biosfera Calakmul, Campeche, México.” In *El Jaguar En El Nuevo Milenio*, 403–17.

Crawshaw, P. G., and H. B. Quigley. 1991. “Jaguar Spacing, Activity and Habitat Use in a Seasonally Flooded Environment in Brazil.” *Journal of Zoology* 223 (3): 357–70.

Crawshaw JR., Peter G., Jan K. Mahler, Cibele Indrusiak, Sandra M. C. Cavalcanti, Maria R. P. Leite-Pitman, and Kirsten M. Silvius. 2004. “Ecology and Conservation of the Jaguar (Panthera Onca) in Iguacu National Park, Brazil.” In *People in Nature: Wildlife Conservation in South and Central America*, KM Silvius, RE Bodmer, and JMV Fragoso, , 286–96. Chapter 17. New York: Columbia University Press.

Crawshaw JR., Peter G., and Howard B. Quigley. 1984. “A Ecologia Do Jaguar Ou Onça-Pintada (Panthera Onca) No Pantanal Mato-Grossense.” Relatório final para o Instituto Brasileiro de Desenvolvimento Florestal-IBDF, Brasília: IBDF.

Fischer, Wagner A., Mario B. Ramos-Neto, Leandro Silveira, and Anah T. A. Jacomo. 2003. “Human Transportation Network as Ecological Barrier for Wildlife on Brazilian Pantanal-Cerrado Corridors.” *Road Ecology Center*, August.

Foster, Rebecca. 2008. “The Ecology of Jaguars (Panthera Onca) in a Human-Influenced Landscape.” University of Southhampton. PhD Thesis.

Jost, Lou. 2008. “GST and Its Relatives Do Not Measure Differentiation.” *Molecular Ecology* 17 (18): 4015–26.

Keenan, Kevin, Philip McGinnity, Tom F. Cross, Walter W. Crozier, and Paulo A. Prodöhl. 2013. “diveRsity: An R Package for the Estimation and Exploration of Population Genetics Parameters and Their Associated Errors.” *Methods in Ecology and Evolution* 4 (8): 782–88.

Kelly, Marcella J., Andrew J. Noss, Mario S. Di Bitetti, Leonardo Maffei, Rosario L. Arispe, Agustin Paviolo, Carlos D. De Angelo, and Yamil E. Di Blanco. 2008. “Estimating Puma Densities from Camera

Trapping across Three Study Sites: Bolivia, Argentina, and Belize." *Journal of Mammalogy* 89 (2): 408–18.

Lindzey, Frederick G., Walter D. Van Sickle, Bruce B. Ackerman, Dan Barnhurst, Thomas P. Hemker, and Steven P. Laing. 1994. "Cougar Population Dynamics in Southern Utah." *The Journal of Wildlife Management* 58 (4): 619–24.

Mazzolli, Marcelo. 2010. "Mosaics of Exotic Forest Plantations and Native Forests as Habitat of Pumas." *Environmental Management* 46 (2): 237–53.

Miotto, Renata A., Marcelo Cervini, Rodrigo A. Begotti, and Pedro M. Galetti Jr. 2012. "Monitoring a Puma (Puma Concolor) Population in a Fragmented Landscape in Southeast Brazil." *Biotropica* 44 (1): 98–104.

Monroy-Vilchis, Octavio, Clarita Rodríguez-Soto, Martha Zarco-González, and Vicente Urios. 2009. "Cougar and Jaguar Habitat Use and Activity Patterns in Central Mexico." *Animal Biology* 59 (2): 145–57.

Nathan, Ran, Wayne M. Getz, Eloy Revilla, Marcel Holyoak, Ronen Kadmon, David Saltz, and Peter E. Smouse. 2008. "A Movement Ecology Paradigm for Unifying Organismal Movement Research." *Proceedings of the National Academy of Sciences* 105 (49): 19052–59.

Nei, M., and R. K. Chesser. 1983. "Estimation of Fixation Indices and Gene Diversities." *Annals of Human Genetics* 47 (3): 253–59.

Nowell, Kristin, and Peter Jackson. 1996. "Wild Cats: Status Survey and Conservation Action Plan. IUCN/SSC Cat Specialist Group." IUCN.

Núñez, Rodrigo, Brian Miller, and Fred Lindzey. 2002. "Ecología Del Jaguar En La Reserva de La Biosfera Chamela-Cuixmala, Jalisco, México." In *El Jaguar En El Nuevo Milenio*, 107–25.

Payan Garrido, C. E. 2009. “Hunting Sustainability, Species Richness and Carnivore Conservation in Colombian Amazonia.” Doctoral Thesis, UCL (University College London).

Rabinowitz, A. R., and B. G. Nottingham Jr. 1986. “Ecology and Behaviour of the Jaguar (Panthers Onca) in Belize, Central America.” *Journal of Zoology* 210 (1): 149–59.

Rabinowitz, Alan, and Kathy A. Zeller. 2010. “A Range-Wide Model of Landscape Connectivity and Conservation for the Jaguar, Panthera Onca.” *Biological Conservation* 143 (4): 939–45.

Revilla, Eloy, Thorsten Wiegand, Francisco Palomares, Pablo Ferreras, Miguel Delibes, and Associate Editor: Rolf A. Ims. 2004. “Effects of Matrix Heterogeneity on Animal Dispersal: From Individual Behavior to Metapopulation-Level Parameters.” *The American Naturalist* 164 (5): E130–53.

Rodríguez-Soto, Clarita, Octavio Monroy-Vilchis, Luigi Maiorano, Luigi Boitani, Juan Carlos Faller, Miguel Á. Briones, Rodrigo Núñez, Octavio Rosas-Rosas, Gerardo Ceballos, and Alessandra Falcucci. 2011. “Predicting Potential Distribution of the Jaguar (Panthera Onca) in Mexico: Identification of Priority Areas for Conservation.” *Diversity and Distributions* 17 (2): 350–61.

Sanderson, Eric W., Kent H. Redford, Cheryl-Lesley B. Chetkiewicz, Rodrigo A. Medellin, Alan R. Rabinowitz, John G. Robinson, and Andrew B. Taber. 2002. “Planning to Save a Species: The Jaguar as a Model.” *Conservation Biology* 16 (1): 58–72.

Schaller, George B., and Peter Gransden Crawshaw. 1980. “Movement Patterns of Jaguar.” *Biotropica* 12 (3): 161–68.

Schumaker, NH. 2016. *HexSim* (version 4.0). Corvallis, Oregon, USA: U.S. Environmental Protection Agency, Environmental Research Laboratory.

Seymour, Kevin. 1989. “Panthera Onca (Linnaeus, 1758)” Mammalian Species Archive 340. *The American Society of Mammalogists*. 1-9.

Sollmann, Rahel, Mariana Malzoni Furtado, Beth Gardner, Heribert Hofer, Anah T. A. Jácomo, Natália Mundim Tôrres, and Leandro Silveira. 2011. “Improving Density Estimates for Elusive Carnivores: Accounting for Sex-Specific Detection and Movements Using Spatial Capture–recapture Models for Jaguars in Central Brazil.” *Biological Conservation* 144 (3): 1017–24.

Sollmann, Rahel, Natália Mundim Tôrres, Mariana Malzoni Furtado, Anah Tereza de Almeida Jácomo, Francisco Palomares, Severine Roques, and Leandro Silveira. 2013. “Combining Camera-Trapping and Noninvasive Genetic Data in a Spatial Capture–recapture Framework Improves Density Estimates for the Jaguar.” *Biological Conservation* 167: 242–47.

Stoner, David C., Wendy R. Rieth, Michael L. Wolfe, Mclain B. Mecham, and Ann Neville. 2008. “Long-Distance Dispersal of a Female Cougar in a Basin and Range Landscape.” *The Journal of Wildlife Management* 72 (4): 933–39.

Stoner, David C., Michael L. Wolfe, Clint Mecham, McLain B. Mecham, Susan L. Durham, and David M. Choate. 2013. “Dispersal Behaviour of a Polygynous Carnivore: Do Cougars Puma Concolor Follow Source-Sink Predictions?” *Wildlife Biology* 19 (3): 289–301.

Sunquist, Fiona, and Mel Sunquist. 2002. *Wild Cats of the World*. 1 edition. Chicago: University of Chicago Press.

Vynne, Carly, Jonah L. Keim, Ricardo B. Machado, Jader Marinho-Filho, Leandro Silveira, Martha J. Groom, and Samuel K. Wasser. 2011. “Resource Selection and Its Implications for Wide-Ranging Mammals of the Brazilian Cerrado.” *PLoS ONE* 6 (12): 1–12.

Weaver, John L., Paul C. Paquet, and Leonard F. Ruggiero. 1996. “Resilience and Conservation of Large Carnivores in the Rocky Mountains.” *Conservation Biology* 10 (4): 964–76.

Weir, B. S., and C. Clark Cockerham. 1984. “Estimating F-Statistics for the Analysis of Population Structure.” *Evolution* 38 (6): 1358–70.

Wultsch, Claudia, Anthony Caragiulo, Isabela Dias-Freedman, Howard Quigley, Salisa Rabinowitz, and George Amato. 2016. “Genetic Diversity and Population Structure of Mesoamerican Jaguars (Panthera Onca): Implications for Conservation and Management.” *PLOS ONE* 11 (10): e0162377.

Zanin, Marina, Begoña Adrados, Noa González, Severine Roques, Daniel Brito, Cuauhtemoc Chávez, Yamel Rubio, and Francisco Palomares. 2016. “Gene Flow and Genetic Structure of the Puma and Jaguar in Mexico.” *European Journal of Wildlife Research*, May, 1–9.

Zeller, Kathy. 2007. “Jaguars in the New Millennium. Data Set Update: The State of the Jaguar in 2006. WCS Report.” *Wildlife Conservation Society, New York*, 1–82.

APPENDIX

Table S1. Geographic data layers used to generate model land-cover maps, barrier maps, and sampling locations.

Geographic Data Layer	Source	Provider/Host	Web Address
Land cover	0.5 km MODIS-based Global Land Cover Climatology	USGS Land Cover Institute (LCI)	http://landcover.usgs.gov/global_climatology.php
Jaguar Conservation Units	Kathy Zeller, Wildlife Conservation Society	Data-Basin	http://databasin.org/datasets/
Elevation	SRTM 90m Digital Elevation Data	CGIAR-CSI GeoPortal	http://srtm.csi.cgiar.org/
Roads	Digital Chart of the World	DIVA-GIS	www.diva-gis.org/Data
Rivers	Digital Chart of the World	DIVA-GIS	www.diva-gis.org/Data